T.C.
DOKUZ EYLÜL UNIVERSITY
SCHOOL OF NATURAL AND APPLIED SCIENCE

ANALYSIS OF STRESS DISTRIBUTIONS IN A BEAM WITH A CIRCULAR HOLE UNDER DIFFERENT CONDITIONS

A Thesis Presented to
the Graduate School of Natural
and Applied Sciences
Dokuz Eylül University

In Partial Fulfillment
of the Requirements for the Masters Degree
in Mechanical Engineering

by

Mesut UYANER

Advisor

Assoc.Prof.Dr. Seçil ERİM

December 1994
İZMİR

ABSTRACT

In this study, a simple beam with a circular hole placed at different locations along the transverse axis is stress analysed under the effect of pure bending by means of Finite Element Method.

Both isotropic (steel) and composite materials (Graphite-epoxy, Scotchply, Kevlar, and Boron) are used as the beam material and stress distributions and stress concentration factors around the hole are determined for each case.

The effect of variations in reinforcing angles upon the stress distribution are also investigated at several angles chosen between 0° and 90° inclusive.

The value of the critical diameter of the hole leading to $(\sigma_{xth})_{max}$ is determined for each **b** distance considered by the FEM. The critical **b** distance leading to $(\sigma_{xth})_{max}$ is computed for the 10 mm hole diameter in the steel beam and in the composites with each different reinforcing angle.

Two-dimensional four-node quadrilateral isoparametric finite element is chosen to solve the problem. The Gaussian numerical integration method is used to determine element stiffness values. Stress distributions and stress concentration factors obtained from prepared computer programs are presented in the form of graphics.

ÖZET

Bu çalışmada enine ekseni üzerinde dairesel delik bulunan bir kiriş basit eğilme etkisinde sonlu elemanlar yöntemiyle incelenmiştir. Delik, sözü edilen eksen boyunca kaydırılmış ve kiriş için hem izotropik (çelik) ve hemde ortotropik (farklı kompozitler) malzemeler kullanılmıştır. Bu suretle değişik her bir durum için delik civarındaki gerilme dağılımı ve gerilme yığılması faktörü belirlenmiştir. Öte yandan fiber takviye açılarındaki değişimin gerilme dağılımı üzerindeki etkisini ortaya çıkarmak amacıyla inceleme, kullanılan her bir kompozit için 0° ile 90° arasındaki muhtelif açılarda tekrarlanmıştır.

İncelenen her **b** mesafesi için en büyük teorik eğilme gerilmesini doğuracak kritik delik çapı değeri Sonlu Elemanlar Yöntemi ile tayin edildi. Ayrıca 10 mm'lik sabit delik çapı için yine en büyük teorik eğilme gerilmesini doğuracak kritik **b** mesafesi çelik ve her bir değişik takviye açılarındaki kompozit kirişler için hesaplandı.

Problemin çözümünde iki boyutlu dört düğümlü izoparametrik eleman modeli kullanılmıştır. Eleman katılık değerlerinin belirlenmesinde Gauss nümerik integrasyon yöntemi izlenmiştir. Gerilme dağılımı ve gerilme yığılma faktörleri yazılan bilgisayar proğramları yardımıyla elde edilmiş ve grafikler halinde sunulmuştur.

ACKNOWLEDGEMENTS

I am in debt to Assoc.Prof.Dr. Seçil ERİM, my advisor, for his constructive suggestions, guidance and his continued interest in my work. It is really a chance to study under his supervision.

I had the benefit of reviews, comments and advices from Prof. Dr Onur Sayman. I express my thanks to him. I also thank all my friends who made many valuable suggestions.

Finally, unbounded thanks for my wife who was a hidden hero behind my study. Her love, encouragement, and patience supported me in this study.

Mesut UYANER

CONTENTS

Page

LIST OF ILLUSTRATIONS

FIGURE PAGE

LIST OF TABLES

NOMENCLATURE

$\mathbf{u}$	Nodal displacement vector
u, v, w	Nodal displacement vector components
$\mathbf{f}$	Force vector
$\mathbf{T}$	Traction force vector
$\mathbf{P}_i$	Point load vector
σ	Stress vector
$\underline{\sigma}$	Ply stress in composites
$\sigma_x, \sigma_y, \sigma_z$	Components of normal stress
$\tau_{yz}, \tau_{xz}, \tau_{xy}$	Components of shear stress
$\partial/\partial x$	Partial differentiation with respect to x
$\mathbf{n}$	Unit normal
ε	Strain vector
$\varepsilon_x, \varepsilon_y, \varepsilon_z$	Components of normal strains
$\gamma_{yz}, \gamma_{xz}, \gamma_{xy}$	Components of engineering shear strains
E	Young's modulus for isotropic material
G	Shear modulus for isotropic material
ν	Poisson's ratio for isotropic material
$\mathbf{D}$	Material matrix
Π	Potential energy of an elastic body
U	Strain energy
WP	Work potential
E_L	Longitudinal modulus
E_T	Transverse modulus

G_{LT}	Longitudinal-transverse shear modulus
Q_{ij}	Modulus components i,j=1,2,6
S_{ij}	Compliance components i,j=1,2,6
W	Stored elastic energy
ν_{LT}	Major Poisson's ratio
ν_{TL}	Minor Poisson's ratio
θ	Reinforcing angle
m	$\cos\theta$
n	$\sin\theta$
U_i	Linear combination of modulus and compliance in multiple angle formulation. Same notation but different definition is used for modulus and compliance
σ'	Transformed stress
ε'	Transformed strain
r	Abscissa in local coordinate system
s	Ordinate in local coordinate system
N_i	Shape functions on a master element, equal to unity at node i.
J	Jacobean matrix
$\mathbf{k^e}$	Element stiffness matrix
σ_{xth}	Bending stress evaluated from elementary beam theory
$(\sigma_{xth})_{max}$	Maximum theoretical bending stress in a beam
σ_{xth}^*	Bending stress for a beam evaluated from elementary beam theory
Y_c	Distance from the longitudinal axis given by $Y_c = y - h/2$
y^*	Distance from point where the stress is calculated on to the neutral axis
I	Second moment of the cross sectional area
I^*	Second moment of cross sectional area of the beam with a hole
σ_1	The maximum principal stress at any point
t	Thickness of the beam

h	Height of the beam
L	Length of the beam
D	Diameter of the hole
$\mathbf{D_{cr}}$	Critical hole diameter
b	Distance from the longitudinal axis to the centre of the hole
a	The moment arm
SCF	Stress concentration factor
SCF*	Stress concentration factor computed regarding σ_{xth}^*
SCF_{locmax}	Maximum local stress concentration factor
SCF_{cr}	Critical stress concentration factor
Sub x	Normal component along x-axis
Sub y	Normal component along y-axis
Sub xy	Shear component in x-y plane

CHAPTER 1

FUNDAMENTAL CONCEPTS

1.1. STRESSES AND EQUILIBRIUM

A three-dimensional body occupying a volume V and having a surface S is shown in Fig. 1.1. Points in the body are located by x, y, z coordinates. The boundary is constrained on some region, where the displacement is specified. On part of the boundary, distributed force per unit area **T**, also called traction, is applied. Under the force, the body deforms. The deformation of a point x (= [x, y, z]^T) is given by the three components of its displacement:

$$\mathbf{u} = [u, v, w]^T \tag{1.1}$$

The distributed force per unit volume, for example, the weight per unit volume, is the vector **f** given by

$$\mathbf{f} = [f_x, f_y, f_z]^T \tag{1.2}$$

The body force acting on the elemental volume dV is shown in Fig. 1.1. The surface traction **T** may be given by its component values at points on the surface.

$$\mathbf{T} = [T_x, T_y, T_z]^T \tag{1.3}$$

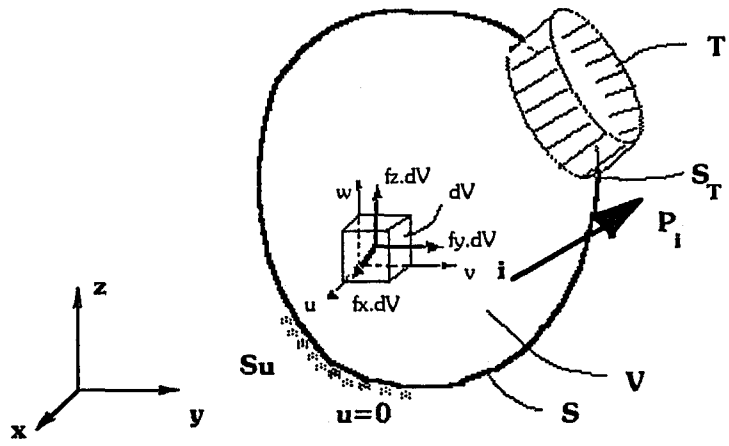

Figure 1.1 Three-dimensional body

Examples of traction are distributed contact force and action of pressure. A load **P** acting at a point *i* is represented by its three components

$$\mathbf{P}_i = [P_x, P_y, P_z]^T_i \tag{1.4}$$

The stress acting on the elemental volume *dV* are shown in Fig 1.2. When the volume dV shrinks to a point, the stress tensor is represented by placing its components in a (3 x 3) symmetric matrix. However, we represent stress by the six independent components as follows:

$$\sigma = [\sigma_x, \sigma_y, \sigma_z, \tau_{yz}, \tau_{xz}, \tau_{xy}]^T \tag{1.5}$$

where σ_x, σ_y, σ_z are normal stress and τ_{yz}, τ_{xz}, τ_{xy} are shear stresses.

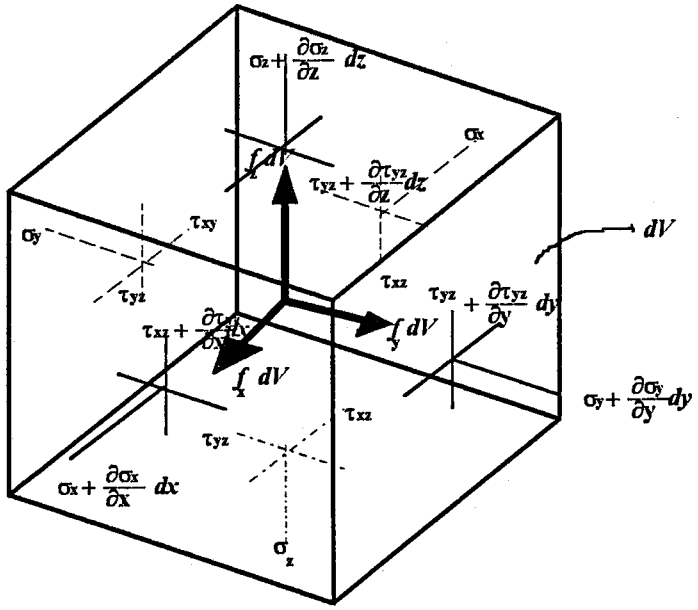

Figure 1.2 Equilibrium of an elemental volume

Let us consider equilibrium of an elemental volume shown in Fig. 1.2. First we get forces on faces by multiplying stress components by the corresponding areas. Writing $\Sigma Fx = 0$, $\Sigma Fy = 0$ and $\Sigma Fz = 0$, and recognising $dV = dx\, dy\, dz$, we get the equilibrium equations:

$$\frac{\partial \sigma_x}{\partial x} + \frac{\partial \tau_{xy}}{\partial y} + \frac{\partial \tau_{xz}}{\partial z} + f_x = 0$$

$$\frac{\partial \tau_{xy}}{\partial x} + \frac{\partial \sigma_y}{\partial y} + \frac{\partial \tau_{yz}}{\partial z} + f_y = 0 \qquad (1.6)$$

$$\frac{\partial \tau_{xz}}{\partial x} + \frac{\partial \tau_{xz}}{\partial y} + \frac{\partial \sigma_z}{\partial z} + f_z = 0$$

1.2. POTENTIAL ENERGY AND EQUILIBRIUM

In mechanics of solids, our problem is to determine the displacement **u** of the body shown in Fig. 1.1, satisfying the equilibrium equations 1.6. Note that stresses are related to strains, which, in turn, are related to displacements. This leads to requiring solution of second-order partial differential equations. Solution of this set of equations is generally referred to as an *exact* solution. Such exact solutions are available for simple geometries and loading conditions, and one may refer to publications in theory of elasticity. For problems of complex geometries and general boundary and loading conditions, obtaining such solutions is an almost impossible task. Approximate solution methods usually employ potential energy or variational methods, which place less stringent conditions on the functions.

Potential Energy, Π

The total potential energy Π of an elastic body, is defined as the sum of total strain energy (U) and the work potential:

$$\Pi = \underset{(U)}{\text{Strain Energy}} + \underset{(WP)}{\text{Work Potential}} \tag{1.7}$$

For linear elastic materials, the strain energy per unit volume in the body is $\frac{1}{2}\sigma^T\varepsilon$. For the elastic body shown in Fig. 1.1, the total strain energy U is given by

$$U = \frac{1}{2} \int_V \sigma^T\varepsilon \, dV \tag{1.8}$$

The work potential WP is given by

$$WP = \int_V \mathbf{u}^T \mathbf{f} dV + \int_S \mathbf{u}^T \mathbf{T} dS - \sum_i \mathbf{u}_i^T \mathbf{P}_i \tag{1.9}$$

The total potential for the general elastic body shown in Fig. 1.1 is

$$\Pi = \tfrac{1}{2} \int_V \sigma^T \varepsilon dV - \int_V \mathbf{u}^T \mathbf{f} dV + \int_S \mathbf{u}^T \mathbf{T} dS - \sum_i \mathbf{u}_i^T \mathbf{P}_i \tag{1.10}$$

We consider here conservative systems, where the work potential is independent of the path taken. In other words, if the system is displaced from a given configuration and brought back to the original state, the forces do zero work regardless of the path followed. The potential energy principle is now stated as follows:

Principle of Minimum Potential Energy: For conservative systems, of all the kinematically admissible displacement fields, those corresponding to equilibrium extremize the total potential energy. If the extremum condition is a minimum, the equilibrium state is stable.

Kinematically admissible displacements are those that satisfy the single-valued nature of displacements (compatibility) and the boundary conditions. In problems where displacements are the unknowns, which is the approach in our study, compatibility is automatically satisfied.

1.3. NOTE ON COMPOSITE MATERIALS

1.3.1 Stiffness Of Unidirectional Composites

The stiffness of unidirectional composites, like any other structural material, can be defined by appropriate stress-strain relations. We will show that material constants of these relations can be packaged in a set of engineering constants, compliance components or modulus components. The components of any one set are directly expressible in terms of the components of the other sets. Each set, however, possesses unique characteristics that make it suitable for specific usage. The stiffness of the unidirectional composites is governed by the same stress-strain relation that is valid for ordinary materials. The number of independent constants are four for composites and two for ordinary materials. Numerical values for the stiffness of several typical unidirectional composites are given in tables.

1.3.1.1 Stress in Composites

In the study of composites three levels of average stress are dealt with:

- Micromechanical stress σ is that calculation based on distinct phases of fiber, matrix, and in some cases interface and voids.
- Calculation of ply stress $\underline{\sigma}$ is based on assumed homogeneity with each ply or ply assembly in which the fiber and matrix are smeared.
- Laminate stress or stress resultant N/h is the average of ply stresses across the thickness of a laminate.

Two levels of this idealization of average stresses are shown in Fig. 1.3. On the micromechanical level in Fig. 1.3a, the fiber and matrix stresses vary from point

to point within each constituent phase. The average of these stresses is the ply stress $\underline{\sigma}$. In a laminate or on the macromechanical level, each ply or ply assembly has its own ply stress. The average of several ply stresses is the laminate stress or stress resultant N/h as shown in Fig. 1.3b.

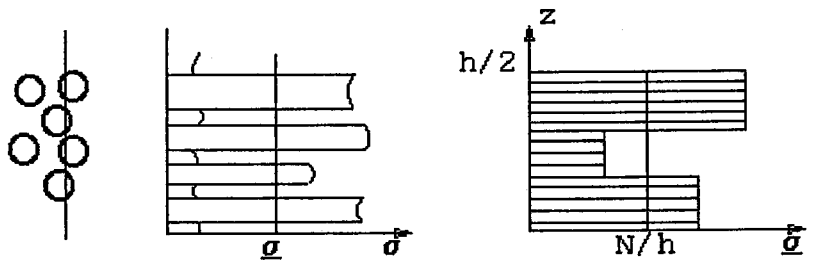

(a) (b)

Figure 1.3 Schematic relations between local and average stresses

The state of stress in a ply or ply assembly is predominantly plane stress. The nonzero components of plane stress are σ_x, σ_y, τ_{xy}. The remaining three components are of secondary and will not be considered in this study.

1.3.1.2 Stress-Strain Relations

We will limit the composites in this section to the linearly elastic materials. The response of materials under stress or strain follows a straight line up to failure in stress or strain space. Assumed linearity moreover permits us to use superposition which is a very powerful tool. For examples, the net result of combining two states of stress is precisely the sum of the two states no more and no less. The sequence of the stress applications is immaterial. We can assemble or dissect components of stress and strain in whatever pattern we choose without affecting result. Combined stress are the sum of simple stresses.

Secondly, elasticity means full reversibility. We can load and unload and reload a material without incurring any hystreresis. Elasticity also means that material's response is instantaneous. There is no time lag, no time or rate dependency.

Experimentally observed behaviour of composites follows closer to linear elasticity than nearly all metals and non-reinforced plastics. The assumed linear elasticity for composites appears to be reasonable. If we are to improve upon this simplification, such as the incorporation of nonlinear elasticity, plasticity and viscoelasticity, the degree of complexity is increased significantly beyond the scope of this study.

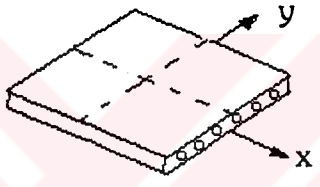

Figure 1.4. Two orthotropic planes of symmetry of unidirectional composites.

For unidirectional composites, the stress-strain relations can be derived by the superposition principle. We must recognise that two orthogonal planes of symmetry exist for unidirectional composites: one plane is parallel to the fibers, and the other, transverse to the fibers. Symmetry exists when the structure of the material on one side of the plane is the mirror image of the structure on the other side. The two orthogonal planes are shown in Fig. 1.4, where the x-axis is along the longitudinal direction of the fiber while the y-axis is in the transverse direction. The stress-strain relation in this section is limited to this special case, which is shown in Fig. 1.4. The off-axis orientation will be discussed in the next section.

The on-axis stress-strain relation can be derived by super-positioning the results of the following simple tests:

a. Uniaxial Longitudinal Tensile Test: The applied uniaxial stress versus the resulting biaxial strain curves for this test are shown in Fig. 1.5. The following stress-strain relations are established from the curves:

$$\varepsilon_x = \frac{1}{E_L}\sigma_x \qquad \varepsilon_y = -\frac{\nu_{LT}}{E_L}\sigma_x \tag{1.11}$$

where E_L = Longitudinal Modulus

ν_{LT} = Major Poisson's Ratio = $-\varepsilon_y/\varepsilon_x$

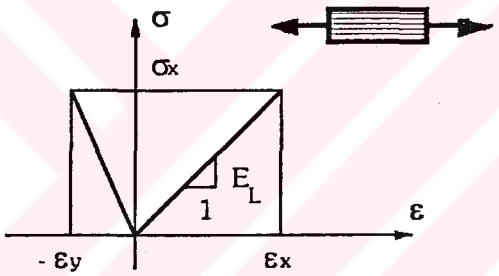

Figure 1.5 Uniaxial longitudinal tensile test

b. Uniaxial Transverse Tensile Test: The applied uniaxial stress and the resulting biaxial strain are shown in Fig. 1.6. The following stress -strain relations can be established from the figure:

$$\varepsilon_y = \frac{1}{E_T}\sigma_y \qquad \varepsilon_x = -\frac{\nu_{TL}}{E_T}\sigma_y \tag{1.12}$$

where E_T = Transverse Modulus

ν_{TL} = Minor Poisson's Ratio = $-\varepsilon_x/\varepsilon_y$

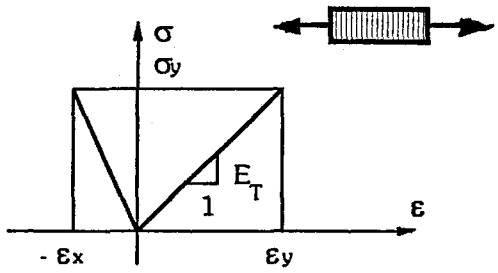

Figure 1.6 Uniaxial transverse tensile test

c. Longitudinal Shear Test: We apply another simple state of stress, the pure shear, to our unidirectional composite. This is shown in Fig. 1.7. The resulting stress- strain relation is:

$$\gamma_{xy} = \frac{1}{G_{LT}} \tau_{xy} \tag{1.13}$$

where G_{LT} = Longitudinal Shear Modulus

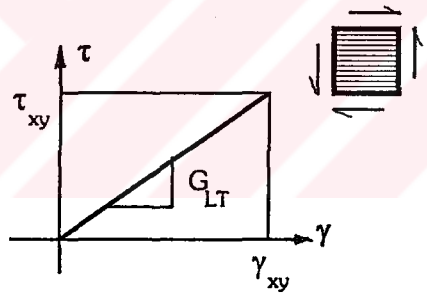

Figure 1.7 Longitudinal shear test

By applying the principle of superposition, we can sum up the contribution of each stress component in Eqs. 1.11, 1.12, and 1.13 to the resulting strain components. The final stress-strain relations for our unidirectional composite are:

$$\varepsilon_x = \frac{1}{E_L}\sigma_x - \frac{\nu_{TL}}{E_T}\sigma_y$$

(1.14)

$$\varepsilon_y = -\frac{\nu_{LT}}{E_L}\sigma_x + \frac{1}{E_T}\sigma_y$$

$$\gamma_{xy} = \frac{1}{G_{LT}}\tau_{xy}$$

These are the on-axis stress-strain relation of a unidirectional composite; i.e., the material is in its orthotropic symmetry orientation.

These simultaneous equations can be repackaged in a matrix multiplication table, where in each row in the table is equal to the sum of products from each column and its column heading. This rule should be self-evident if we compare the first of Eq. 1.14 with the first row of Table 1.

Table 1. ON -AXIS STRESS-STRAIN RELATION FOR UNIDIRECTIONAL COMPOSITES IN TERMS OF ENGINEERING CONSTANTS

	σ_x	σ_y	τ_{xy}
ε_x	$1/E_L$	$-\nu_{TL}/E_T$	0
ε_y	$-\nu_{LT}/E_L$	$1/E_T$	0
γ_{xy}	0	0	$1/G_{LT}$

All the material constants of the stress-strain relation shown in this table are called engineering constants. They are the familiar constants used for ordinary materials with subscripts added to denote the directionality of properties. Many design formulas for structural elements are written in terms of engineering constants. Thus the use of engineering constants will often facilitate the use of composites for structural applications. However, engineering constants for composites are clumsy, and should be replaced by the components of

compliance and modulus. A change of notation from engineering constants in Table 1 to components of compliance in Table 2 can be done by direct substitution.

Table 2. ON-AXIS STRESS-STRAIN RELATION FOR UNIDIRECTIONAL COMPOSITES IN TERMS OF COMPLIANCE

	σ_x	σ_y	τ_{xy}
ε_x	S_{11}	S_{12}	0
ε_y	S_{21}	S_{22}	0
γ_{xy}	0	0	S_{66}

The relations between these two sets of elastic constants are:

$$S_{11} = 1/E_L \qquad S_{22} = 1/E_T$$
$$S_{12} = -\nu_{TL}/E_T \qquad S_{21} = -\nu_{LT}/E_L \qquad S_{66} = 1/G_{LT} \tag{1.15}$$

or conversely,

$$E_L = 1/S_{11} \qquad E_T = 1/S_{12}$$
$$\nu_{LT} = -S_{21}/S_{11} \qquad \nu_{TL} = -S_{12}/S_{22} \qquad G_{LT}=1/S_{66} \tag{1.16}$$

From Eq. 1.14 we can solve for stress in terms of strain for which we have the following equations:

$$\begin{aligned} \sigma_x &= m\, E_L\, [\, \varepsilon_x + \nu_{TL}.\varepsilon_y \,] \\ \sigma_y &= m\, E_T\, [\, \nu_{LT}.\varepsilon_x + \varepsilon_y \,] \\ \tau_{xy} &= G_{LT}.\gamma_{xy} \end{aligned} \tag{1.17}$$

where $m = (1 - \nu_{LT}.\nu_{TL})^{-1}$

In order to eliminate the clumsiness of engineering constants in this stress-strain relation, we will introduce components of modulus in Table 3.

Table 3. ON -AXIS STRESS-STRAIN RELATION FOR UNIDIRECTIONAL COMPOSITES IN TERMS OF MODULUS

	ε_x	ε_y	γ_{xy}
σ_x	Q_{11}	Q_{12}	0
σ_y	Q_{21}	Q_{22}	0
τ_{xy}	0	0	Q_{66}

The following relations exist between engineering constants and the components of modulus:

$$Q_{11} = m E_L \qquad Q_{22} = m E_T$$
$$Q_{21} = m \nu_{TL} E_L \qquad Q_{12} = m \nu_{LT} E_T \qquad Q_{66} = G_{LT} \tag{1.18}$$

or conversely

$$E_L = Q_{11}/m \qquad E_T = Q_{22}/m$$
$$\nu_{LT} = Q_{21}/Q_{22} \qquad \nu_{TL} = Q_{12}/Q_{11} \qquad G_{LT} = Q_{66} \tag{1.19}$$

where $m = (1 - (Q_{12}.Q_{21})/(Q_{11}.Q_{22}))^{-1}$

We have seen three sets of material constants, any of which can completely describe the stiffness of on-axis unidirectional composites. The characteristics of each set is summarized in the following:

- Modulus is used to calculate the stress from the strain. This is the basic set needed for the stiffness of multidirectional laminates.
- Compliance is used to calculate the strain from the stress. This is the set needed for the calculation of engineering constants.

- Engineering constants are the carryover from the ordinary materials.

As stated earlier, from one set of constants we can readily find the other sets. They are all equivalent. There is a direct relationship between the modulus and compliance. One is the inverse of the other.

1.3.1.3 Symmetry Of Compliance and Modulus

The coupling components of compliance and those of modulus are equal, or in the terminology of matrix algebra, the compliance and modulus matrices are symmetric. Since the only coupling that we have seen thus far is the Poisson coupling, the symmetry condition states that the coupling components are equal, as follows:

$$S_{21} = S_{12}\,, \quad Q_{12} = Q_{21}$$

The validity of these equalities from the stored elastic energy in a body subjected to stress and strain can be demonstrated. Lets the stored energy at a point in the orthotropic body be

$$W = \tfrac{1}{2}[\, \sigma_x \varepsilon_x + \sigma_y \varepsilon_y + \tau_{xy} \gamma_{xy} \,] \tag{1.20}$$

From this definition we see

$$\frac{\partial W}{\partial \sigma_x} = \varepsilon_x, \quad \frac{\partial W}{\partial \sigma_y} = \varepsilon_y, \quad \frac{\partial W}{\partial \tau_{xy}} = \gamma_{xy} \tag{1.21}$$

Substituting the stress-strain relation from Table 2 into Eq. 1.20,

$$W = \tfrac{1}{2}[\, S_{11} \sigma_x^2 + \tfrac{1}{2}(S_{12}+S_{21})\, \sigma_x \sigma_y + S_{22} \sigma_y^2 + S_{66} \tau_{xy}^2 \,] \tag{1.22}$$

We will obtain the stress-strain relation by differentiation of this energy term in accordance with Eq. 1.22,

$$\varepsilon_x = S_{11}\,\sigma_x + \tfrac{1}{2}(S_{12} + S_{21})\,\sigma_y$$
$$\varepsilon_y = \tfrac{1}{2}(S_{12} + S_{21})\,\sigma_x + S_{22}\,\sigma_y \qquad (1.23)$$

Matching the like constants between this set and those in Table 2, the only condition that satisfies both sets is

$$S_{21} = S_{12} \qquad (1.24)$$

By substituting the modulus relations in Table 3 into Eq. 15 can also show that

$$Q_{12} = Q_{21} \qquad (1.25)$$

The last two equations state the symmetry conditions of the Poisson coupling. A similar symmetry condition can be applied to engineering constants. From Eq. 1.15, for example , we have

$$\nu_{LT}\,E_T = \nu_{TL}\,E_L \qquad (1.26)$$

With these symmetry conditions, the number of independent constants for the on-axis orthotropic unidirectional composite are reduced by one, from five to four in Table 1 to 3. If additional symmetry conditions exist, the number of constants can be further reduced.

In summary, the stress-strain relations which govern the stiffness of all materials have the identical form for unidirectional composites as for ordinary materials. No additional terms or more complex relationships exist. The only difference is the number of independent constants; four for composites versus two for ordinary

materials. Ordinary materials can be treated as special cases of composites.

1.3.2 Off-Axis Stiffness Of Unidirectional Composites

The stiffness of unidirectional composites with off-axis ply orientation are important because composite laminates normally consist of many off-axis plies in addition to on-axis plies. We must know how to determine the contribution to the laminate stiffness by each ply or ply assembly. We will need the transformation of modulus and compliance to determine the off-axis stiffness. These transformation relations can be formulated in terms of power functions, the multiple angle functions and the invariants. And they are called as the modulus transformation equations.

1.3.2.1 Off-Axis Modulus

In Fig. 1.8, the off-axis modulus can be determined in three steps in each of the following cases: the off-axis to on-axis strain transformation, and the inverse or the on-axis to off-axis stress transformation. This process is initiated by a given strain and led us eventually to the induced stress in Fig. 1.8(d). The off-axis compliance can be similarly derived in three steps. The purpose here is to derive the off-axis modulus and the off-axis stress-strain relation for this arbitrary angle of orientation. Then we can go directly from (a) to (d) in Fig. 1.8 in one step.These steps are shown in Fig. 1.8

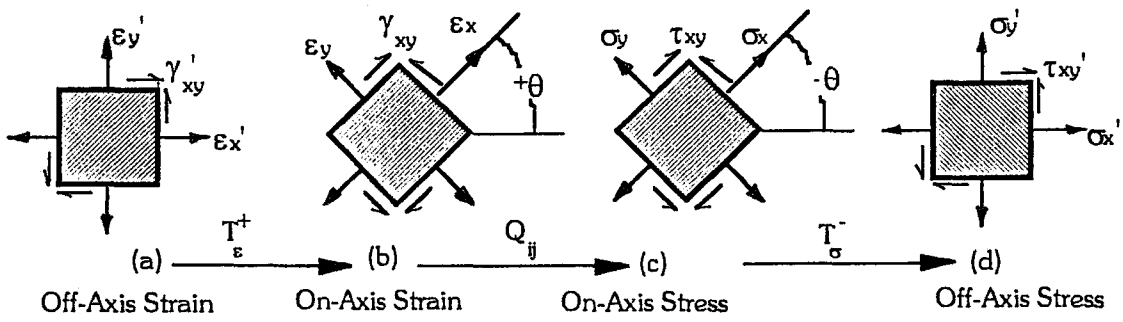

Figure 1.8. Determination of the off-axis modulus:

To go from (a) to (b), we need the strain transformation as follows:

$$\begin{aligned}\varepsilon_x &= m^2 \varepsilon_x' + n^2 \varepsilon_y' + mn\, \gamma_{xy}' \\ \varepsilon_y &= n^2 \varepsilon_x' + m^2 \varepsilon_y' - mn\, \gamma_{xy}' \\ \gamma_{xy} &= -2mn\, \varepsilon_x' + 2mn\, \varepsilon_y' + (m^2-n^2)\, \gamma_{xy}'\end{aligned} \tag{1.27}$$

To go from (b) to (c) in Fig. 1.8 , we need the on-axis, orthotropic stress-strain relation in modulus as listed in Table 3, which when combined with results in Eq. 1.27 produces:

$$\begin{aligned}\sigma_x &= Q_{11}(m^2 \varepsilon_x' + n^2 \varepsilon_y' + mn\, \gamma_{xy}') + Q_{12}(n^2 \varepsilon_x' + m^2 \varepsilon_y' - mn\, \gamma_{xy}') \\ &= (m^2Q_{11} + n^2Q_{12})\varepsilon_x' + (n^2Q_{11} + m^2Q_{12})\varepsilon_y' + (mnQ_{11} - mn\, Q_{12})\gamma_{xy}'\end{aligned} \tag{1.28}$$

similarly,

$$\sigma_y = (m^2Q_{12} + n^2Q_{22})\varepsilon_x' + (n^2Q_{12} + m^2Q_{22})\varepsilon_y' + (mnQ_{12} - mn\, Q_{22})\gamma_{xy}' \tag{1.29}$$

$$\tau_{xy} = -2mnQ_{66}\varepsilon_x' + 2mnQ_{66}\varepsilon_y' + (m^2-n^2)Q_{66}\gamma_{xy}' \tag{1.30}$$

To go from (c) to (d) in Fig. 1.8, we need inverse or negative stress transformation. The angle of rotation is now negative, however, and the primed

and the unprimed are interchanged. The unprimed is now the old (before transformation), and the primed is now the new (after transformation).

$$\begin{aligned}\sigma_x' &= Q_{11}'\varepsilon_x' + Q_{12}'\varepsilon_y' + Q_{16}'\gamma_{xy}' \\ \sigma_y' &= Q_{21}'\varepsilon_x' + Q_{22}'\varepsilon_y' + Q_{26}'\gamma_{xy}' \\ \tau_{xy}' &= Q_{61}'\varepsilon_x' + Q_{62}'\varepsilon_y' + Q_{66}'\gamma_{xy}'\end{aligned} \tag{1.31}$$

This is the off-axis stress-strain relation that directly relates the given strain in Fig. 1.8(a) to the resulting stress in 1.8(d), and re drawn in Fig. 1.9. This relation can also be arranged in a matrix multiplication table as follows:

Table 4. OFF-AXIS STRESS-STRAIN RELATION FOR UNIDIRECTIONAL COMPOSITES IN TERMS OF MODULUS

	ε_x'	ε_y'	γ_{xy}'
σ_x'	Q_{11}'	Q_{12}'	Q_{16}'
σ_y'	Q_{21}'	Q_{22}'	Q_{26}'
τ_{xy}'	Q_{61}'	Q_{62}'	Q_{66}'

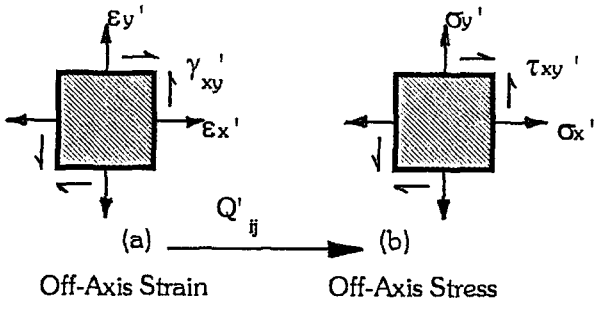

Figure 1.9. The off-axis stress-strain relations in modulus.

Since the choice of the primed and unprimed notation is arbitrary, this table remains valid if all primes are eliminated. Then the relation applies to the unprimed coordinates shown in Fig. 1.10.

We have merged the three steps in Fig. 1.8 into one. The relationship remains valid if all primes are omitted in Fig. 1.9. This new unprimed applies to the coordinates of Fig. 1.10.

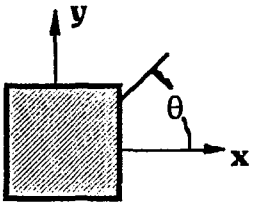

Figure 1.10. A new, unprimed coordinate system.

Unprimed coordinates are now the off-axis configuration. The major difference between the on-axis stress-strain relation in Table 3 and the off-axis relation in Table 4 lies in the additional components in the modulus. Those terms with the subscripts 16 and 26 are shear coupling terms that relate the shear strain to normal stress, or normal strain to shear stress. Such coupling does not exist in ordinary materials, or in unidirectional composites in their on-axis orientation. Geometric illustration of the shear coupling effects will be done when we develop the generally orthotropic compliance. Symmetry of these components can also be demonstrated in a manner similar to that used for the Q_{12} component in the previous section. The strored energy in Eq. 1.22 must contain interaction terms of $\sigma_x\tau_{xy}$ and $\sigma_y\tau_{xy}$, or their equivalent strain components $\varepsilon_x\gamma_{xy}$ and $\varepsilon_y\gamma_{xy}$.

The relationship between the modulus components of the on-axis and the off-axis orientations can be summarized in Table 5, where matrix multiplication is implied. These relations result from the derivation of Eq. 1.31. These relations are limited to transformation from the on-axis, orthotropic orientation where

shear coupling components are zero. Q_{16} and Q_{26} do not appear as column headings in this table.*

Table 5. TRANSFORMATION OF MODULUS FROM ON-AXIS UNIDIRECTIONAL COMPOSITES IN POWER FUNCTIONS

	Q_{11}	Q_{22}	Q_{12}	Q_{66}
Q_{11}'	m^4	n^4	$2m^2n^2$	$4m^{2\,2}$
Q_{22}'	n^4	m^4	$2m^2n^2$	$4m^2n^2$
Q_{12}'	m^2n^2	m^2n^2	m^4+n^4	$-4m^2n^2$
Q_{66}'	m^2n^2	m^2n^2	$-2m^2n^2$	m^2-n^2
Q_{16}'	m^3n	$-mn^3$	mn^3-m^3n	$2(mn^3-m^3n)$
Q_{26}'	mn^3	$-mn^3$	m^3n-mn^3	$2(m^3n-mn^3)$

$m = \cos\theta, \quad n = \sin\theta$

Apparently, all the sums of exponents of the trigonometric functions in this table are in the fourth power which are by definition characteristic of the 4th rank tensor. The stress transformation equations are governed by the 2nd power functions and belong to the 2nd rank tensor . The strain transformation equations are also governed by 2nd power functions, but are different from those for stress because engineering shear strain is used which is twice the tensorial shear strain.

The critical issue again is the sign convention. The angle used in this table is the ply orientation. Because of its importance, Fig. 1.10 is shown here again for emphasis. Although the primed versus unprimed coordinates may be interchanged from situation, it is imperative that the sign convention is clearly

*If the transformation is from one off-axis orientation to another, additional columns for Q_{16} and Q_{26} must be present.

understood. For unidirectional composites, the on-axis, orthotropic, and material symmetry axes coincide. We normally use the unprimed axes to denote this configuration. The off-axis, generally orthotropic configuration refers to ply orientations other than 0° or
90° degrees. We normally use the primed axes for the off-axis situation. This is shown in Fig. 1.11(a).

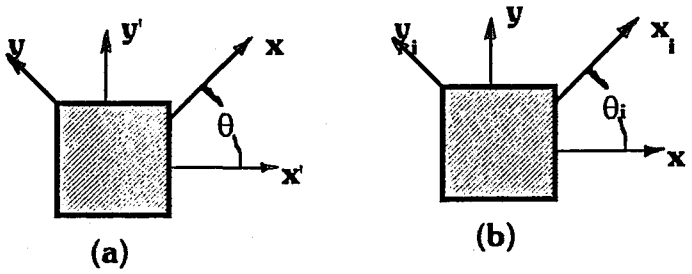

Figure 1.11. Positive ply orientation.

The notation for unidirectional composites normally follows that in Fig. 11(a) and that for multidirectional composites, in Fig. 1.11(b). Where θ_i is the orientation of the i-th ply or ply assembly, primes have been deleted

A multiple-angle formulation for the modulus transformation can be further developed in place of the power functions in Table 5. This process can be done directly by substituting the following trigonometric identities into Table 5.

$$
\begin{aligned}
m^4 &= (3 + 4\cos2\theta + \cos4\theta) / 8 \\
m^3n &= (2\sin2\theta + \sin4\theta) / 8 \\
m^2n^2 &= (1 - \cos4\theta) / 8 \\
mn^3 &= (2\sin2\theta - \sin4\theta) / 8 \\
n^4 &= (3 - 4\cos2\theta + \cos4\theta) / 8
\end{aligned}
\qquad (1.32)
$$

Substitution of values from Eq. 1.32 into Table 5 we get:

$$
\begin{aligned}
Q_{11}' &= m^4Q_{11} + n^4Q_{22} + 2m^2n^2 (Q_{12} + 2Q_{66}) \\
&= (3 + 4\cos2\theta + \cos4\theta)\ Q_{11} / 8 + (3 - 4\cos2\theta + \cos4\theta)\ Q_{22} / 8
\end{aligned}
$$

$$
\begin{aligned}
&+ \tfrac{1}{4}(1 - \cos 4\theta)(Q_{12} + 2Q_{66}) \\
&= (3Q_{11} + 3Q_{22} + 2Q_{12} + 4Q_{66}) / 8 + \tfrac{1}{2}(Q_{11} - Q_{22}) \cos 2\theta \\
&\quad + (Q_{11} + Q_{22} - 2Q_{12} - 4Q_{66}) \cos 4\theta / 8 \\
&= U_1 + U_2 \cos 2\theta + U_3 \cos 4\theta
\end{aligned} \tag{1.33}
$$

We can repeat the process for the other five components of the off-axis modulus and list the results in Table 6 in matrix multiplication format and using the following definitions of the linear combinations of modulus U_i:

$$
\begin{aligned}
U_1 &= (3Q_{11} + 3Q_{22} + 2Q_{12} + 4Q_{66}) / 8 \\
U_2 &= (Q_{11} - Q_{22}) / 2 \\
U_3 &= (Q_{11} + Q_{22} - 2Q_{12} - 4Q_{66}) / 8 \\
U_4 &= (Q_{11} + Q_{22} + 6Q_{12} - 4Q_{66}) / 8 \\
U_5 &= (Q_{11} + Q_{22} - 2Q_{12} + 4Q_{66}) / 8
\end{aligned} \tag{1.34}
$$

Table 6. TRANSFORMED MODULUS FROM ON-AXIS UNIDIRECTIONAL COMPOSITES IN MULTIPLE-ANGLE FUNCTIONS

	1	U_2	U_3
Q'_{11}	U_1	$\cos 2\theta$	$\cos 4\theta$
Q'_{22}	U_1	$-\cos 2\theta$	$\cos 4\theta$
Q'_{12}	U_4	0	$-\cos 4\theta$
Q'_{66}	U_5	0	$-\cos 4\theta$
Q'_{16}	0	$\frac{1}{2} \sin 2\theta$	$\sin 4\theta$
Q'_{26}	0	$\frac{1}{2} \sin 2\theta$	$-\sin 4\theta$

CHAPTER 2

INTRODUCTION

2.1. DEFINITION OF THE PROBLEM

The problem is to investigate stress distributions and stress concentration factors in a simple beam with a circular hole. The centre of the hole is located on the transverse axis of the beam at several distances from the longitudinal axis. The portion of the beam between the points of application of the forces is subjected to pure bending.

The beam investigated is shown in Fig 2.1

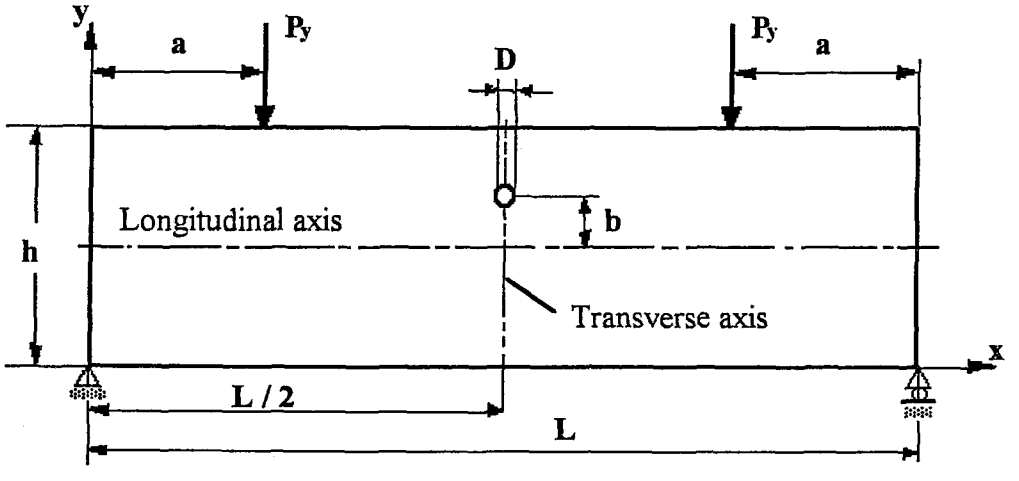

Figure 2.1 The Beam With A Hole

In the present study, the thickness, height and length of the beam are defined by ***t***, ***h***, and ***L*** ,respectively. The beam analysed is subjected to two vertical shearing force ***Py***. The general orthotropic configuration occurs in a composite beam in cases where the reinforcing angle is different from 0° or 90°. And the stress distribution is not symmetrical in such cases. Therefore the entire beam is considered throughout this study for the analysis of stress distribution in both steel and composite beams with any reinforcing angle.

2.2. METHOD AND PROCEDURE

2.2.1 Finite Element Method

Lets consider a spring element shown in Fig. 2.2. The relation between force and displacement in spring is given by

$$\mathbf{P = k.x} \tag{2.1}$$

Here, **P**, **x**, and **k** represent force, displacement, and spring constant, respectively.

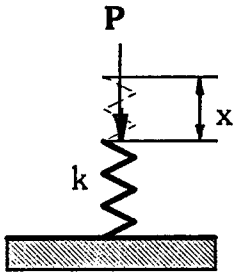

Figure 2.2. A spring element

Eq. 2.1 is valid not only for a spring element but also for a spring system. For spring system Eq. 2.1 becomes

$$\mathbf{f} = \mathbf{D}.\mathbf{q} \tag{2.2}$$

Here, **f** is the force vector and **q** is the displacement vector. They are given by

$$\begin{aligned} \mathbf{f} &= [\, F_1, F_2, \ldots\ldots, F_n]^T \\ \mathbf{q} &= [\, q_1, q_2, \ldots\ldots, q_n]^T \end{aligned} \tag{2.3}$$

D is a stiffness matrix in (n x n) dimensions.

Using above approach, we can form **f** and **D** matrices for any element by subdividing it into many elements.

2.2.1.1 Displacement Evaluation

Lets multiply both sides of Eq. 2.2 by the inverse of **D**.

$$[\mathbf{D}]^{-1}.\mathbf{f} = [\mathbf{D}]^{-1}.[\mathbf{D}].\mathbf{q} \tag{2.4}$$

Since $[\mathbf{D}]^{-1}.[\mathbf{D}]$ is equal to identity matrix I and recalling that multiplying any matrix by identity matrix I will not change result, we can write,

$$\mathbf{q} = [\mathbf{D}]^{-1}.\mathbf{f} \tag{2.5}$$

Obtaining the displacements is realised in the following three steps:

1. Forming the stiffness matrix **D**,
2. Finding the inverse of **D**,
3. Multiplying the result by the force vector **f**.

Matrix **D** is determined depending upon the element characteristics. In order to take the inverse of matrix **D**, boundary conditions should be applied.

2.2.1.2 Stress Calculation

Hooke's law is valid for small displacements. It is given by;

$$\sigma = \mathbf{E}\varepsilon \tag{2.6}$$

Here, σ, **E**, and ε represent stress, modulus of elasticity, and strain, respectively. We can write Eq. 2.6 in matrix form

$$\sigma = \mathbf{D}\varepsilon \tag{2.7}$$

Here, σ is the stress vector and ε is the strain vector. For two-dimensional problem they are given by

$$\begin{aligned} \sigma &= [\, \sigma_x, \sigma_y, \tau_{xy} \,]^T \\ \varepsilon &= [\, \varepsilon_x, \varepsilon_y, \gamma_{xy} \,]^T \end{aligned} \tag{2.8}$$

D is a stiffness matrix in (3 x 3) dimensions for two-dimensional problems.

Relation between the strain and the displacement is given by

$$\varepsilon = \mathbf{B}\mathbf{q} \tag{2.9}$$

Here, **q** is the nodal displacement vector and **B** is the transformation matrix. Substituting Eq. 2.9 into Eq. 2.7 we get

$$\sigma = \mathbf{D}\mathbf{B}\mathbf{q} \tag{2.10}$$

where σ is the stress vector and **q** is the element nodal displacement vector within an element.

In this procedure, both definition of **D** and evaluating **B** matrices show differences depending on chosen finite element. They will be mentioned in the following sections.

In the two-dimensional finite element formulation, the displacements, traction components, and distributed body force values are the functions of the position indicated by (x,y).The displacement vector **u** is given as

$$\mathbf{u} = [\, u,\, v \,]^T \tag{2.11}$$

where u and v are the x and y components of u, respectively. From Fig. 2.3, representing the two-dimensional problem in a general setting, the body force, traction vector, and elemental volume are given by

$$\mathbf{f} = [\, f_x\,,\, f_y \,]^T \qquad \mathbf{T} = [\, T_x\,,\, T_y \,]^T \qquad \text{and} \qquad dV = t\,dA \tag{2.12}$$

where t is the thickness along the z direction. The body force **f** has dimensions of force per unit volume, while the traction force **T** has dimensions of force per unit area. The strain-displacement relations are given by

$$\boldsymbol{\varepsilon} = \left[\, \frac{\partial u}{\partial x},\ \frac{\partial v}{\partial y},\ \frac{\partial u}{\partial y} + \frac{\partial v}{\partial x} \,\right]^T \tag{2.13}$$

Stresses and strain are related by (see Eq. 1.18)

$$\boldsymbol{\sigma} = \mathbf{D}\boldsymbol{\varepsilon} \tag{2.14}$$

The region is discretized with the idea of expressing the displacements in terms of values at discrete points.

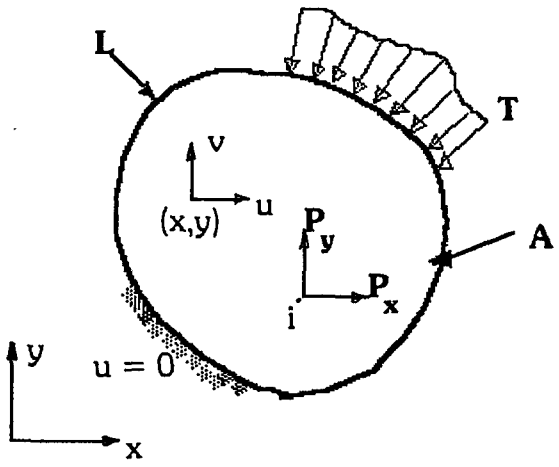

t : thickness at (x,y)

fx , fy: body force components per unit volume at (x,y)

Figure 2.3 Two-dimensional problem

2.2.2. Finite Element Modelling

In this section, we develop what are popularly called *isoparametric* elements for our problem and apply them to stress analysis. The two-dimensional four-node quadrilateral element is used in this study. The process in isoparametric elements consists of deriving shape functions at first and then generating the element stiffness matrix using numerical integration.

2.2.3 The Four-Node Quadrilateral

Consider the general quadrilateral element shown in Fig. 2.4. The local nodes are numbered as 1, 2, 3, and 4 in a *counter clockwise* fashion as shown, and (x_i, y_i) are the coordinates of node *i*. The vector $\mathbf{q} = [\, q_1, q_2, \ldots\ldots, q_8 \,]^T$ denotes the element displacement vector. The displacement of an interior point *P* located at (x,y) is represented as

$$\mathbf{u} = [\, u(x,y), v(x,y) \,]^T.$$

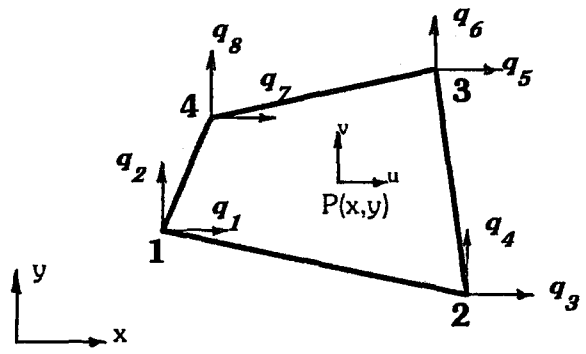

Figure 2.4 Four-node quadrilateral element

2.2.3.1 Shape Functions

Lets develop the shape functions on a master element, shown in Fig. 2.4. The master element is defined in r, s coordinates (or natural coordinates), and is square shaped. The Lagrange shape functions N_i, where i = 1, 2, 3, 4, are defined such that N_i is equal to unity at node i and is zero at other nodes. In particular, consider the definition of N_1:

$$N_1 = 1 \quad \text{at node 1}$$
$$N_1 = 0 \quad \text{at nodes 2, 3, 4} \tag{2.15}$$

Now, the requirement that $N_1 = 0$ at nodes 2, 3, and 4 is equivalent to requiring that $N_1 = 0$ along edges r = +1 and s = +1 (Fig. 2.5). Thus, N_1 has to be of the form

$$N_1 = c\,(1 - r)(1 - s) \tag{2.16}$$

where c is some constant. The constant is determined from the condition $N_1 = 1$ at node 1. Since r = -1, s = -1 at node 1, we have $1 = c\,(2)(2)$ which yields $c = 1/4$. Thus,

$$N_1 = \tfrac{1}{4}(1 - r)(1 - s) \tag{2.17}$$

All the shape functions can be written as

$$N_1 = \tfrac{1}{4}(1 - r)(1 - s)$$
$$N_2 = \tfrac{1}{4}(1 + r)(1 - s)$$
$$N_3 = \tfrac{1}{4}(1 + r)(1 + s) \qquad (2.18)$$
$$N_4 = \tfrac{1}{4}(1 - r)(1 + s)$$

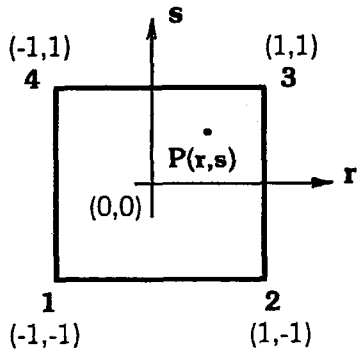

Figure 2.5 The quadrilateral element in r, s space

While implementing in a computer program, the following compact representation of Eq. 2.18 is useful:

$$N_i = \tfrac{1}{4}(1 - r\, r_i)(1 + s\, s_i) \qquad (2.19)$$

where (r_i, s_i) are the natural coordinates of node *i*.

We now express the displacement field within the element in terms of the nodal values. Thus, if $\mathbf{u} = [u, v]^T$ represents the displacement components of a point located at (r, s), and $\mathbf{q}$, dimension (8 x 1), is the element displacement vector, then

$$u = N_1 q_1 + N_2 q_3 + N_3 q_5 + N_4 q_7$$
$$v = N_1 q_2 + N_2 q_4 + N_3 q_6 + N_4 q_8 \qquad (2.20a)$$

Which can be written in matrix form as

$$\mathbf{u} = \mathbf{N}\mathbf{q} \tag{2.20b}$$

where

$$\mathbf{N} = \begin{bmatrix} N_1 & 0 & N_2 & 0 & N_3 & 0 & N_4 & 0 \\ 0 & N_1 & 0 & N_2 & 0 & N_3 & 0 & N_4 \end{bmatrix} \tag{2.21}$$

In the isoparametric formulation, we use the same shape functions N_i to also express the coordinates of a point within the element in terms of nodal coordinates. Thus,

$$\begin{aligned} x &= N_1x_1 + N_2x_2 + N_3x_3 + N_4x_4 \\ y &= N_1y_1 + N_2y_2 + N_3y_3 + N_4y_4 \end{aligned} \tag{2.22}$$

Subsequently, we will need to express the derivatives of a function in x, y coordinates in terms of its derivatives in r, s coordinates. This is done as follows. A function

$f = f(x,y)$, in view of Eqs. 2.22, can be considered to be implicit function of r and s as $f = f[x(r,s),y(r,s)]$. Using the chain rule of differentiation, we have

$$\begin{aligned} \frac{\partial f}{\partial r} &= \frac{\partial f}{\partial x}\frac{\partial x}{\partial r} + \frac{\partial f}{\partial y}\frac{\partial y}{\partial r} \\ \frac{\partial f}{\partial s} &= \frac{\partial f}{\partial x}\frac{\partial x}{\partial s} + \frac{\partial f}{\partial y}\frac{\partial y}{\partial s} \end{aligned} \tag{2.23}$$

or

$$\begin{Bmatrix} \frac{\partial f}{\partial r} \\ \frac{\partial f}{\partial s} \end{Bmatrix} = \mathbf{J} \begin{Bmatrix} \frac{\partial f}{\partial x} \\ \frac{\partial f}{\partial y} \end{Bmatrix} \tag{2.24}$$

where **J** is the Jacobean matrix

$$\mathbf{J} = \begin{bmatrix} \dfrac{\partial x}{\partial r} & \dfrac{\partial y}{\partial r} \\ \dfrac{\partial x}{\partial s} & \dfrac{\partial y}{\partial s} \end{bmatrix} \tag{2.25}$$

In view of Eqs. 2.18 and 2.22, we have

$$\mathbf{J} = \begin{bmatrix} J_{11} & J_{12} \\ J_{21} & J_{22} \end{bmatrix} \tag{2.26a}$$

$$\begin{aligned} J_{11} &= \tfrac{1}{4}[-(1-s)x_1 + (1-s)x_2 + (1+s)x_3 - (1+s)x_4] \\ J_{12} &= \tfrac{1}{4}[-(1-s)y_1 + (1-s)y_2 + (1+s)y_3 - (1+s)y_4] \\ J_{21} &= \tfrac{1}{4}[-(1-r)x_1 + (1+r)x_2 + (1+r)x_3 + (1-r)x_4] \\ J_{22} &= \tfrac{1}{4}[-(1-r)y_1 + (1+s)y_2 + (1+r)y_3 + (1-r)y_4] \end{aligned} \tag{2.26b}$$

Equation 2.24 can be inverted as

$$\begin{Bmatrix} \dfrac{\partial f}{\partial x} \\ \dfrac{\partial f}{\partial y} \end{Bmatrix} = \mathbf{J}^{1} \begin{Bmatrix} \dfrac{\partial f}{\partial r} \\ \dfrac{\partial f}{\partial s} \end{Bmatrix} \tag{2.27a}$$

or

$$\begin{Bmatrix} \dfrac{\partial f}{\partial x} \\ \dfrac{\partial f}{\partial y} \end{Bmatrix} = \frac{1}{\det \mathbf{J}} \begin{bmatrix} J_{22} & -J_{12} \\ -J_{21} & J_{11} \end{bmatrix} \begin{Bmatrix} \dfrac{\partial f}{\partial r} \\ \dfrac{\partial f}{\partial s} \end{Bmatrix} \tag{2.27b}$$

The expressions will be used in the derivation of the element stiffness matrix.

An additional result that will be needed is the relation

$$dx\,dy = \det \mathbf{J}\; dr\,ds \tag{2.28}$$

2.2.3.2 Element Stiffness Matrix

The stiffness matrix for the quadrilateral element can be derived from the strain energy in the body, given by

$$U = \int_V \tfrac{1}{2}\sigma^T \varepsilon\, dV \tag{2.29}$$

or

$$U = \sum_e t_e \int_e \tfrac{1}{2}\sigma^T \varepsilon\, dA \tag{2.30}$$

where t_e is the thickness of element e.

The strain-displacement relations are

$$\varepsilon = [\,\varepsilon_x, \varepsilon_y, \gamma_{xy}\,]^T = \begin{bmatrix} \dfrac{\partial u}{\partial x}, & \dfrac{\partial v}{\partial y}, & \dfrac{\partial u}{\partial y} + \dfrac{\partial v}{\partial x} \end{bmatrix}^T \tag{2.31}$$

By considering $f \equiv u$ in Eq. 2.27b, we have

$$\begin{Bmatrix} \dfrac{\partial u}{\partial x} \\ \dfrac{\partial u}{\partial y} \end{Bmatrix} = \frac{1}{\det \mathbf{J}} \begin{bmatrix} J_{22} & -J_{12} \\ -J_{21} & J_{11} \end{bmatrix} \begin{Bmatrix} \dfrac{\partial u}{\partial r} \\ \dfrac{\partial u}{\partial s} \end{Bmatrix} \tag{2.32a}$$

Similarly

$$\begin{Bmatrix} \frac{\partial v}{\partial x} \\ \frac{\partial v}{\partial y} \end{Bmatrix} = \frac{1}{\det \mathbf{J}} \begin{bmatrix} J_{22} & -J_{12} \\ -J_{21} & J_{11} \end{bmatrix} \begin{Bmatrix} \frac{\partial v}{\partial r} \\ \frac{\partial v}{\partial s} \end{Bmatrix} \tag{2.32b}$$

Equations 2.31 and 2.32a,b yield

$$\varepsilon = \mathbf{A} \begin{bmatrix} \frac{\partial u}{\partial r}, \frac{\partial u}{\partial s}, \frac{\partial v}{\partial r}, \frac{\partial v}{\partial s} \end{bmatrix}^T \tag{2.33}$$

Where **A** is given by

$$\mathbf{A} = \frac{1}{\det \mathbf{J}} \begin{bmatrix} J_{11} & -J_{11} & 0 & 0 \\ 0 & 0 & -J_{21} & J_{11} \\ -J_{21} & J_{11} & J_{11} & -J_{11} \end{bmatrix} \tag{2.34}$$

Now, from the interpolation equations Eq. 2.20a, we have

$$\begin{bmatrix} \frac{\partial u}{\partial r}, \frac{\partial u}{\partial s}, \frac{\partial v}{\partial r}, \frac{\partial v}{\partial s} \end{bmatrix}^T = \mathbf{Gq} \tag{2.35}$$

Where

$$\mathbf{G} = \tfrac{1}{4}\begin{bmatrix} -(1-s) & 0 & (1-s) & 0 & (1+s) & 0 & -(1+s) & 0 \\ 0 & -(1-s) & 0 & (1-s) & 0 & (1+s) & 0 & -(1+s) \\ -(1-r) & 0 & -(1+r) & 0 & (1+r) & 0 & (1-r) & 0 \\ 0 & -(1-r) & 0 & -(1+r) & 0 & (1+r) & 0 & (1-r) \end{bmatrix} \quad (2.36)$$

Equations 2.33 and 2.35 now yield

$$\varepsilon = \mathbf{Bq} \quad (2.37)$$

Where

$$\mathbf{B} = \mathbf{AG} \quad (2.38)$$

The relation $\varepsilon = \mathbf{Bq}$ is the desired result. The strain in the element is expressed in terms of its nodal displacements. The stress is now given by

$$\sigma = \mathbf{DBq} \quad (2.39)$$

Where D is a (3x3) material matrix. The strain energy in Eq. 2.30 becomes

$$U = \sum_e \tfrac{1}{2}\mathbf{q}^T \begin{bmatrix} t_e \int_{-1}^{1}\int_{-1}^{1} \mathbf{B}^T\mathbf{D}\mathbf{B}\,\det\mathbf{J}\,dr\,ds \end{bmatrix} \mathbf{q} \quad (2.40a)$$

$$U = \sum_e \tfrac{1}{2}\mathbf{q}^T\mathbf{k}^e\mathbf{q} \quad (2.40b)$$

where

$$\mathbf{k}^e = t_e \int_{-1}^{1}\int_{-1}^{1} \mathbf{B}^T\mathbf{D}\mathbf{B}\,\det\mathbf{J}\,dr\,ds \quad (2.41)$$

is the element stiffness matrix of dimension (8 x 8).

We note here that quantities **B** and det**J** in the above integral are involved functions of r and s, and so the integration has to be performed numerically. Numerical method chosen in this study is given subsequently.

2.2.3.3 Element Force Vectors

Here, we do not treat body force and traction force due to loading configuration since our study sample is subjected only to point loads. Point loads are considered in the usual manner by having a structural node at that point and simply adding them to the global load vector **F**.

2.2.4. Numerical Integration

Consider the problem of numerically evaluating a one-dimensional integral of the form

$$I = \int_{-1}^{1} f(r)\, dr \tag{2.42}$$

The *Gaussian quadrature* approach for evaluating I is given below. This method has proved most useful in finite element work. Extension to integrals in two-dimensions follows readily.

Consider the *n*-point approximation

$$I = \int_{-1}^{1} f(r)\,dr - w_1 f(r_1) + w_2 f(r_2) + \ldots\ldots\ldots + w_n f(r_n) \qquad (2.43)$$

where $w_1, w_2, \ldots\ldots, w_n$ are the **weights** and $r_1, r_2, \ldots\ldots, r_n$ are the sampling points or **Gauss points**. The idea behind Gaussian quadrature is to select the n Gauss points and n weights such that Eq. 2.43 provides an exact answer for polynomials $f(r)$ of as large a degree as possible. In other words, the idea is that if the n-point integration formula is exact for all polynomials up to as high a degree as possible, then the formula will work well even if f is not a polynomial. To get some intuition for the method, the one-point and two point approximations are given below.

2.2.4.1 One-point formula

Consider the formula with $n = 1$ as

$$I = \int_{-1}^{1} f(r)\,dr \cong w_1 f(r_1) \qquad (2.44)$$

Since there are two parameters, w_1 and r_1, we consider requiring the formula in Eq. 2.44 to be exact when $f(r)$ is a polynomial of order one. Thus, if $f(r) = a_0 + a_1 r$ then we require

$$\text{Error} = \int_{-1}^{1} (a_0 + a_1 r)\,dr - w_1 f(r_1) = 0 \qquad (2.45a)$$

$$\text{Error} = 2a_0 - w_1(a_0 + a_1 r_1) = 0 \qquad (2.45b)$$

$$\text{Error} = a_0(2 - w_1) - w_1 a_1 r_1 = 0 \tag{2.45c}$$

From Eq. 2.45c, we see that the error is zeroed if

$$w_1 = 2\,, \quad r_1 = 0 \tag{2.46}$$

For any general f, then, we have

$$I = \int_{-1}^{1} f(r)\, dr \cong 2f(0) \tag{2.47}$$

which is seen to be familiar *midpoint rule.*

2.2.4.2 Two-point formula

Consider the formula with $n = 2$ as

$$I = \int_{-1}^{1} f(r)dr \cong w_1 f(r_1) + w_2 f(r_2) \tag{2.48}$$

We have two parameters to choose: w_1, w_2, r_1, and r_2. We can therefore expect the formula in Eq. 2.49 to be exact for a cubic polynomial. Thus, choosing $f(r) = a_0 + a_1 r + a_2 r^2 + a_3 r^3$ yields

$$\text{Error} = \int_{-1}^{1} (a_0 + a_1 r + a_2 r^2 + a_3 r^3)dr - [w_1 f(r_1) + w_2 f(r_2)] \tag{2.49}$$

Requiring zero error yields

$$\begin{aligned} w_1 + w_2 &= 2 \\ w_1 r_1 + w_2 r_2 &= 0 \\ w_1 r_1^2 + w_2 r_2^2 &= 2/3 \\ w_1 r_1^3 + w_2 r_2^3 &= 0 \end{aligned} \tag{2.50}$$

TABLE 7. GAUSS POINTS AND WEIGHTS FOR GAUSSIAN QUADRATURE

$$I = \int_{-1}^{1} f(r)\, dr \cong \sum_{i=1}^{n} w_i f(r_i)$$

# of points, n	Location, r_i	Weights, w_i
1	0.0	2.0
2	$1/\sqrt{3} = 0.5773502962$	1.0
3	0.7745966692	0.5555555556
	0.0	0.8888888889
4	0.8611363116	0.3478548451
	0.3399810436	0.6521451549
5	0.9061798459	0.2369268851
	0.5384693101	0.4786286705
	0.0	0.5688888889
6	0.9324695142	0.1713244924
	0.6612093865	0.3607615730
	0.2386191861	0.4679139346

These non-linear equations have the unique solution

$$w_1 = w_2 = 1 \quad -r_1 = r_2 = 1/\sqrt{3} = 0.5773502691.. \tag{2.51}$$

From above, we conclude that n-point Gaussian quadrature will provide an exact answer if f is a polynomial of order $(2n - 1)$ or less. Table 7 gives the values of w_i and r_i for Gauss quadrature formulas of orders $n = 1$ to $n = 6$. Note that the Gauss points are located symmetrically with respect to origin, and that symmetrically placed points have the same weights. Moreover, the large number of digits given in Table 7 should be used in the calculations for accuracy; i.e., use double precision on the computer.

2.2.4.3 Two-Dimensional Integrals

The extension of Gaussian quadrature to two-dimensional integrals of the form

$$I = \int_{-1}^{1} \int_{-1}^{1} f(r, s)\, dr\, ds \tag{2.52}$$

follows readily, since

$$I = \int_{-1}^{1} \left[\sum_{i=1}^{n} w_i f(r_i, s) \right] ds$$

$$I \approx \sum_{j=1}^{n} w_j \left[\sum_{i=1}^{n} w_i f(r_i, s_i) \right]$$

or

$$I \approx \sum_{i=1}^{n} \sum_{j=1}^{n} w_i w_j f(r_i, s_j) \tag{2.53}$$

2.2.5. Stiffness Integration

To illustrate the use of Eq. 2.53, consider the element stiffness for a quadrilateral element

$$\mathbf{k}^e = t_e \int_{-1}^{1} \int_{-1}^{1} \mathbf{B}^T\mathbf{D}\mathbf{B}\, \det\mathbf{J}\, dr\, ds$$

where **B** and det**J** are functions of r and s. Note that the integral above actually consists of the integral of each element in an (8 x 8) matrix. However, using the

fact that $\mathbf{k}^e$ is symmetric, we do not need to integrate elements below the main diagonal.

Let F represent the ijth element in the integrand. That is,

$$F(r,s) = t_e(\mathbf{B}^T\mathbf{D}\mathbf{B}\ \det\mathbf{J})_{ij} \tag{2.54}$$

Then, if we use a *2 x 2 rule*, we get

$$\boldsymbol{k}_{ij} \approx w_1^2 F(r_1,s_1) + w_1 w_2 F(r_1,s_2) + w_2 w_1 F(r_2,s_1) + w_2^2 F(r_2,s_2) \tag{2.55a}$$

where $w_1=w_2=1.0$, $r_1=s_1=-0.57735..$, and $r_2=s_2=+0.57735$. The Gauss points for the two-point rule used above are shown in Fig. 2.6. Alternatively, if we label the Gauss points as 1, 2, 3, and 4, then $\boldsymbol{k}_{ij}$ in Eq. 2.55a can also be written as

$$\boldsymbol{k}_{ij} = \sum_{IP=1}^{4} W_{IP} F_{IP} \tag{2.55b}$$

where F_{IP} is the value of F and W_{IP} is the weight factor at integration point IP. We note that $W_{IP} = (1)(1) = 1$. Computer implementation is sometimes easier using Eq. 2.55b. We may readily follow the implementation of the above integration procedure in our program SOLVCZ.BAS.

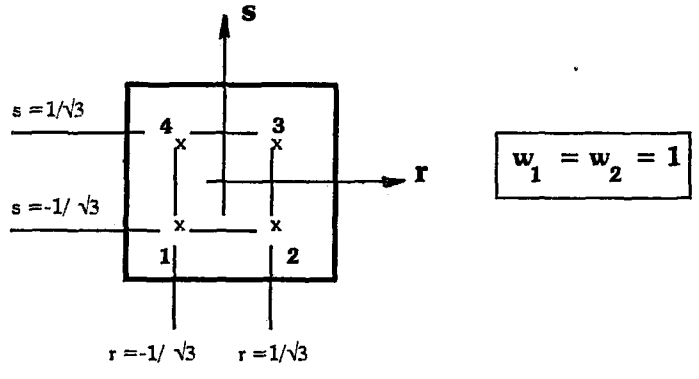

Figure 2.6 Gaussian quadrature in two-dimensions using the 2x2 rule

2.2.6. Stress Calculation

The stresses $\sigma = \mathbf{DBq}$ in the quadrilateral element are not constant within the element; they are functions of r, s and consequently vary within the element. In practise, the stresses are evaluated at the Gauss points. They are also the points used for numerical evaluation of $\mathbf{k}^e$, where they are found to be accurate. For a quadrilateral with 2x2 integration, this gives four sets of stress values. This approach is used in SOLVCZ.BAS.

2.2.7. Calculation of Stress Concentration Factor

Beams are slender members that are used for supporting transverse loading. Long horizontal members used in buildings, bridges, and shafts supported in bearings are some examples of beams. Beams with cross sections that are symmetric with respect to plane of loading are considered in our problem. For small deflections, we recall from elementary beam theory that

$$\sigma = \frac{-M}{I} y \tag{2.56}$$

where σ is the normal stress, M is the bending moment at the section, and I is the moment of inertia of the section about the neutral axis (z axis passing through the centroid). y is the distance from the neutral axis. To determine y within the finite element we can also use Lagrangian Eqs. (Eq. 2.18).

$$y = N_1 y_1 + N_2 y_2 + N_3 y_3 + N_4 y_4 \tag{2.57}$$

For rectangular cross section the moment of inertia is given by

$$I = \frac{th^3}{12} \tag{2.58}$$

In the above equation t and h are the thickness and height of the beam, respectively.

We define the stress concentration factor SCF at any point along the transverse axis and all around the circular hole as following :

$$SCF = \frac{\sigma_1}{\sigma_{xth}} \tag{2.59}$$

Here σ_1 is the greatest absolute principle stress at the point considered and σ_{xth} is the stress evaluated from elementary beam theory at the same point. On calculating σ_{xth}, we assume that the beam has no hole.

2.2.8. Positioning of Local Coordinates

The element connectivity numbers for master element shown in Fig. 2.5 are in order 1, 2, 3, and 4. 1-2 direction is parallel to r axis and 2-3 direction is parallel to s axis. 1-2 and 2-3 directions indicate $+r$ and $+s$ directions, respectively. By this definition we can determine locations of the Gauss points exactly. For instance, lets find the local coordinates in elements #225 and #236 shown in Fig. 2.7a. Element connectivity numbers are

for the element #225 271, 272, 284, 283

for the element #236 273, 274, 283, 284

Using same approach explained above, direction 271-272 and direction 272-284 show +r and +s directions, respectively. Direction 273-274 and direction 274-

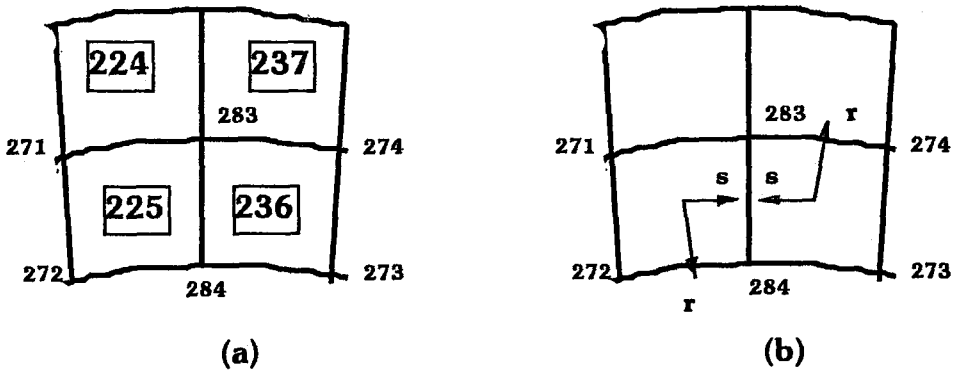

Figure 2.7 Sample problem for positioning of local coordinates

2.2.9 Mesh Generation

The plane domain of the problem is subdivided into four-node quadrilateral finite elements. The basic idea of a mesh generation scheme is to generate element connectivity and nodal coordinate data by reading in input data for a few key points. This theory of a mesh generation scheme is suggested by Zienkiewicz and Philips. This scheme is done by a computer programme named MESHQUAC.BAS . We do not deal with details of theory and only use its results.

In this scheme, a complex region is divided into eight-noded quadrilaterals. They are then viewed in the form of a rectangular block. In general, a complex region is viewed as a rectangle, composed of rectangular blocks, with some blocks left as void and some edges identified to be merged.

Region of the problem is shown in Fig 2.8 below.

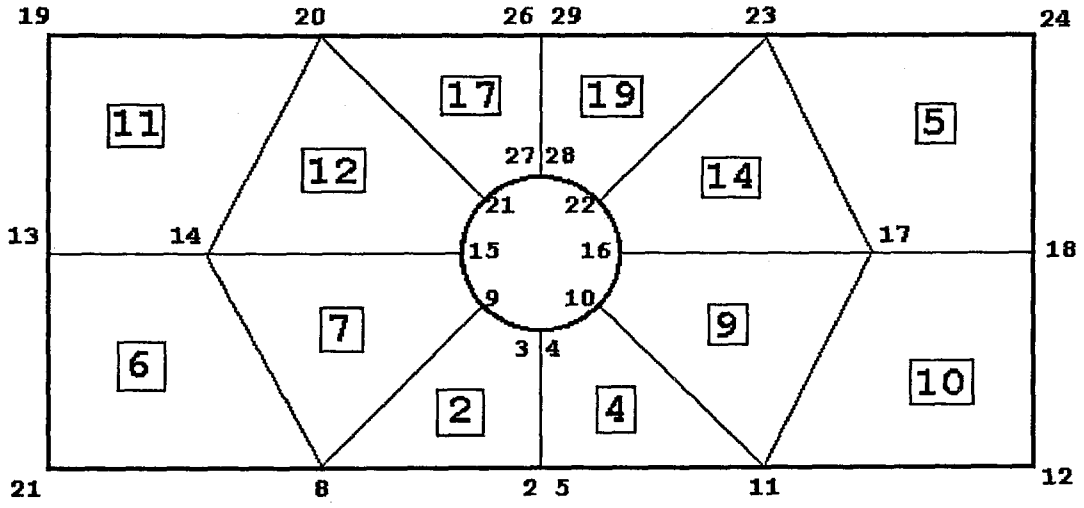

Figure 2.8 Region of the problem

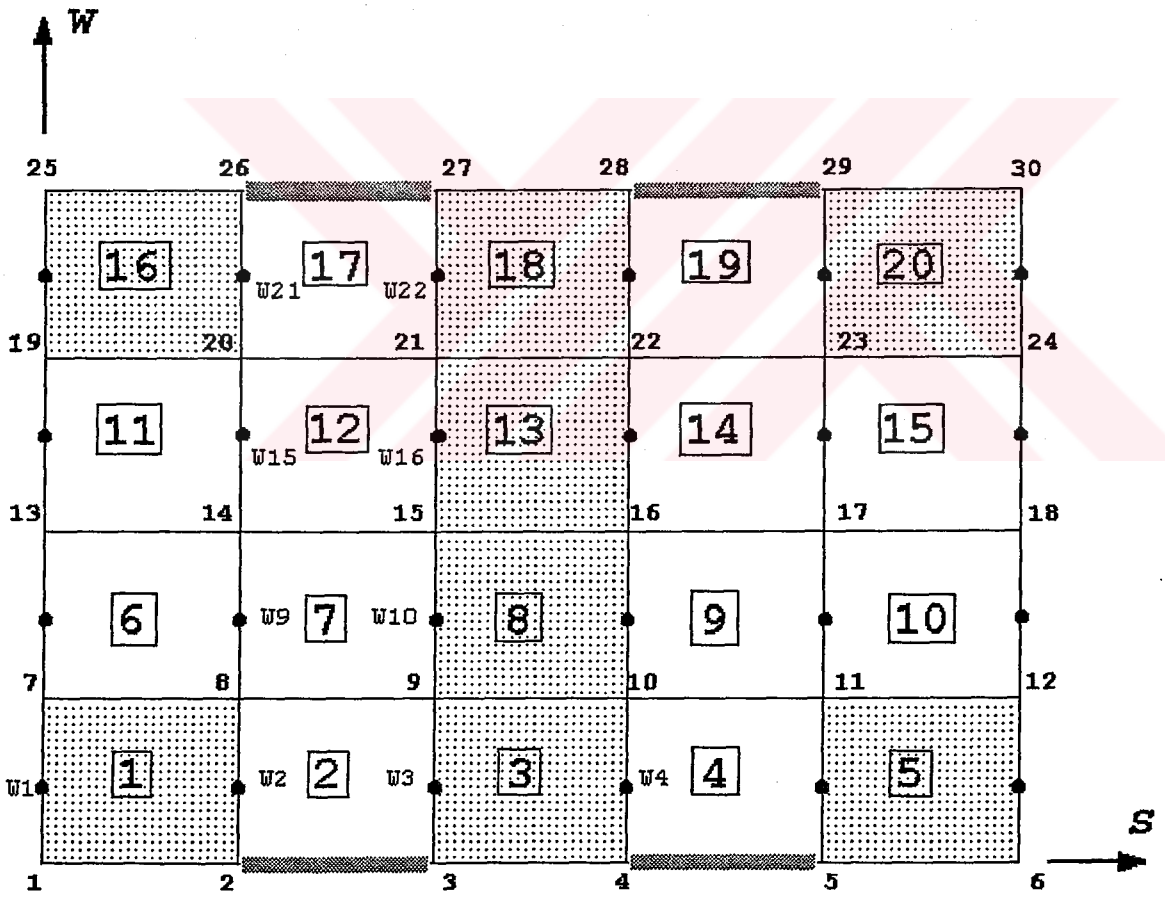

Figure 2.9 Block diagram of the problem

The block diagram of the problem is also shown in Fig 2.9. The full rectangular block pattern is convenient for numbering. To match the pattern in the region,

the shaded blocks are to be treated as void and four hatched edges 2-3, 27-26 and 4-5, 29-28 need to be merged. The points W_3, W_4, ..., W_{22}, are used for forming the curvature of the circular hole. The sides to be merged which are identified by the end-node numbers of sides, number of void blocks, key points for block diagram, and, curvature indicating nodes (W_3, W_4, etc.) are given in the form of a data file in the mesh generation program MESHQUAC.BAS. The following are obtained as numerical values using above raw data (See App. A):

In the first row of the data file the followings are present; number of node (NN), number of element (NE), number of constrained degrees of freedom (ND), number of applied load (NL), number of material (NM), Dimension of the problem (NDIM), number of nodes that finite element has (NEN).
Then in their proper sequence;

- coordinates of all nodes,
- element connectivity numbers,
- element's material identifiers,
- constrained DOF numbers corresponding magnitude of element in mm,
- calendar number of DOF of a node where the corresponding load is applied and corresponding magnitude of load** in N are listed.

In the last row; Young's modulus and Poisson's ratio for steel or longitudinal and transverse Young's modulus (E_L and E_T), Poisson's ratio (ν_{LT}), and rigidity modulus (G_{LT}) for composites are given.

**The constrained *degrees of freedom* (DOF) and coordinates of those points at which the loads are applied are known (Eqs. 2.60 and 2.61). Using a simple program, their DOF can be found easily. Using these values and rewriting MESHQUAC.BAS one can obtain complete mesh generation program.

In our study each node has two DOF. Typically the DOF of node *I* are Q_{2i-1} and Q_{2i}. DOF Q_{2i-1} indicates the vertical direction and Q_{2i} indicates the transverse direction.

Study sample subdivided into 240 elements is shown in Fig. 2.10.

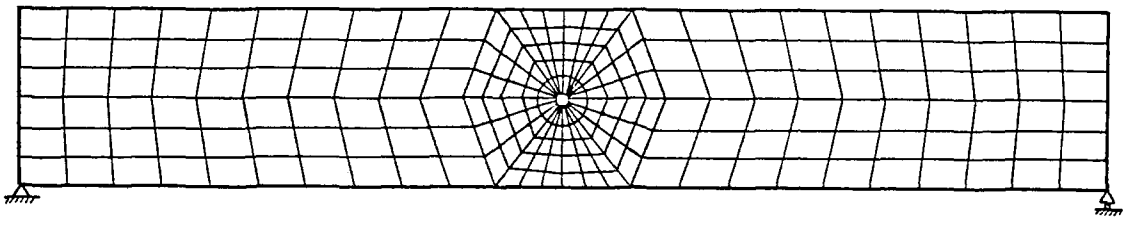

Figure 2.10 Study sample subdivided into 240 elements

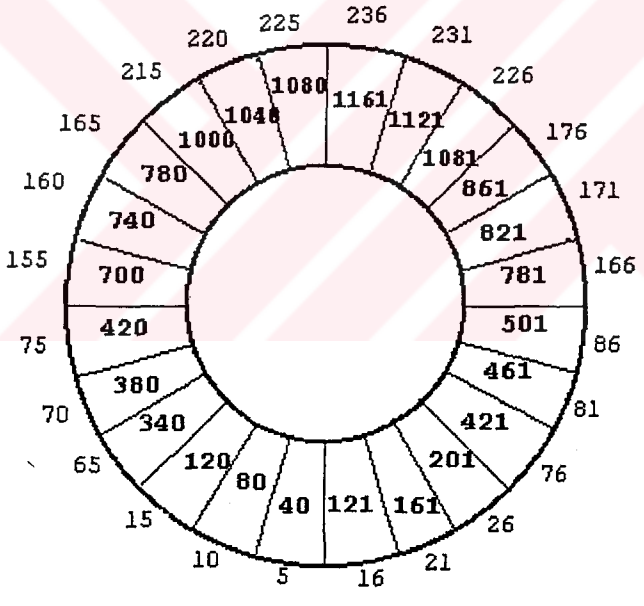

(a) Numbers of the elements around the hole
Bold type numbers belong to sample
subdivided into 1200 elements

Figure 2.11 The Investigated Domain

To indicate all numbers of elements and nodes is immaterial, because investigation is made only around the circular hole and along **A-B** direction. The domain investigated is shown in Fig. 2.11.

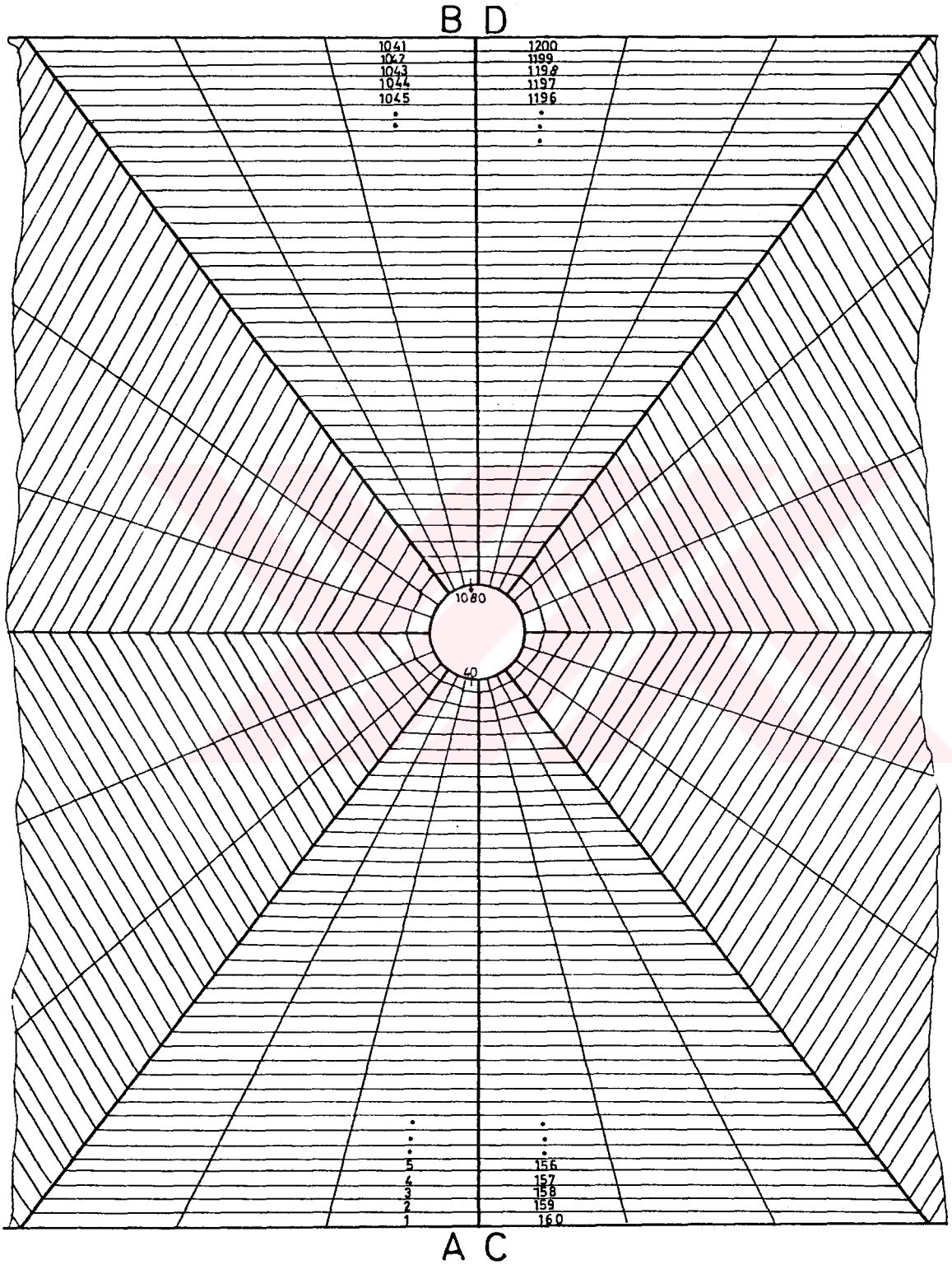

(b) Directions A-B and C-D

Figure 2.11 The Investigated Domain

2.2.10 Boundary Conditions

It is seen that on the fixed support vertical and horizontal displacements are zero and on the sliding support, there is no horizontal displacement. In summary, we can write the boundary conditions as following:

$$\begin{aligned} u = v = 0 \quad & \text{at } x = 0, \quad y = 0 \\ v = 0 \quad & \text{at } x = \boldsymbol{L}, \quad y = 0 \end{aligned} \tag{2.60}$$

Two vertical loads are applied at the two points below:

$$\begin{aligned} F = 1000\ N \quad & \text{at } x = \mathbf{a}, \quad y = \boldsymbol{h} \\ F = 1000\ N \quad & \text{at } x = \boldsymbol{L} - \mathbf{a}, \quad y = \boldsymbol{h} \end{aligned} \tag{2.61}$$

2.2.11 Numerical Data

In the calculations, geometric dimensions and loads are taken as

Height of the beam,	**h** = 120 mm
Length of the beam,	**L** = 800 mm
Thickness of the beam,	**t** = 5 mm
Diameter of the hole	**D** = 10 mm
Distance from longitudinal axis to the centre of the hole,	**b** = varies from 0 mm to 54 mm
The moment arm	**a** = 210 mm
Vertical point load	**P**y = 1000 N

The material properties for steel are

Modulus of elasticity $\mathbf{E} = 210$ GPa

Poisson's ratio $\nu = 0.3$

The material properties for composites are given in the table below.

Table 8. ENGINEERING CONSTANTS, FIBER VOLUME AND SPECIFIC GRAVITY OF TYPICAL UNIDIRECTIONAL COMPOSITES

Type	Material	E_L (GPa)	E_T (GPa)	ν_{LT}	G_{LT} (GPa)	v_f %	Sp. Grav.
T300/5208	Gr/Ep	181	10.3	0.28	7.17	0.70	1.6
B(4)/5505	B/Ep	204	18.5	0.23	5.59	0.5	2.0
Scotchply /1002	Gl/Ep	38.6	8.27	0.26	4.14	0.45	1.8
Kevlar49 /Epoxy	Aramid/Ep	76	5.5	0.34	2.3	0.60	1.46

CHAPTER 3

RESULTS AND DISCUSSION

3.1. STRESSES

In the following comparisons the stress occurring at any point along the transverse axis of the beam without a hole is denoted by σ_{xth}. And the numerical values that σ_{xth} takes are calculated by the so-called flexure formula (Eq. 2.56). Flexure formula is valid not only for isotropic beams but also for orthotropic beams without a hole. So the numerical values that σ_{xth} takes (in composite beams) are also calculated by the same formula. In cases the hole is present, stress occurring at any point along the transverse axis is calculated by the Finite Element Method and it is denoted by σ_x.

3.1.1. Steel

- At the position where **b**=0, σ_x and σ_{xth} take almost the same numerical values up to the boundaries of the hole as shown in Fig. 3.1.
- As the distance b increases, σ_x gradually takes greater values than σ_{xth} does. The gradual increase starts at certain points from the top and bottom of the hole. And it lasts as far as the hole is reached from both sides.

- At b=30 mm position, the stress occurring just above the hole reaches the maximum value of the theoretical stress. For cases where **b**=40 mm and **b**=50 mm, the stress occurs just above the hole takes greater values than $(\sigma_{xth})_{max}$ does.
- σ_x values of those points above the hole are always greater than those below the hole.

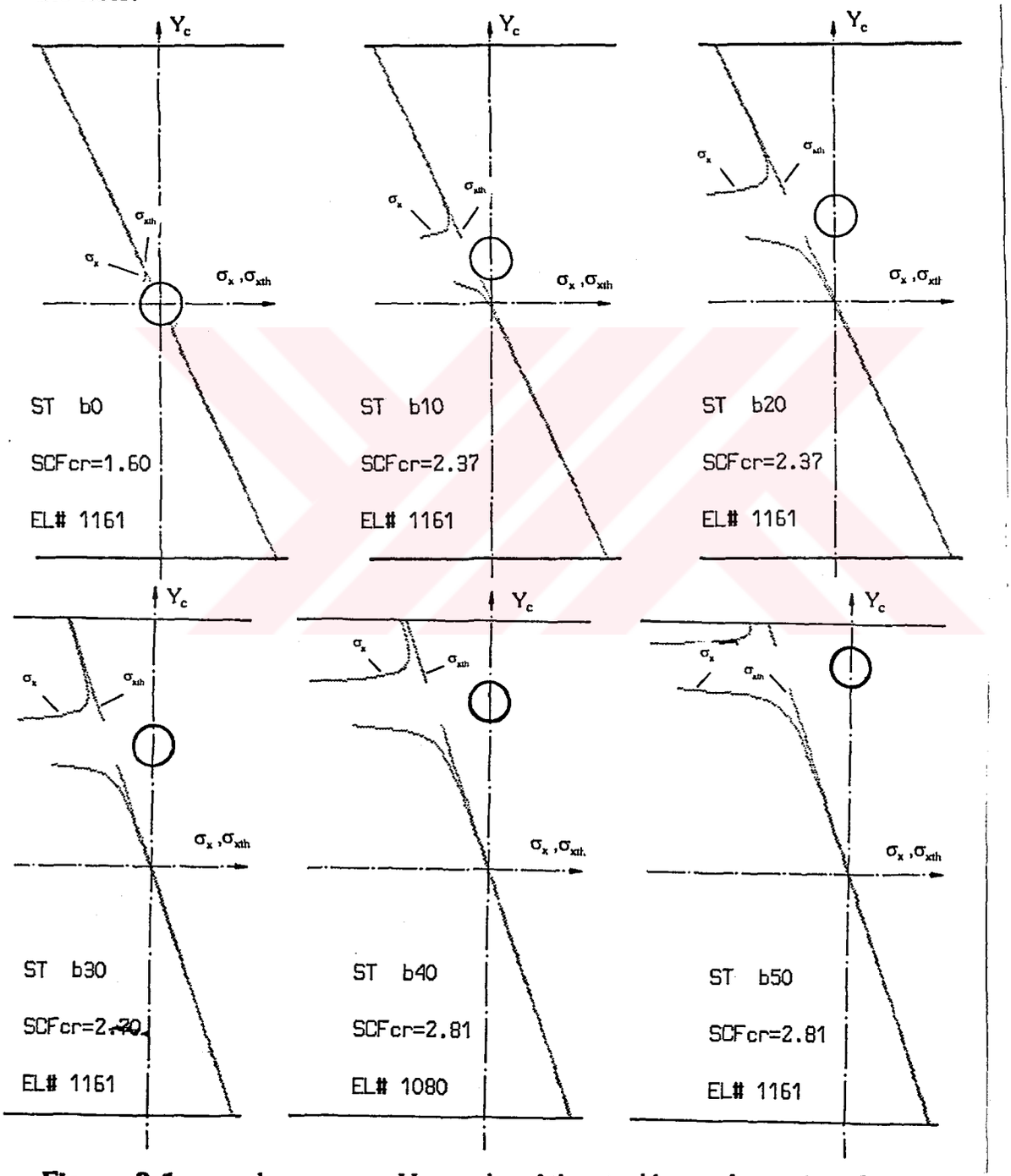

Figure 3.1 σ_x and σ_{xth} versus Y_c graphs of the steel beam for various **b** distances

3.1.2. Composites

In the most of the graphics plotted for composites, small broken lines are shown at Gauss points. It is the consequence of the sensitivity of the Finite Element Method for composites in off-axis. Reinforcing angle is again denoted by θ here.

3.1.2.1 Graphite-Epoxy

θ = 0° case

- The graphics plotted for this case are similar to those of steel for each **b** distance.
- As the distance **b** increases, σ_x gradually takes greater values than σ_{xth} does. The gradual increase starts at certain points from the top and bottom of the hole and it continues up to hole.
- At position **b**= 20 mm, the stresses occurring just above the hole are always greater than those below the hole.

θ = 30° case

In this case, at those points above the hole, σ_x always takes greater values than σ_{xth}. The situation below the hole is in complete opposition.

θ = 45° case

The graphics plotted for this case are similar to those of the case θ=30°.

θ = 60° case

Again the graphics plotted for this case are similar to those of steel for each **b** distance. At those points above hole, σ_x always takes greater values than σ_{xth} does. The situation below the hole is in complete opposition.

θ = 90° case

The graphics plotted for this case are similar to those of steel for each **b** distance. At those points above hole, σ_x always takes smaller values than σ_{xth} . The situation below the hole is in complete opposition.

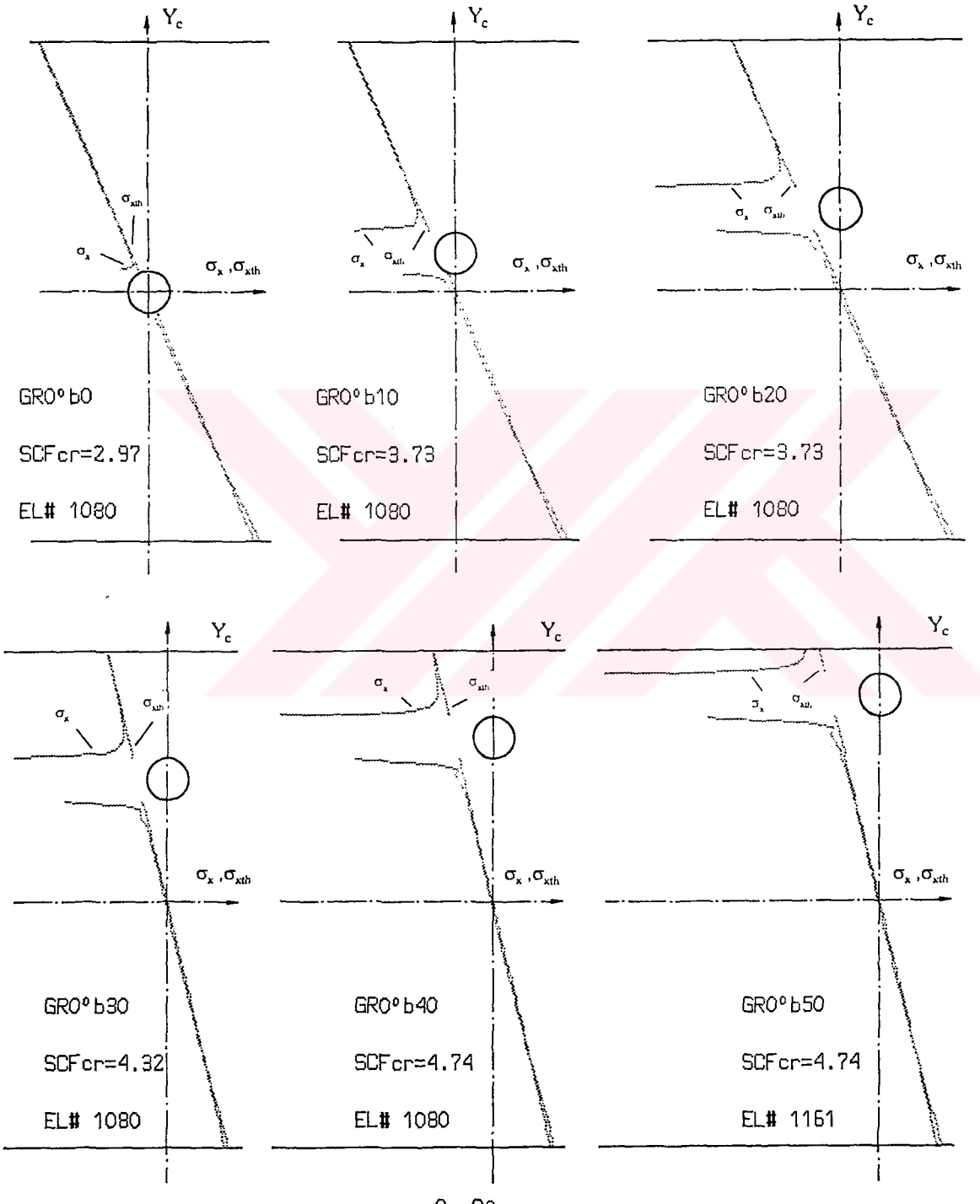

Figure 3.2a σ_x and σ_{xth} versus Y_c graphs of the Graphite-Epoxy for various **b** distances

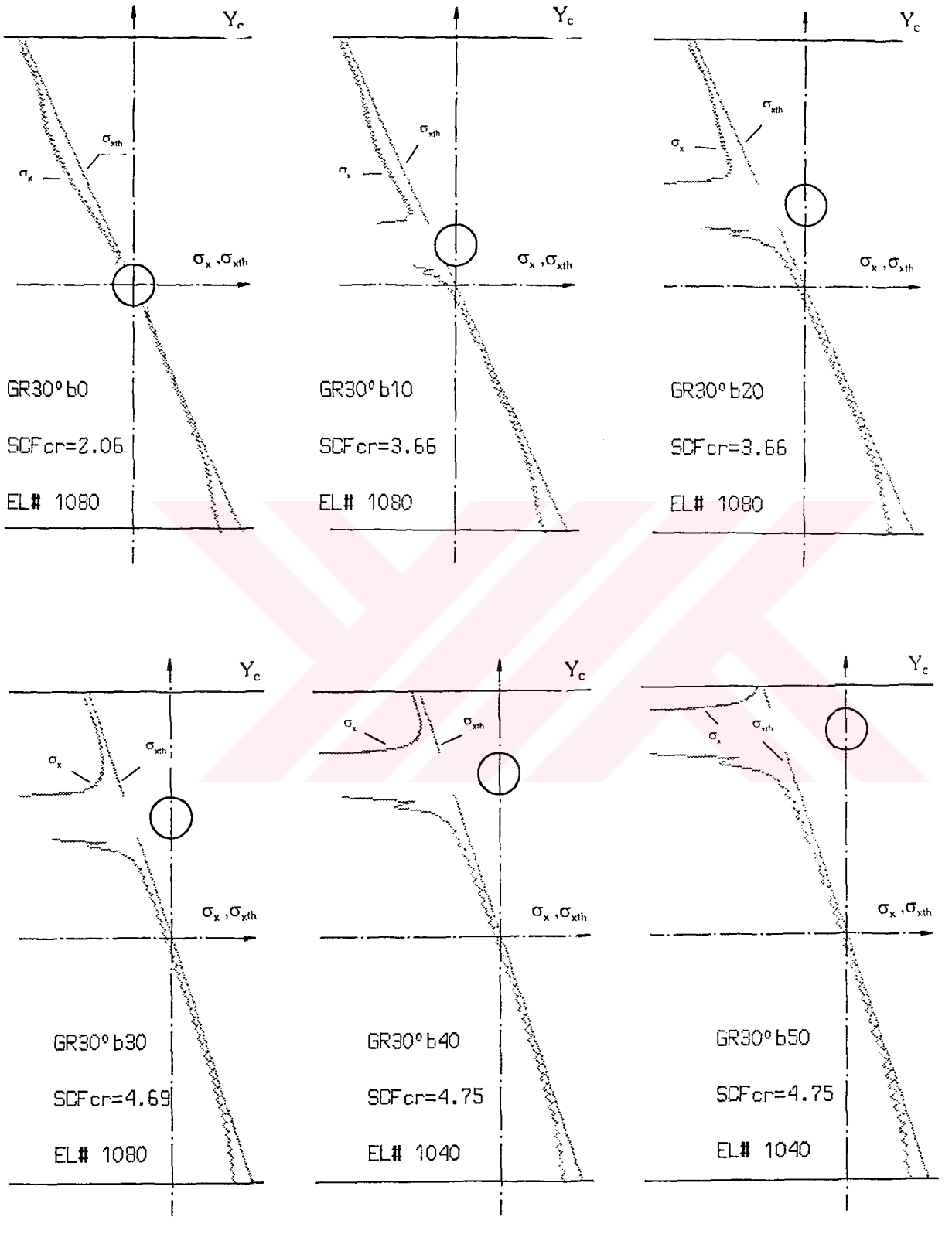

θ=30°

Figure 3.2b σ_x and σ_{xth} versus Y_c graphs of the Graphite-Epoxy for various **b** distances

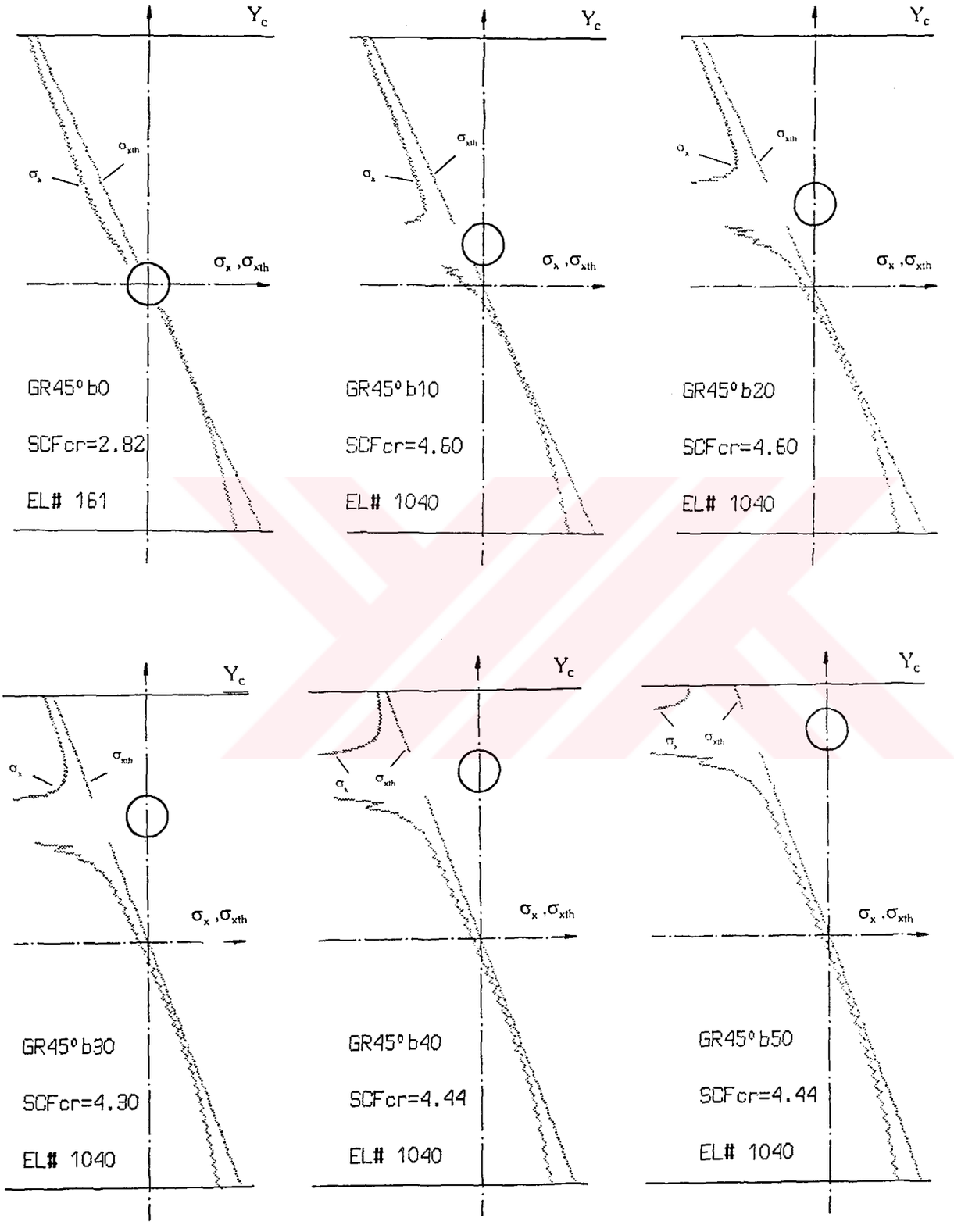

θ=45°

Figure 3.2c σ_x and σ_{xth} versus Y_c graphs of the Graphite-Epoxy for various **b** distances

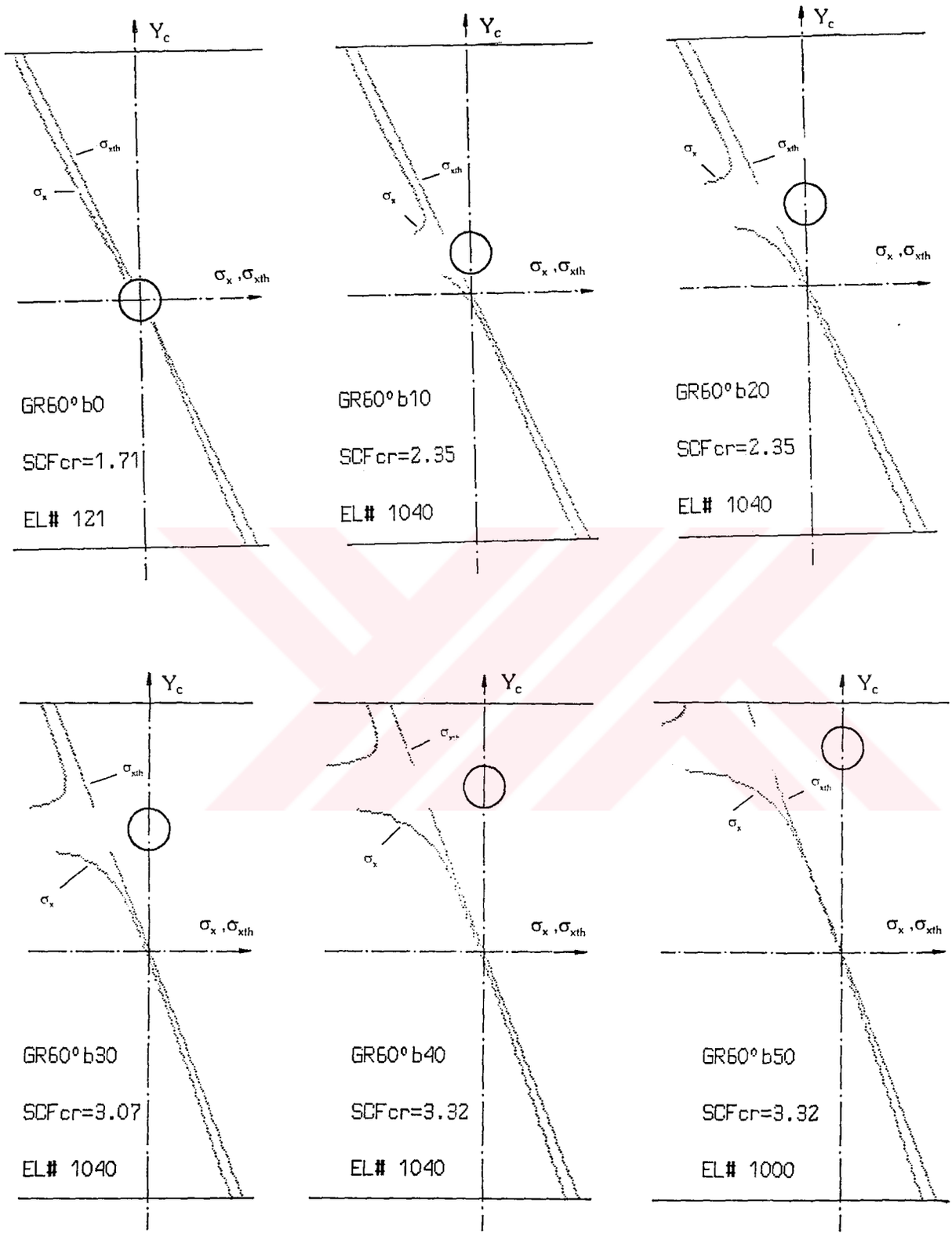

θ=60°

Figure 3.2d σ_x and σ_{xth} versus Y_c graphs of the Graphite-Epoxy for various **b** distances

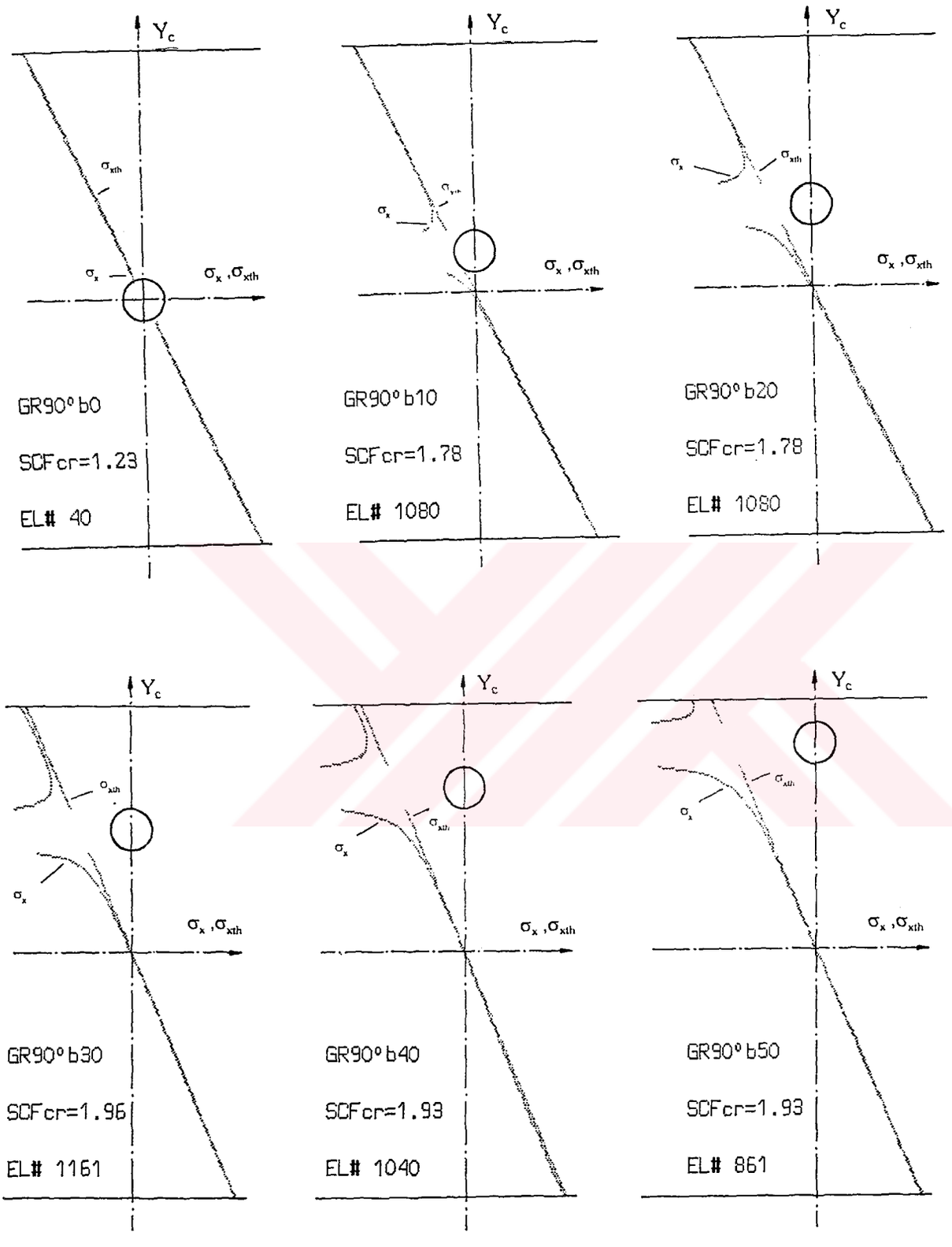

θ=90°

Figure 3.2e σ_x and σ_{xth} versus Y_c graphs of the Graphite-Epoxy for various **b** distances

3.1.2.2 Scotchply

θ = 0° case

- As the distance **b** increases, σ_x gradually takes greater values than σ_{xth} does. The gradual increase starts at certain points from the top and bottom of the hole. And it continues as far as the hole is reached from both sides.
- At position **b**=20 mm, the stress occurring just above the hole reaches $(\sigma_{xth})_{max}$. For cases **b**=30 mm to 50 mm, the stress occurs just above the hole takes greater values than $(\sigma_{xth})_{max}$ does.
- σ_x values of those points above the hole are always greater than those below the hole.

θ = 30° and 40° cases

The graphics plotted for these cases are similar to those for Graphite-epoxy of the case θ=30° .

θ = 60° case

The graphics plotted for this case are similar to those for the same material of the case θ=0° .

θ = 90° case

In this case, the characteristics of all σ_x-Y_c graphics are similar to the characteristics displayed by the steel beam.

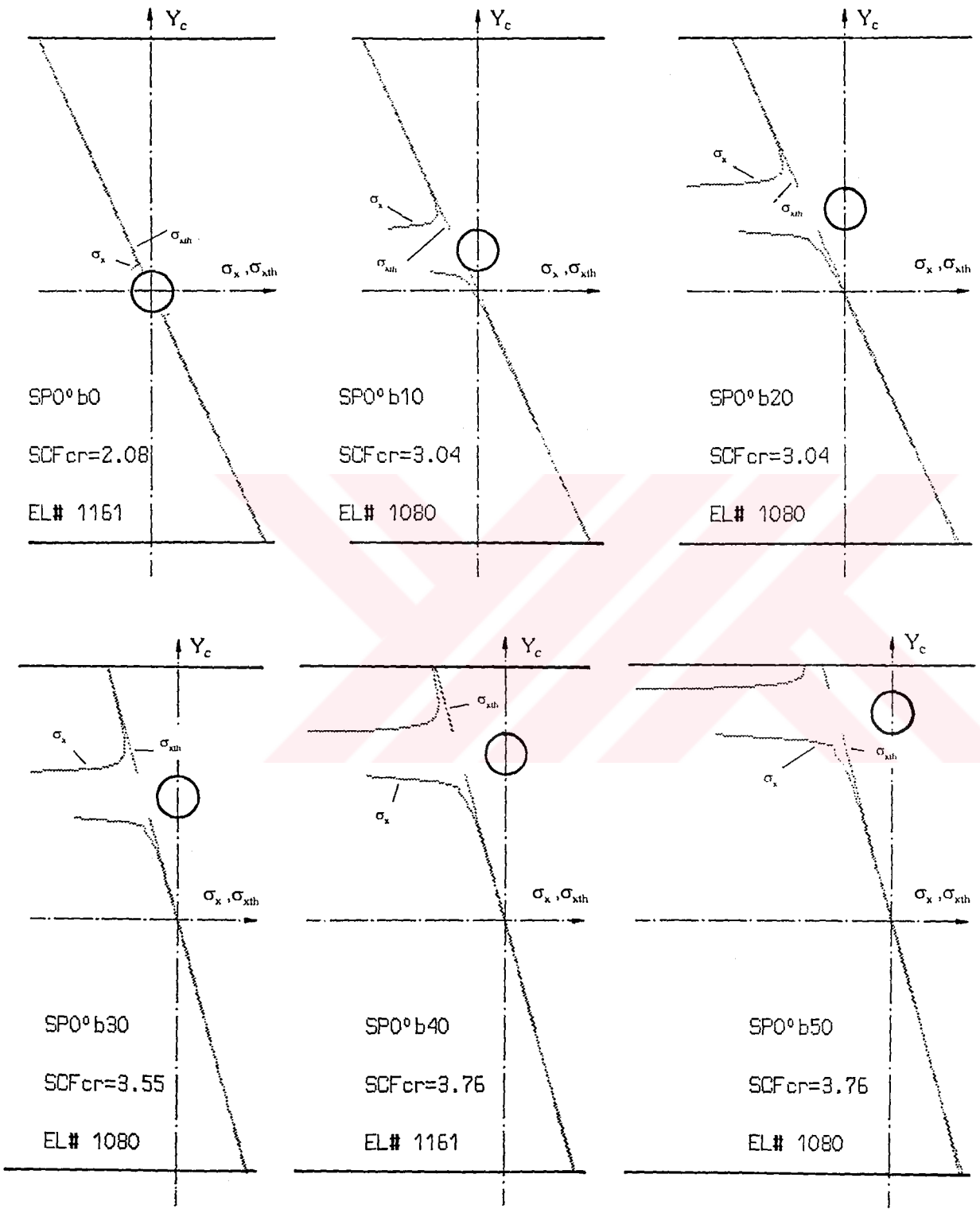

θ=0°

Figure 3.3a σ_x and σ_{xth} versus Y_c graphs of the Scotchply for various **b** distances

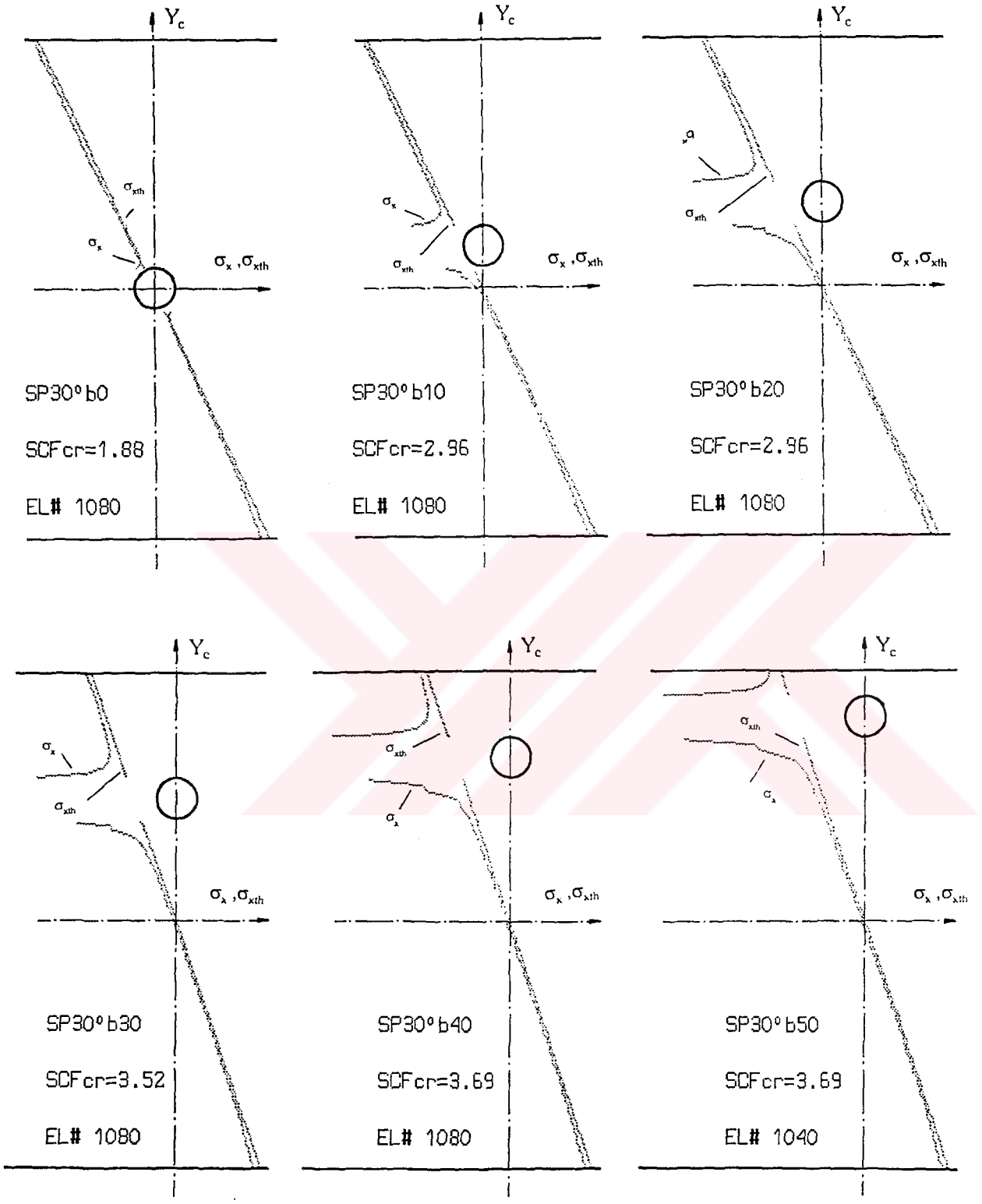

$\theta=30°$

Figure 3.3b σ_x and σ_{xth} versus Y_c graphs of the Scotchply for various **b** distances

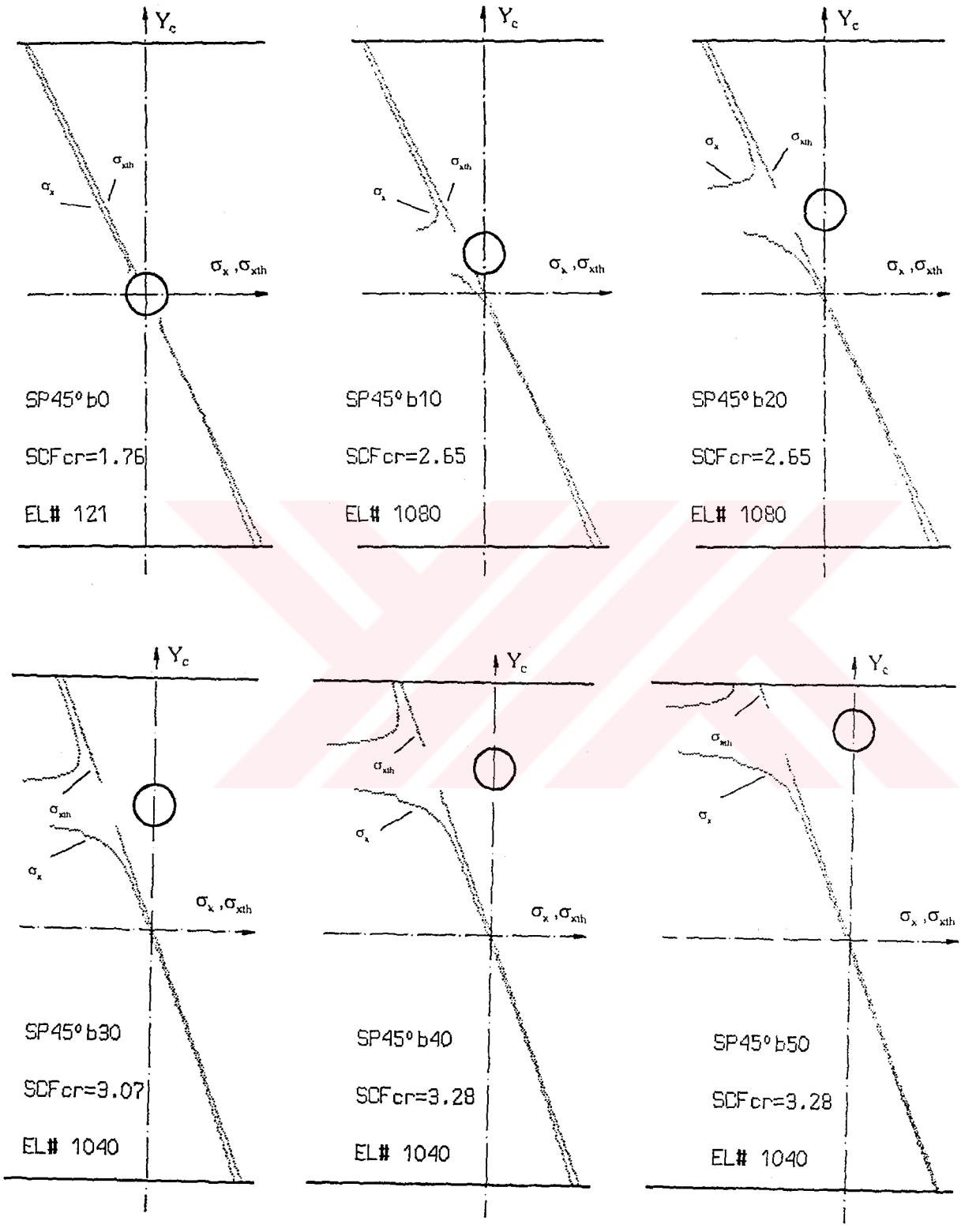

θ=45°

Figure 3.3c σ_x and σ_{xth} versus Y_c graphs of the Scotchply for various **b** distances

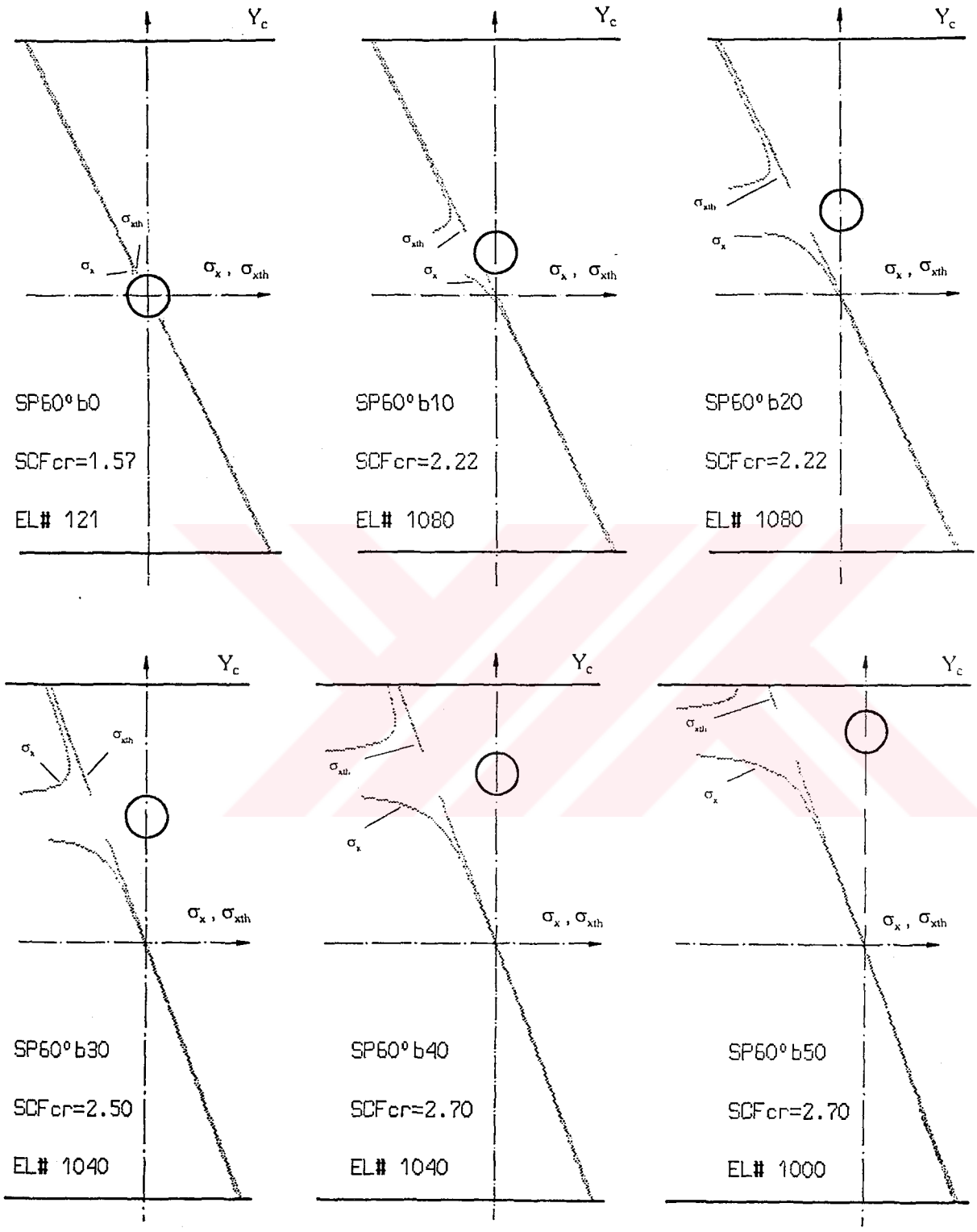

θ=60°

Figure 3.3d σ_x and σ_{xth} versus Y_c graphs of the Scotchply for various **b** distances

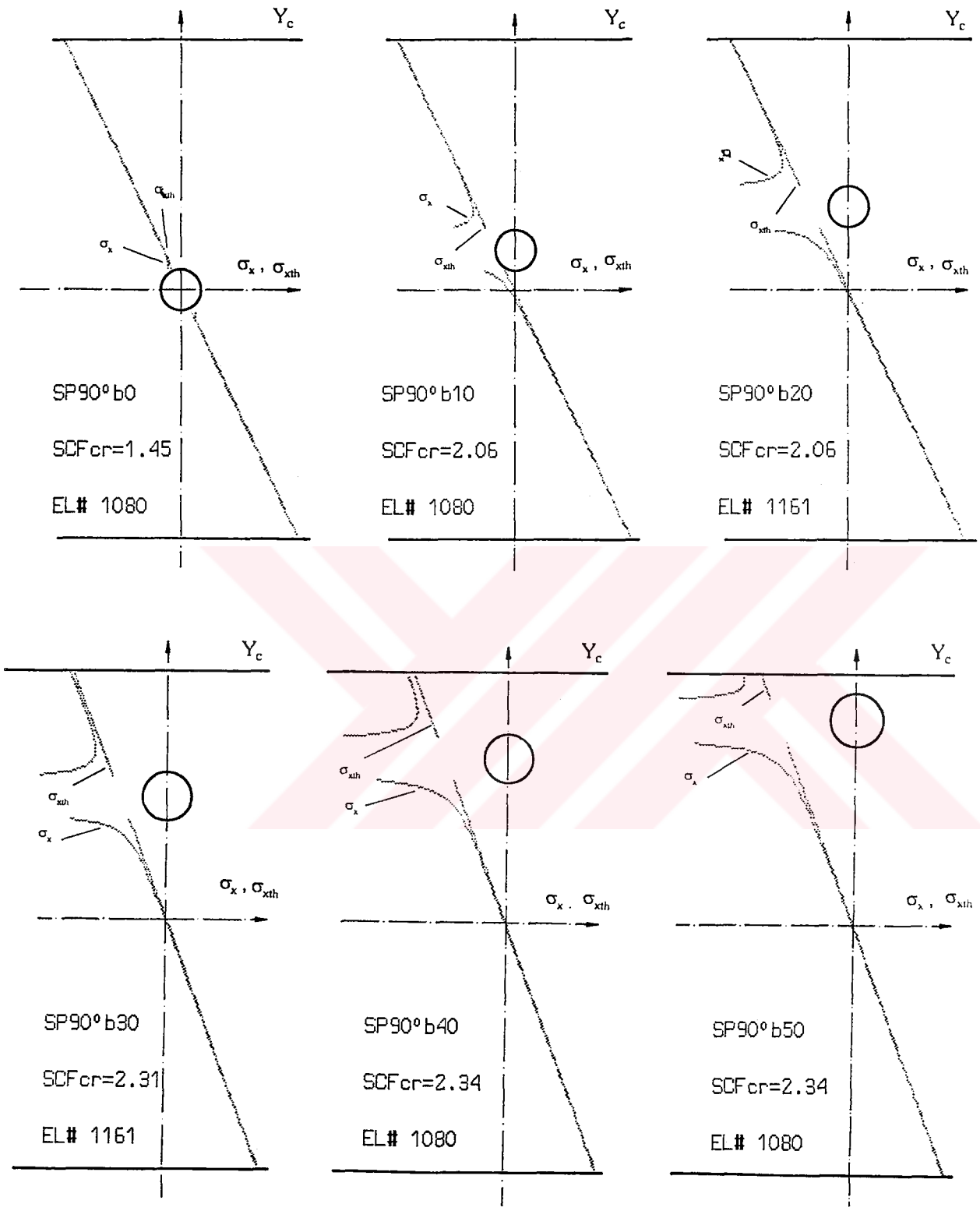

θ=90°

Figure 3.3e σ_x and σ_{xth} versus Y_c graphs of the Scotchply for various **b** distances

3.1.2.3 Kevlar

The whole σ_x-Yc graphics for Kevlar are similar to those for Graphite-epoxy.

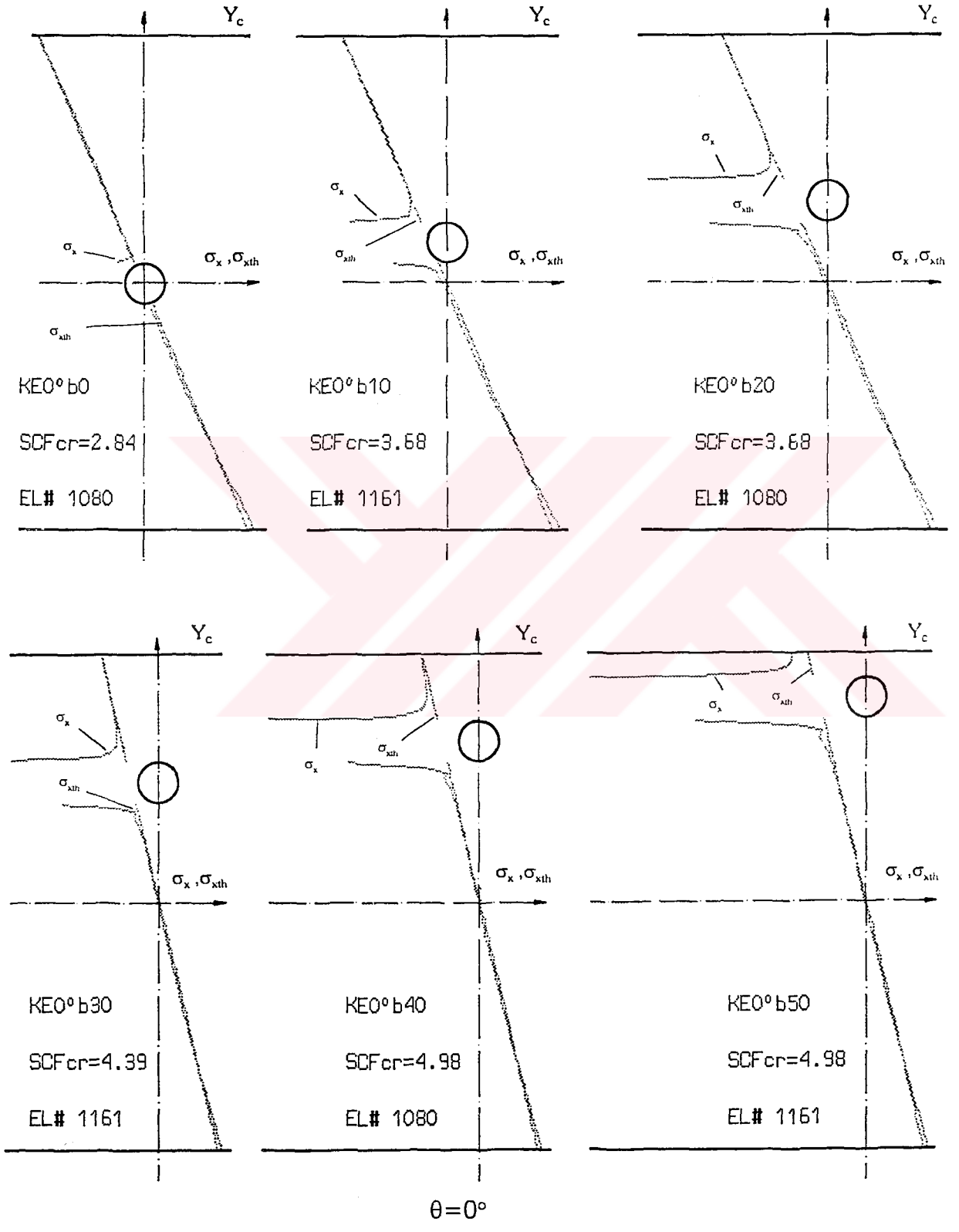

Figure 3.4a σ_x and σ_{xth} versus Y_c graphs of the Kevlar for various **b** distances

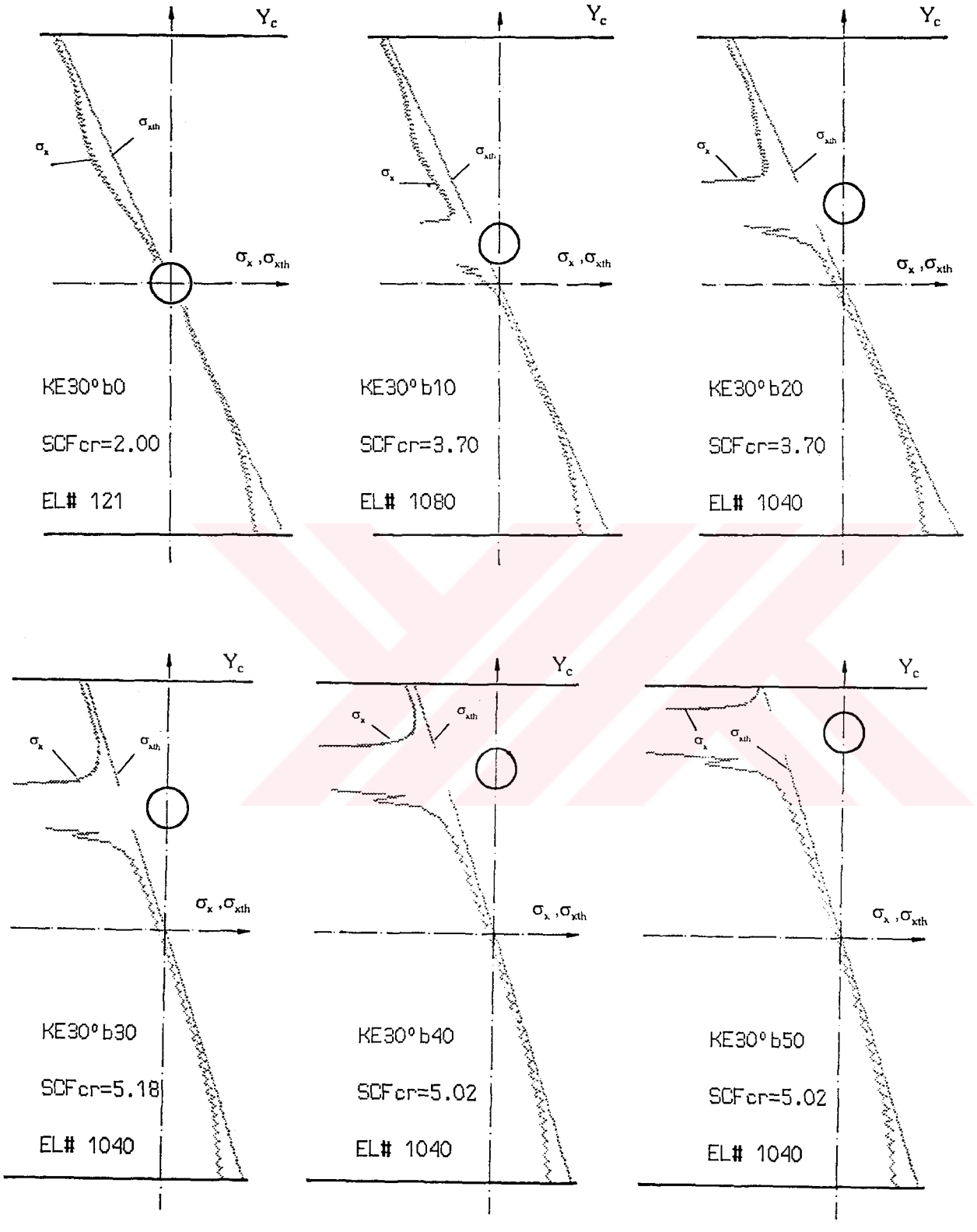

θ=30°

Figure 3.4b σ_x and σ_{xth} versus Y_c graphs of the Kevlar for various **b** distances

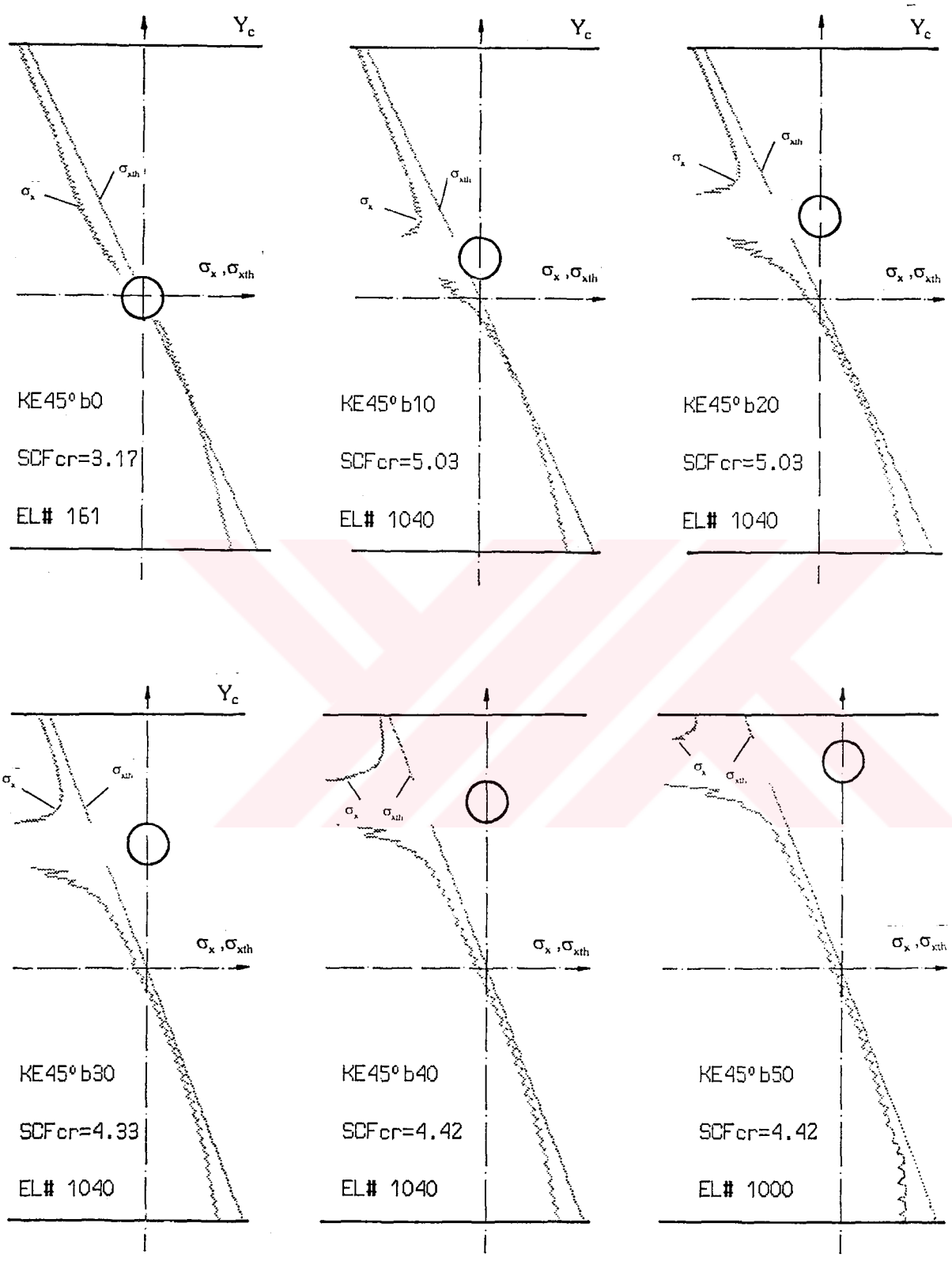

θ=45°

Figure 3.4c σ_x and σ_{xth} versus Y_c graphs of the Kevlar for various **b** distances

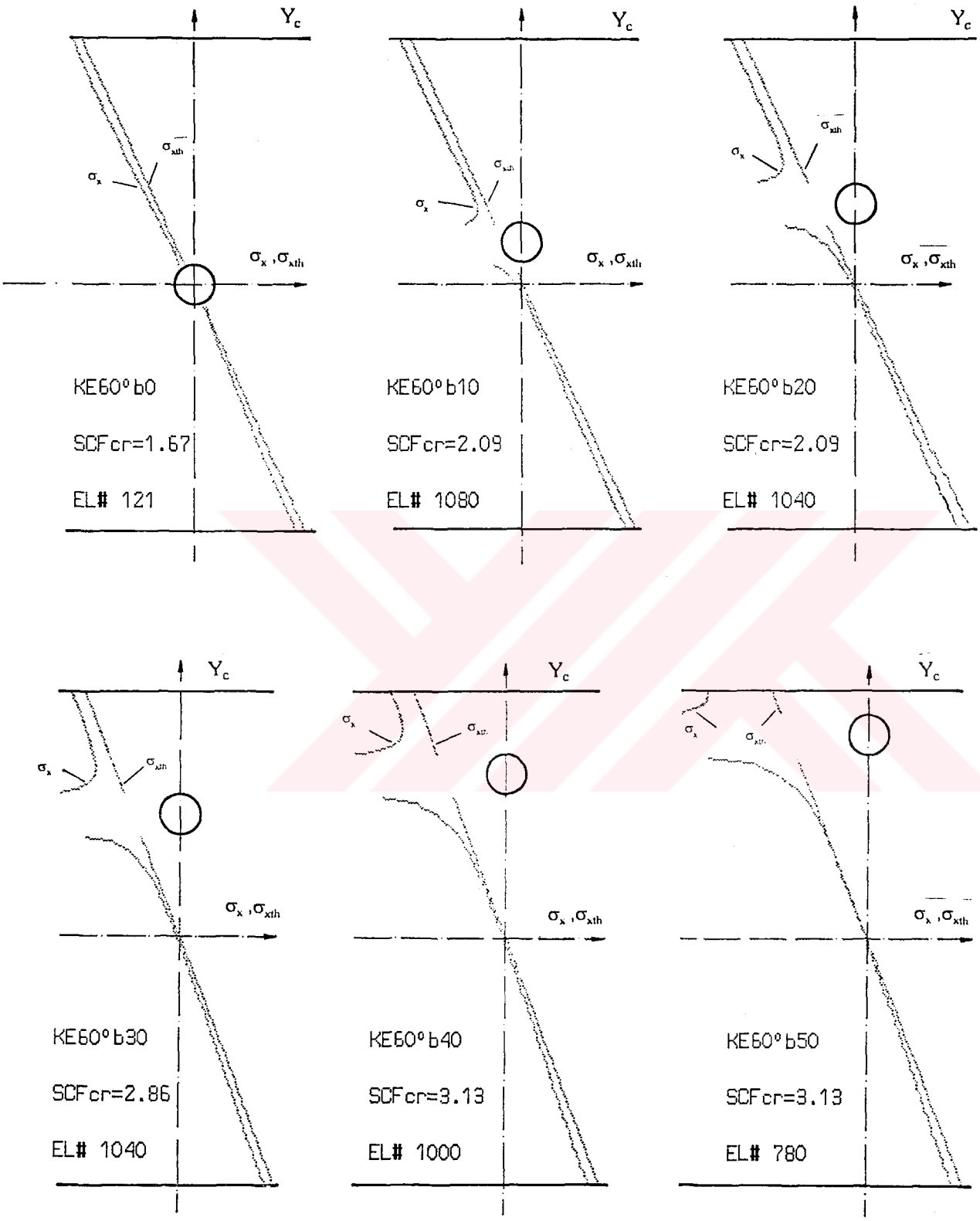

θ=60°

Figure 3.4d σ_x and σ_{xth} versus Y_c graphs of the Kevlar for various **b** distances

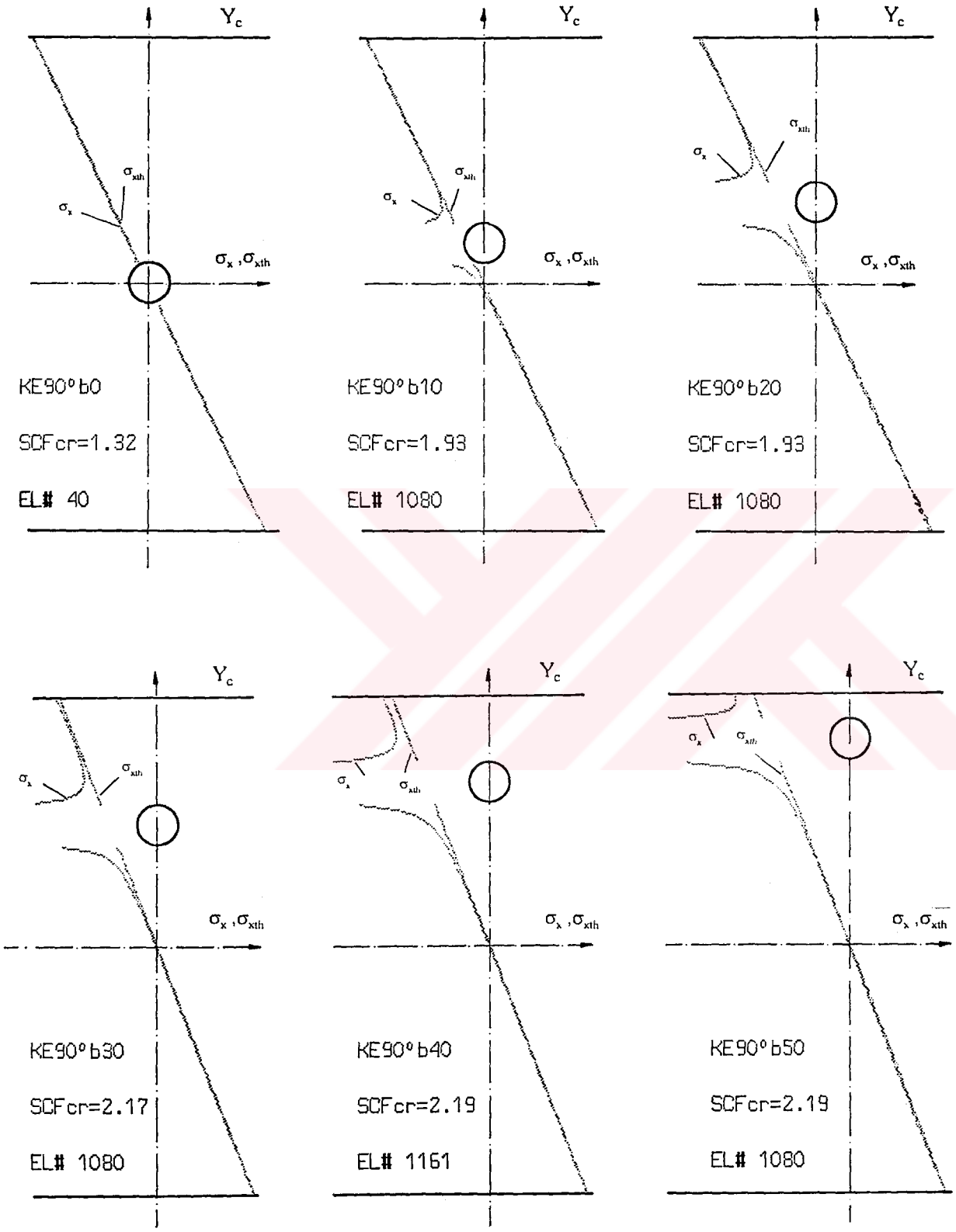

θ=90°

Figure 3.4e σ_x and σ_{xth} versus Y_c graphs of the Kevlar for various **b** distances

3.1.2.4 Boron

The whole σ_x-Yc graphics for Kevlar are similar to those for Graphite-epoxy.

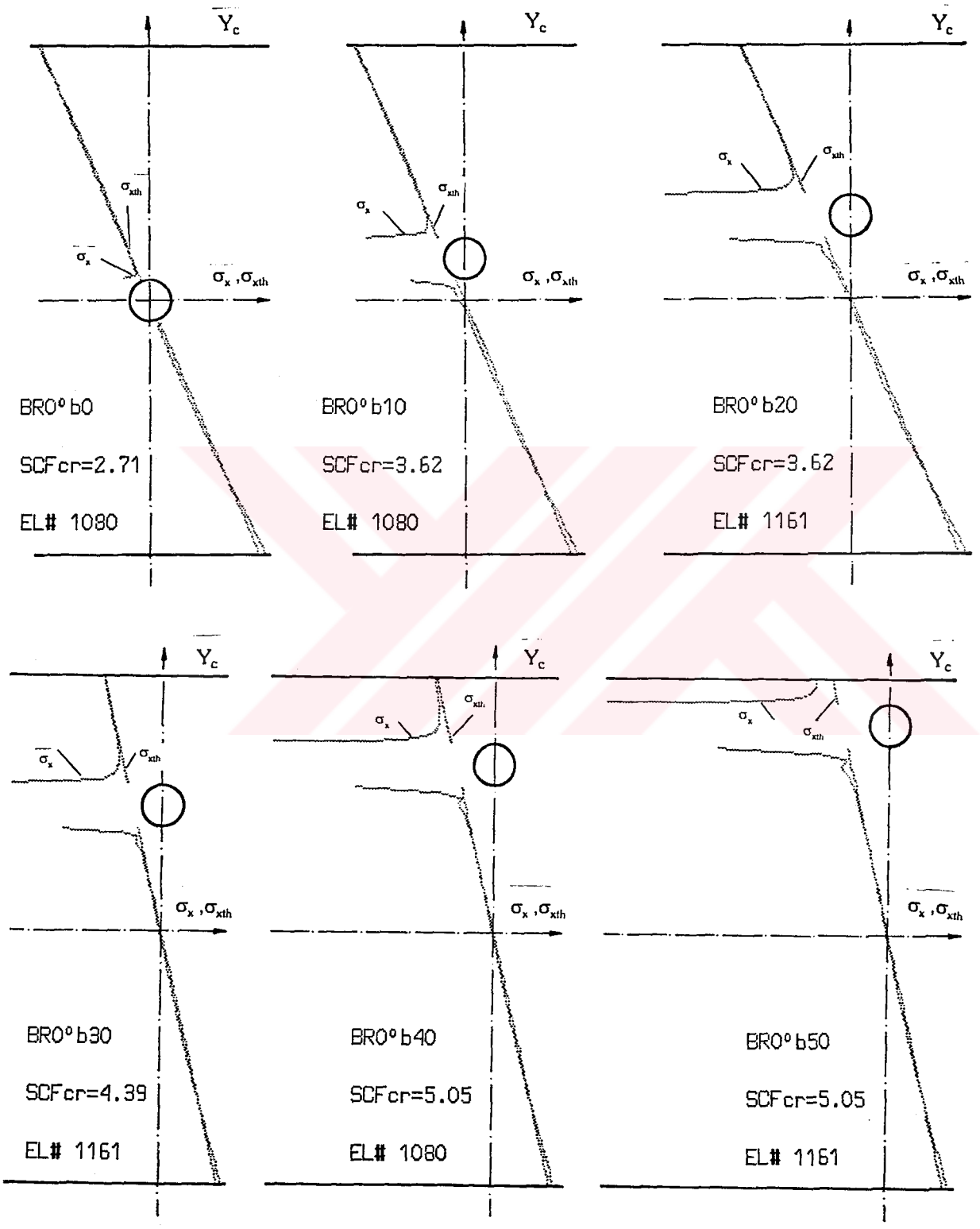

θ=0°

Figure 3.5a σ_x and σ_{xth} versus Y_c graphs of the Boron for various **b** distances

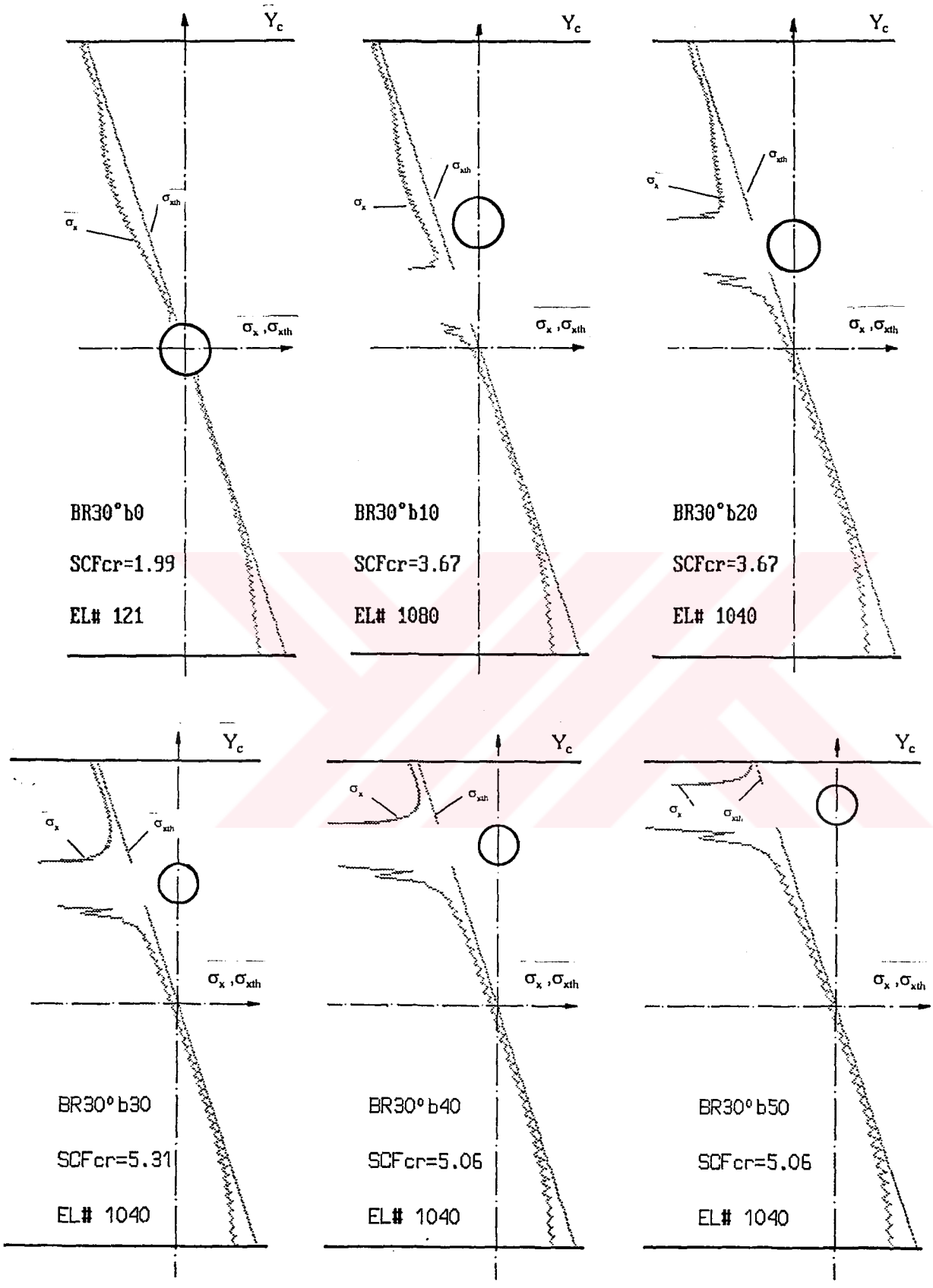

Figure 3.5b σ_x and σ_{xth} versus Y_c graphs of the Boron for various **b** distances

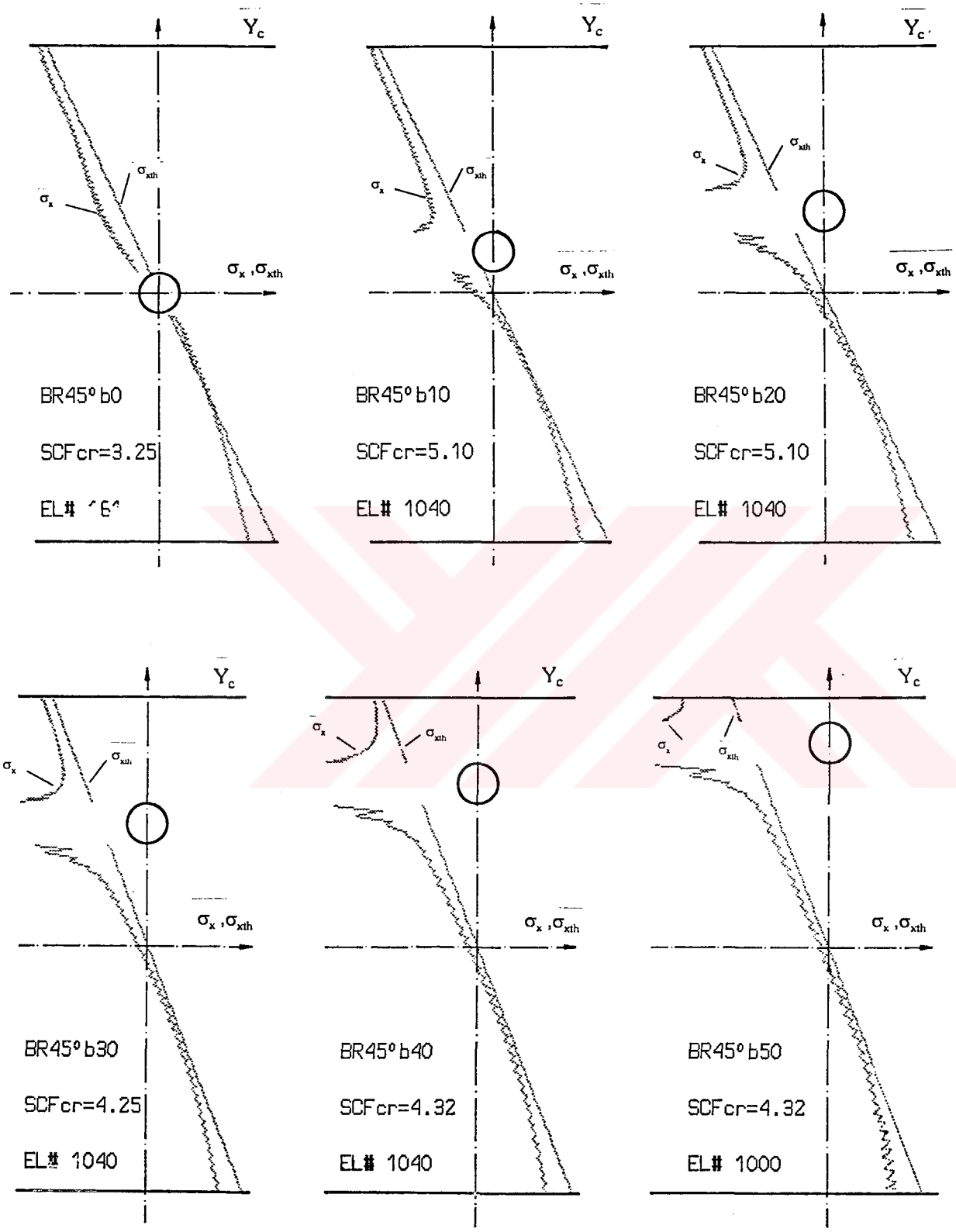

θ=45°

Figure 3.5c σ_x and σ_{xth} versus Y_c graphs of the Boron for various **b** distances

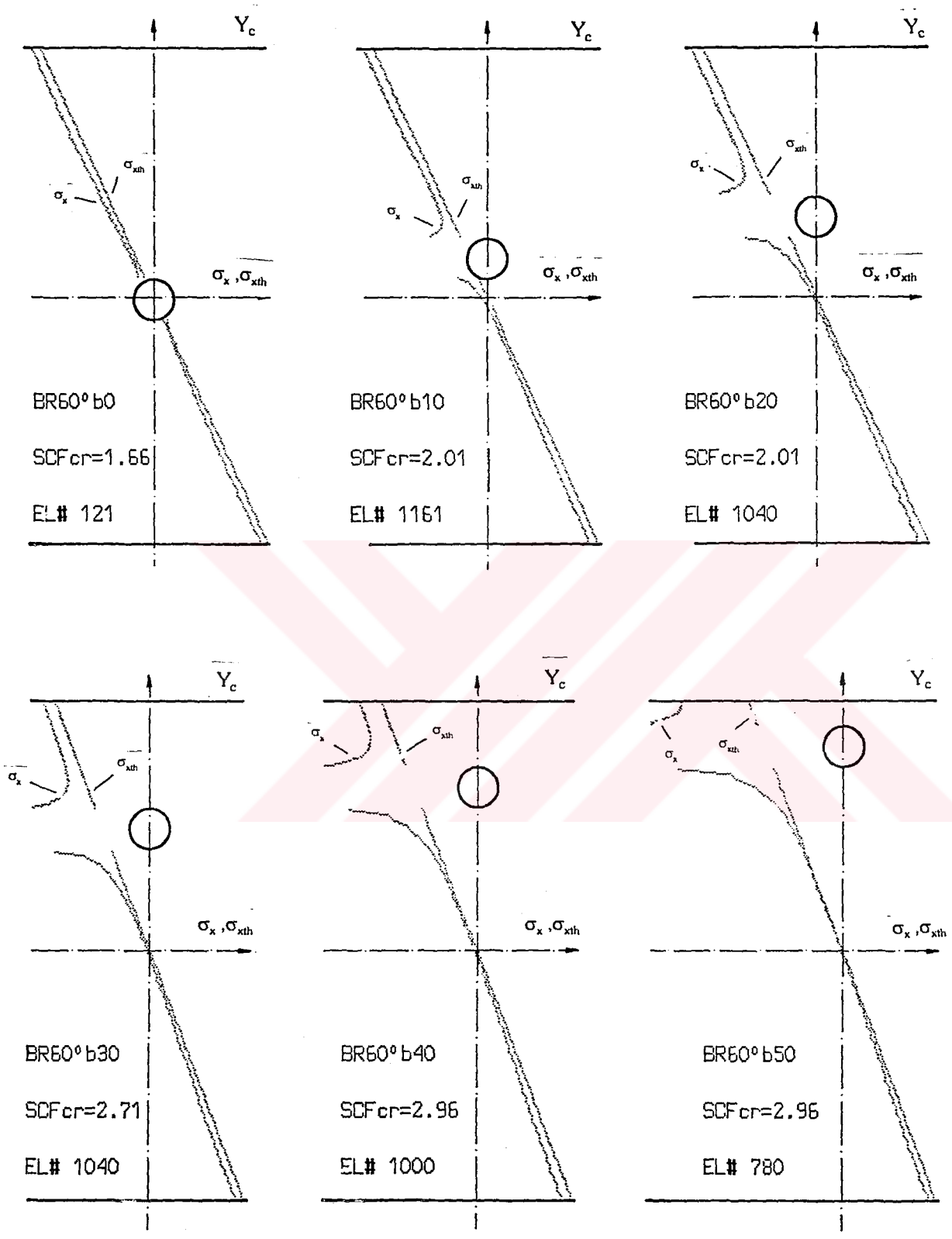

$\theta=60°$

Figure 3.5d σ_x and σ_{xth} versus Y_c graphs of the Boron for various **b** distances

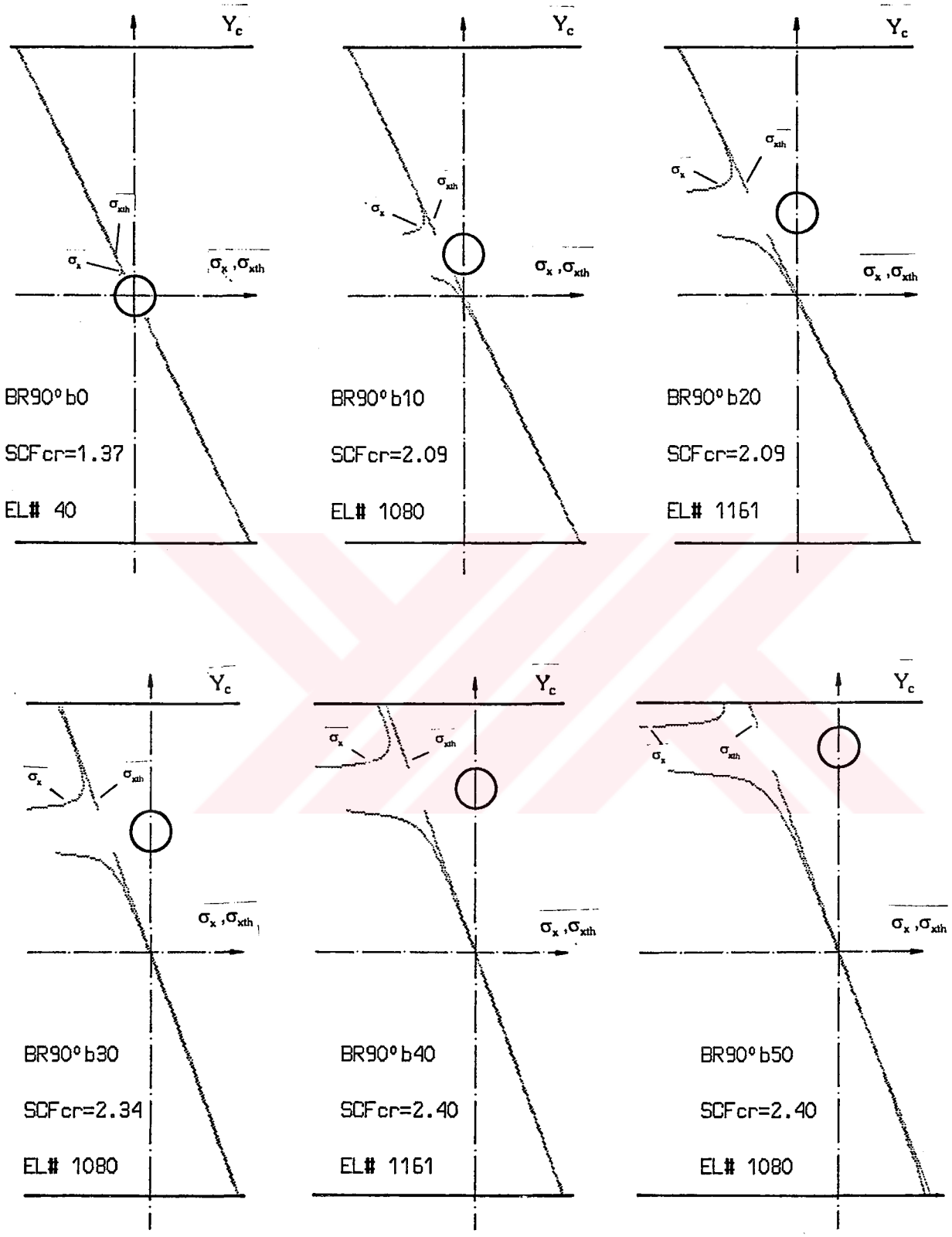

θ=90°

Figure 3.5e σ_x and σ_{xth} versus Y_c graphs of the Boron for various **b** distances

3.2. STRESS CONCENTRATION FACTORS

We define stress concentration factor SCF for a beam subjected to pure bending in the previous section as follows:

$$SCF = \frac{\sigma_1}{\sigma_{xth}} \tag{3.1}$$

Where σ_1 is the greatest maximum principal stress occurring at any point. σ_{xth} is the theoretical bending stress at the same point, calculated by the flexure formula (Eq. 2.56). The principal stresses (σ_1 and σ_2) are computed at each point analysed considering plane stress condition. We define two SCF around the hole.

The principal stress having the greater absolute value computed at each point is divided by the theoretical stress computed at the same point. So the local stress concentration factor is obtained for each and every point analysed around the hole. The maximum one is chosen among these as the local maximum stress concentration factor, SCF_{Locmax} . It is given by

$$SCF_{Locmax} = \frac{\sigma_1}{\sigma_{xth}} \tag{3.2}$$

Among the greater principal stresses computed as above at each point we choose the maximum one and then divide it by the theoretical stress at the same point. The result so obtained is called as the critical stress concentration factor and is given by

$$SCF_{cr} = \frac{(\sigma_1)_{max}}{\sigma_{xth}} \tag{3.3}$$

As it is clearly seen from Eqs. 3.4 and 3.5 one can obtain σ_1 by using σ_{xth} and in practice it is easier to compute it.

The above definitions of SCF and SCF* are valid for both SCF_{Locmax} and SCF_{cr}. To avoid confusion of many indices, we drop "Locmax" and "cr".

The σ_x / σ_{xth} , SCF_{Locmax} , and SCF_{cr} values are given in the tables below. In addition, SCF_{Locmax} versus b and SCF_{cr} versus b graphs are given in Figures 3.6 - 3.9.

Table 9. NUMERICAL VALUES OBTAINED FOR STEEL BEAM

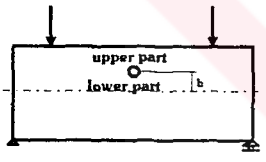

		b (mm)					
		0	10	20	30	40	50
Upper part	σ_x (MPa)	2.41	-5.39	-13.02	-20.58	-28.05	-35.56
	σ_{xth} (MPa)	1.53	-1.37	-4.27	-7.17	-10.07	-12.97
	σ_x / σ_{xth}	1.57	3.93	3.05	2.87	2.78	2.74
	σ_1 / σ_{xth}	1.60	3.94	3.05	2.87	2.79	2.74
Lower part	σ_x (MPa)	-2.45	-10.50	-18.88	-27.65	-36.86	-41.42
	σ_{xth} (MPa)	-1.53	-4.43	-7.34	-10.24	-13.14	-16.04
	σ_x / σ_{xth}	1.60	2.37	2.57	2.70	2.81	2.58
	σ_1 / σ_{xth}	1.62	2.37	2.57	2.70	2.81	2.59

Table 10. NUMERICAL VALUES OBTAINED FOR GRAPHITE-EPOXY

b=0 mm	Reinforcing Angle θ (°)					Max.	Min.
	0	30	45	60	90	value at	value at
σ_x / σ_{xth}	1.12	1.54	1.10	1.22	1.18	30°	45°
SCF_{locmax}	2.97	2.06	3.08	1.71	1.23	45°	90°
SCF_{cr}	2.97	2.06	2.82	1.71	1.23	0°	90°

b=10 mm	Reinforcing Angle θ (°)					Max.	Min.
	0	30	45	60	90	value at	value at
σ_x / σ_{xth}	6.65	6.65	7.74	4.31	2.98	45°	90°
SCF_{locmax}	6.65	5.28	5.28	3.54	2.98	0°	90°
SCF_{cr}	3.73	3.66	4.60	2.35	1.78	45°	90°

b=20 mm	Reinforcing Angle θ (°)					Max.	Min.
	0	30	45	60	90	value at	value at
σ_x / σ_{xth}	4.65	3.70	3.28	2.56	2.30	0°	90°
SCF_{locmax}	4.65	4.86	5.42	3.14	2.30	45°	90°
SCF_{cr}	4.07	4.20	4.45	2.73	1.90	45°	90°

b=30 mm	Reinforcing Angle θ (°)					Max.	Min.
	0	30	45	60	90	value at	value at
σ_x / σ_{xth}	4.13	3.54	2.95	2.38	2.19	0°	90°
SCF_{locmax}	4.32	4.72	4.34	3.07	2.19	30°	90°
SCF_{cr}	4.32	4.69	4.30	3.07	1.96	30°	90°

b=40 mm	Reinforcing Angle θ (°)					Max.	Min.
	0	30	45	60	90	value at	value at
σ_x / σ_{xth}	4.00	3.42	2.74	2.32	2.06	0°	90°
SCF_{locmax}	4.74	4.75	4.44	3.35	2.06	30°	90°
SCF_{cr}	4.74	4.75	4.44	3.32	1.93	30°	90°

b=50 mm	Reinforcing Angle θ (°)					Max.	Min.
	0	30°	45	60	90	value at	value at
σ_x / σ_{xth}	3.90	3.26	2.58	2.24	2.08	0°	90°
SCF_{locmax}	5.06	5.67	4.45	4.31	2.36	30	90°
SCF_{cr}	5.06	5.67	4.45	4.31	2.36	30°	90°

Table 11. NUMERICAL VALUES OBTAINED FOR SCOTCHPLY

b=0 mm	Reinforcing Angle θ (°)					Max. value at	Min. value at
	0	30	45	60	90		
σ_x / σ_{xth}	1.69	1.60	1.48	1.44	1.41	0°	90°
SCF_{locmax}	2.08	1.88	1.76	1.57	1.45	0°	90°
SCF_{cr}	2.08	1.88	1.76	1.57	1.45	0°	90°

b=10 mm	Reinforcing Angle θ (°)					Max. value at	Min. value at
	0	30	45	60	90		
σ_x / σ_{xth}	5.17	4.08	3.61	3.32	3.36	0°	60°
SCF_{locmax}	5.17	4.91	4.45	3.58	3.36	0°	90°
SCF_{cr}	3.04	2.96	2.65	2.22	2.06	0°	90°

b=20 mm	Reinforcing Angle θ (°)					Max. value at	Min. value at
	0	30	45	60	90		
σ_x / σ_{xth}	3.85	3.20	2.83	2.62	2.63	0°	60°
SCF_{locmax}	3.85	3.74	3.38	2.80	2.63	0°	90°
SCF_{cr}	3.33	3.28	2.88	2.39	2.21	0°	90°

b=30 mm	Reinforcing Angle θ (°)					Max. value at	Min. value at
	0	30	45	60	90		
σ_x / σ_{xth}	3.56	3.02	2.68	2.46	2.49	0°	60°
SCF_{locmax}	3.56	3.52	3.11	2.61	2.48	0°	90°
SCF_{cr}	3.55	3.52	3.07	2.50	2.31	0°	90°

b=40 mm	Reinforcing Angle θ (°)					Max. value at	Min. value at
	0	30	45	60	90		
σ_x / σ_{xth}	3.44	2.94	2.58	2.40	2.40	0°	60°
SCF_{locmax}	3.76	3.69	3.28	2.70	2.40	0°	90°
SCF_{cr}	3.76	3.69	3.28	2.70	2.34	0°	90°

b=50 mm	Reinforcing Angle θ (°)					Max. value at	Min. value at
	0	30	45	60	90		
σ_x / σ_{xth}	3.40	2.91	2.51	2.33	2.35	0°	60°
SCF_{locmax}	3.94	3.86	3.44	2.80	2.35	0°	90°
SCF_{cr}	3.94	3.86	3.44	2.80	2.14	0°	90°

Table 12. NUMERICAL VALUES OBTAINED FOR KEVLAR

b=0 mm	Reinforcing Angle θ (°)					Max.	Min.
	0	30	45	60	90	value at	value at
σ_x / σ_{xth}	1.15	1.48	1.00	1.27	1.27	30°	45°
SCF_{locmax}	2.84	2.00	3.74	1.67	1.32	45°	90°
SCF_{cr}	2.84	2.00	3.17	1.67	1.32	45°	90°

b=10 mm	Reinforcing Angle θ (°)					Max.	Min.
	0	30	45	60	90	value at	value at
σ_x / σ_{xth}	6.51	4.76	4.59	3.29	3.32	0°	60°
SCF_{locmax}	6.51	7.00	8.84	4.01	3.33	45°	90°
SCF_{cr}	3.68	3.70	5.03	2.09	1.93	45°	90°

b=20 mm	Reinforcing Angle θ (°)					Max.	Min.
	0	30	45	60	90	value at	value at
σ_x / σ_{xth}	4.64	3.67	3.26	2.55	2.57	0°	60°
SCF_{locmax}	4.64	5.09	5.97	2.90	2.57	45°	90°
SCF_{cr}	4.11	4.49	4.57	2.47	2.10	45°	90°

b=30 mm	Reinforcing Angle θ (°)					Max.	Min.
	0	30	45	60	90	value at	value at
σ_x / σ_{xth}	4.14	3.59	2.90	2.40	2.41	0°	60°
SCF_{locmax}	4.39	5.18	4.65	2.86	2.41	30°	90°
SCF_{cr}	4.39	5.18	4.33	2.86	2.17	30°	90°

b=40 mm	Reinforcing Angle θ (°)					Max.	Min.
	0	30	45	60	90	value at	value at
σ_x / σ_{xth}	4.09	3.45	2.66	2.32	2.34	0°	60°
SCF_{locmax}	4.98	5.02	4.42	3.13	2.34	30°	90°
SCF_{cr}	4.98	5.02	4.42	3.13	2.19	30°	90°

b=50 mm	Reinforcing Angle θ (°)					Max.	Min.
	0	30	45	60	90	value at	value at
σ_x / σ_{xth}	3.99	3.24	2.48	2.28	2.27	0°	90°
SCF_{locmax}	5.29	5.85	4.44	4.24	2.28	30°	90°
SCF_{cr}	5.29	5.85	4.44	4.24	2.10	30°	90°

Table 13. NUMERICAL VALUES OBTAINED FOR BORON

b=0 mm	Reinforcing Angle θ (°)					Max.	Min.
	0	30	45	60	90	value at	value at
σ_x / σ_{xth}	1.23	1.45	0.96	1.32	1.36	30°	45°
SCF_{locmax}	2.71	1.99	3.96	1.66	1.40	45°	90°
SCF_{cr}	2.71	1.99	3.25	1.66	1.37	45°	90°

b=10 mm	Reinforcing Angle θ (°)					Max.	Min.
	0	30	45	60	90	value at	value at
σ_x / σ_{xth}	6.36	4.72	4.58	3.30	3.57	0°	60°
SCF_{locmax}	6.36	7.12	9.12	3.79	3.57	45°	90°
SCF_{cr}	3.62	3.67	5.10	2.01	2.09	45°	60°

b=20 mm	Reinforcing Angle θ (°)					Max.	Min.
	0	30	45	60	90	value at	value at
σ_x / σ_{xth}	4.59	3.64	3.25	2.59	2.74	0°	60°
SCF_{locmax}	4.59	5.15	6.15	2.80	2.74	45°	90°
SCF_{cr}	4.09	4.59	4.56	2.35	2.26	30°	90°

b=30 mm	Reinforcing Angle θ (°)					Max.	Min.
	0	30	45	60	90	value at	value at
σ_x / σ_{xth}	4.12	3.59	2.87	2.44	2.56	0°	60°
SCF_{locmax}	4.39	5.31	4.72	2.71	2.56	30°	90°
SCF_{cr}	4.39	5.31	4.25	2.71	2.34	30°	90°

b=40 mm	Reinforcing Angle θ (°)					Max.	Min.
	0	30	45	60	90	value at	value at
σ_x / σ_{xth}	4.10	3.45	2.62	2.35	2.50	0°	60°
SCF_{locmax}	5.05	5.06	4.32	2.96	2.51	30°	90°
SCF_{cr}	5.05	5.06	4.32	2.96	2.40	30°	90°

b=50 mm	Reinforcing Angle θ (°)					Max.	Min.
	0	30	45	60	90	value at	value at
σ_x / σ_{xth}	4.02	3.20	2.45	2.38	2.59	0°	60°
SCF_{locmax}	5.37	5.83	4.41	4.15	2.60	30°	90°
SCF_{cr}	5.37	5.83	4.41	4.15	2.49	30°	90°

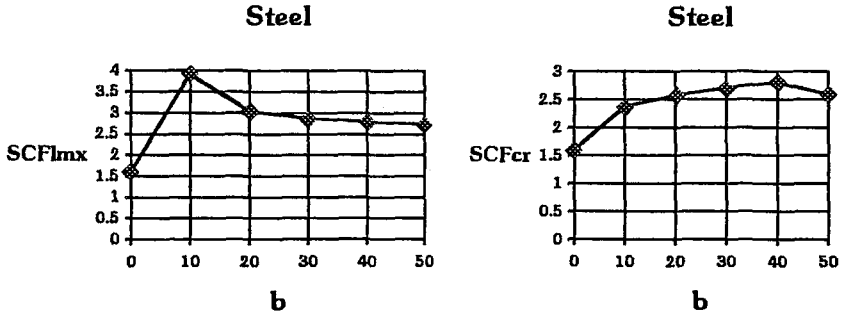

(a) (b)

Figure 3.6 SCF_{locmax} versus **b** and SCF_{cr} versus **b** graphs of the steel beam

It is seen from Fig. 3.6a that SCF_{locmax} increases with **b** up to the point where **b**=10mm and at this point SCF_{locmax} reaches its maximum value of 3.9 . From this point on SCF_{locmax} decreases as the distance **b** increases and at **b**=50mm it takes the minimum value of 2.7 .

In Fig. 3.6b the graph for steel beam reveals that there is a steady increase in SCF_{cr} as the distance b extends up to 40mm, thereafter a slight decrease is noticed.

The same trend is observed from the graph of Scotchply in Fig. 3.8.

As to the other composites, the plotted SCF_{cr} versus b graphs are similar to that of the steel with the exception of the case where the reinforcing angle is 45° Fig. 3.8. Failure in achieving the same trend at this angle may result from the lack of sensitivity of the FEM in this case.

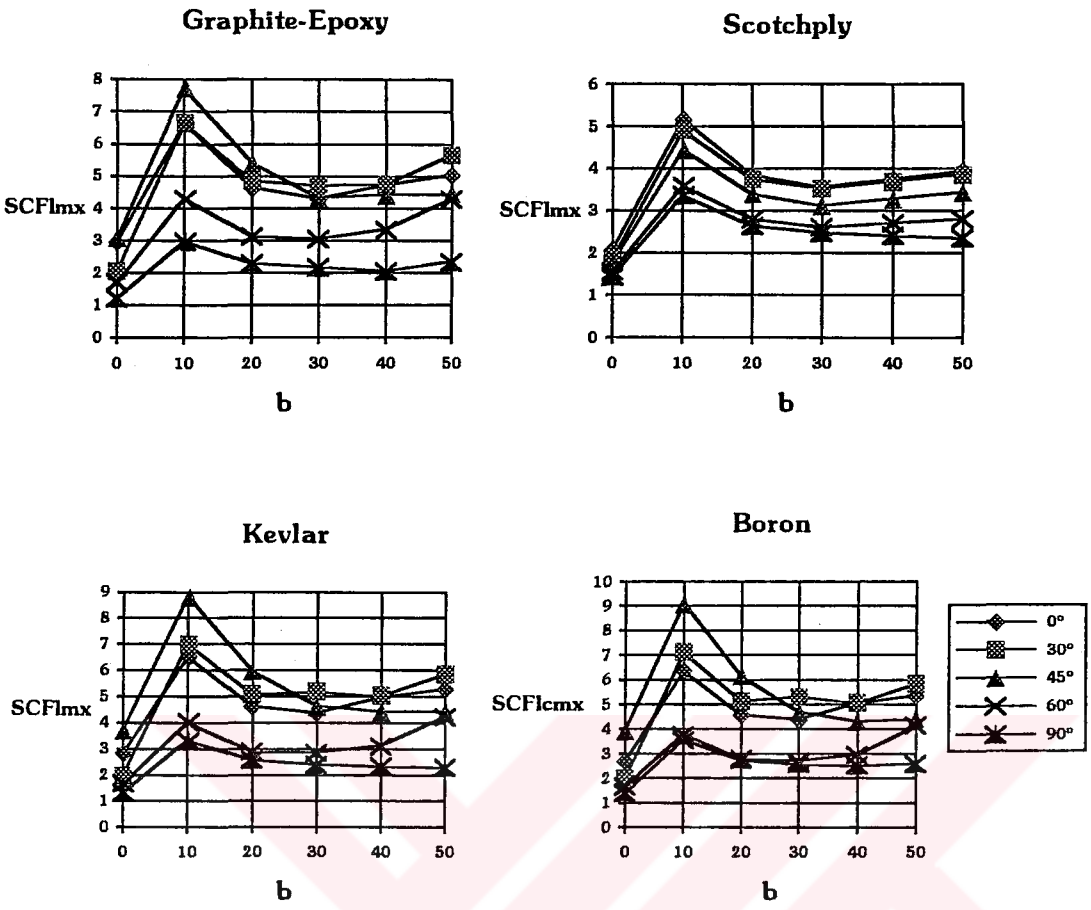

Figure 3.7 SCF_{locmax} versus **b** graphs of the composites

The plotted SCF_{locmax} versus **b** graphs of the composites for all reinforcing angles are similar to the graph of the steel Fig. 3.6a.

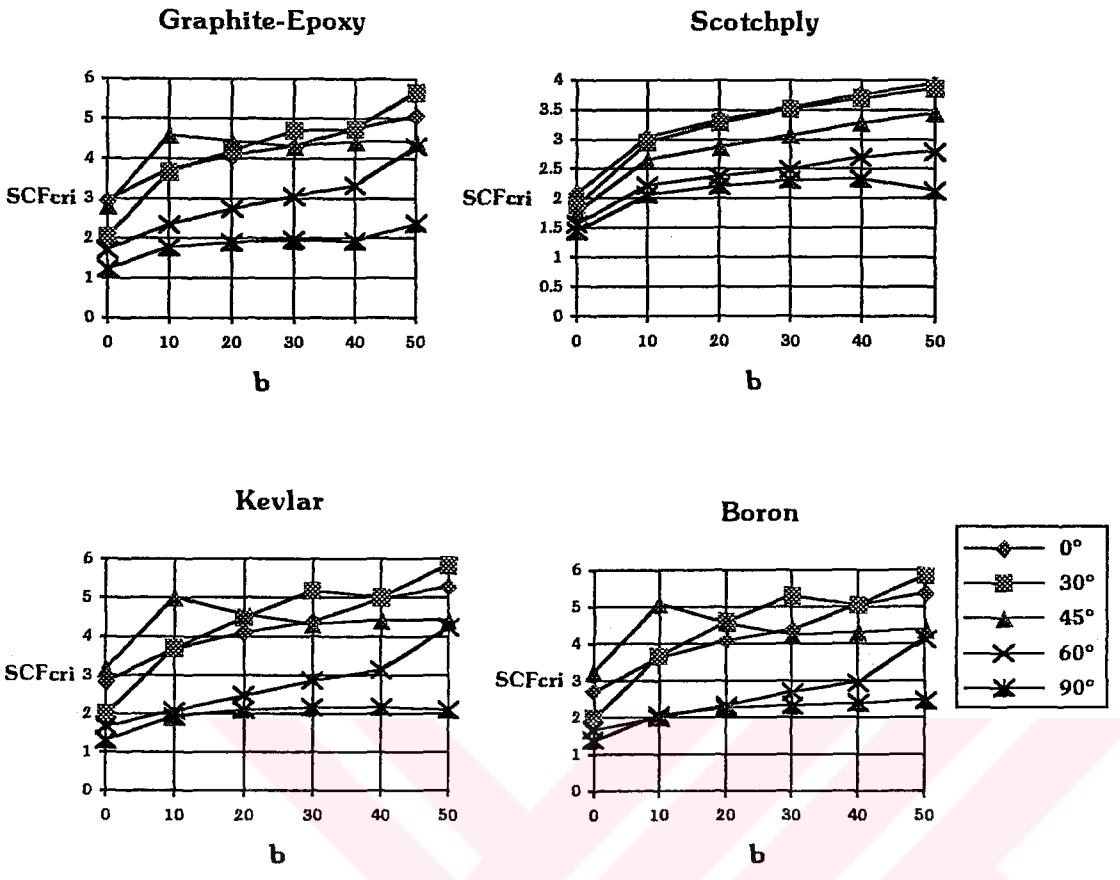

Figure 3.8 SCF_{cr} versus **b** graphs of the composites

Variation of the SCF around the hole is given in the following figures.

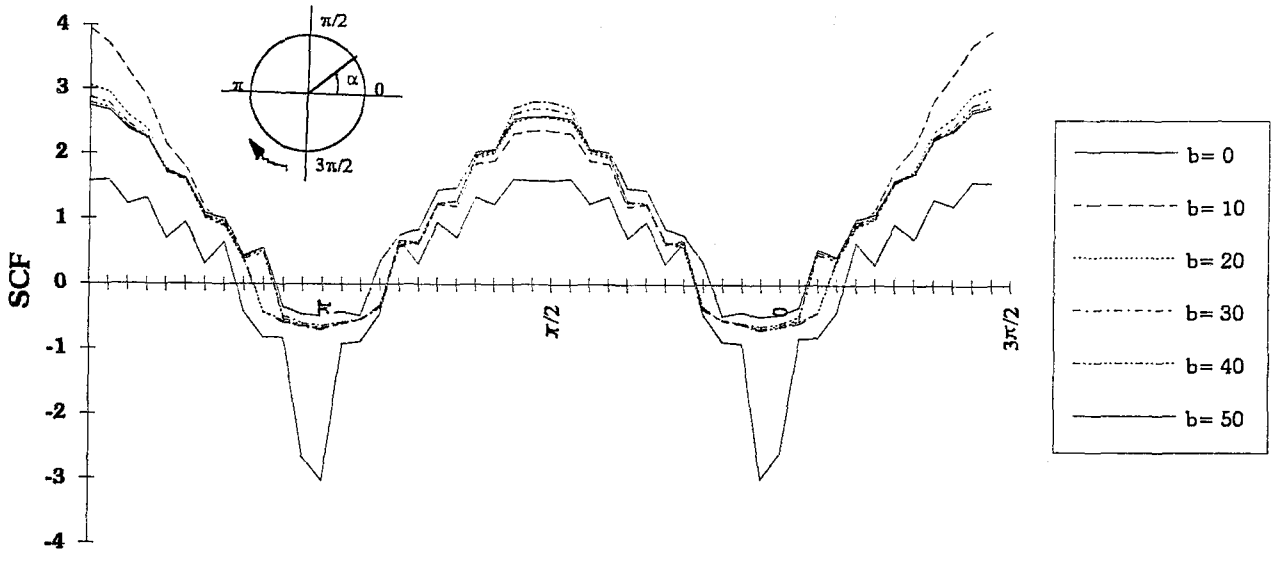

Figure 3.9 Variation of the SCF around the hole for the steel beam

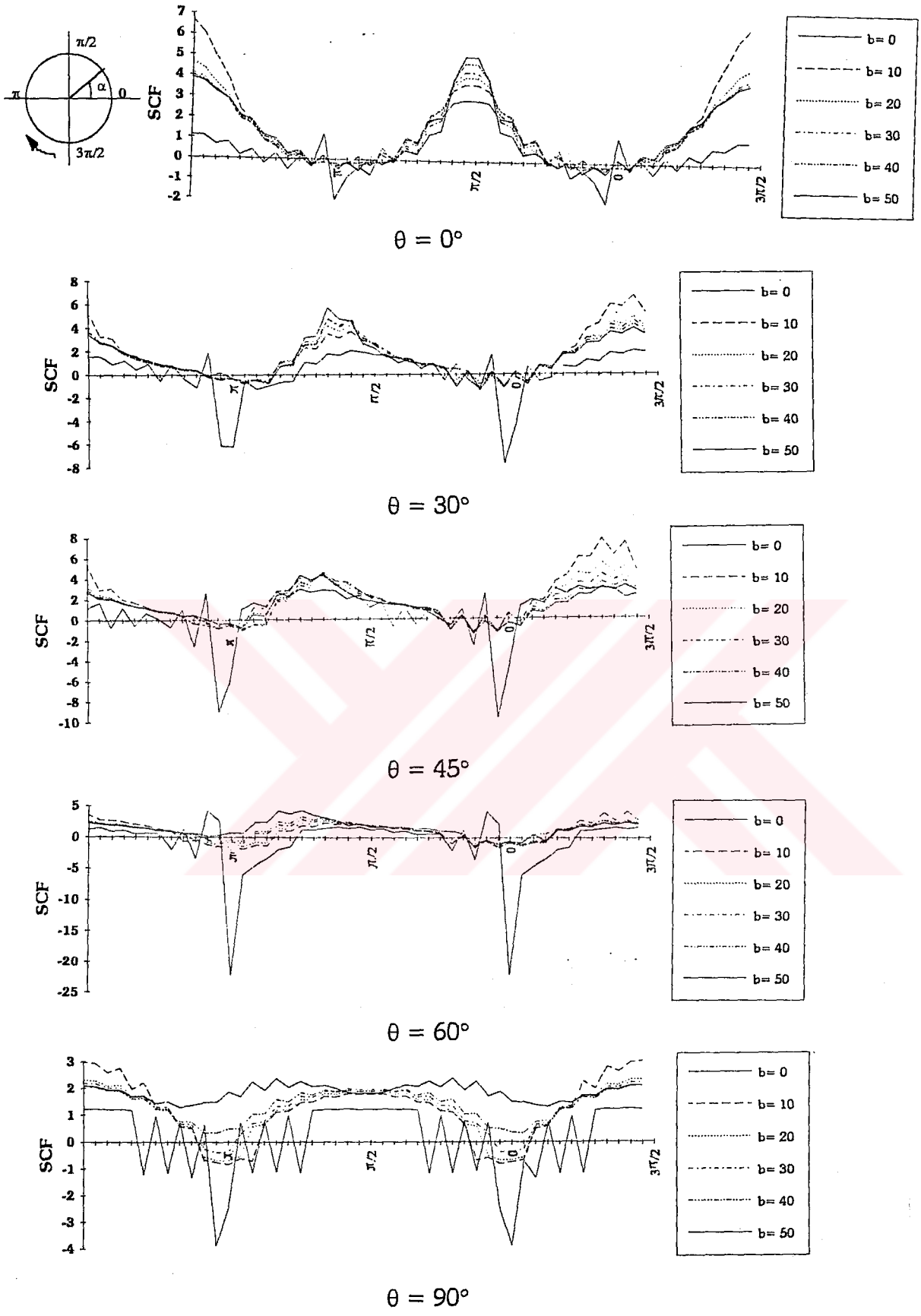

Figure 3.10 Variation of the SCF around the hole for Graphite-Epoxy

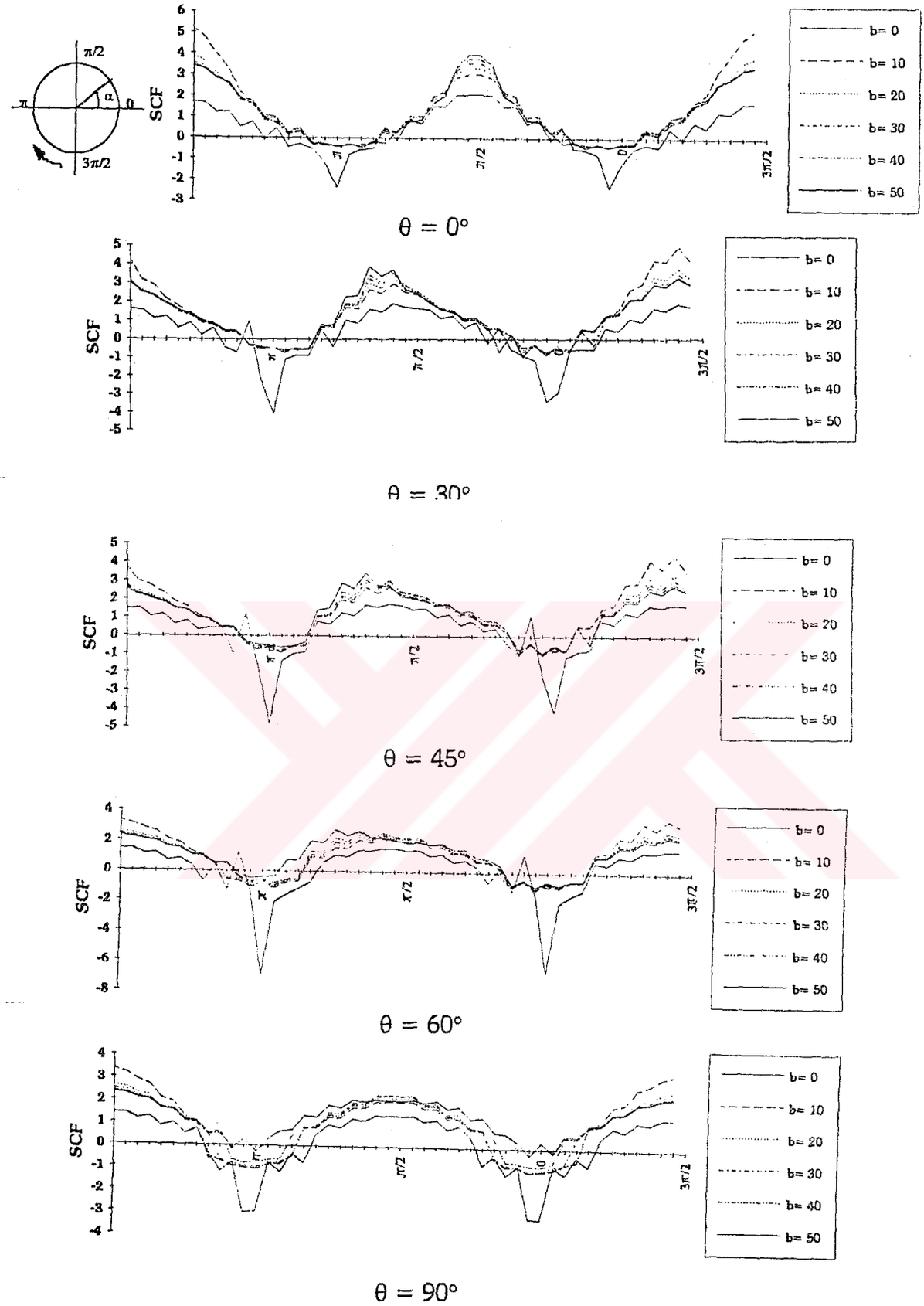

Figure 3.11 Variation of the SCF around the hole for Scotchply

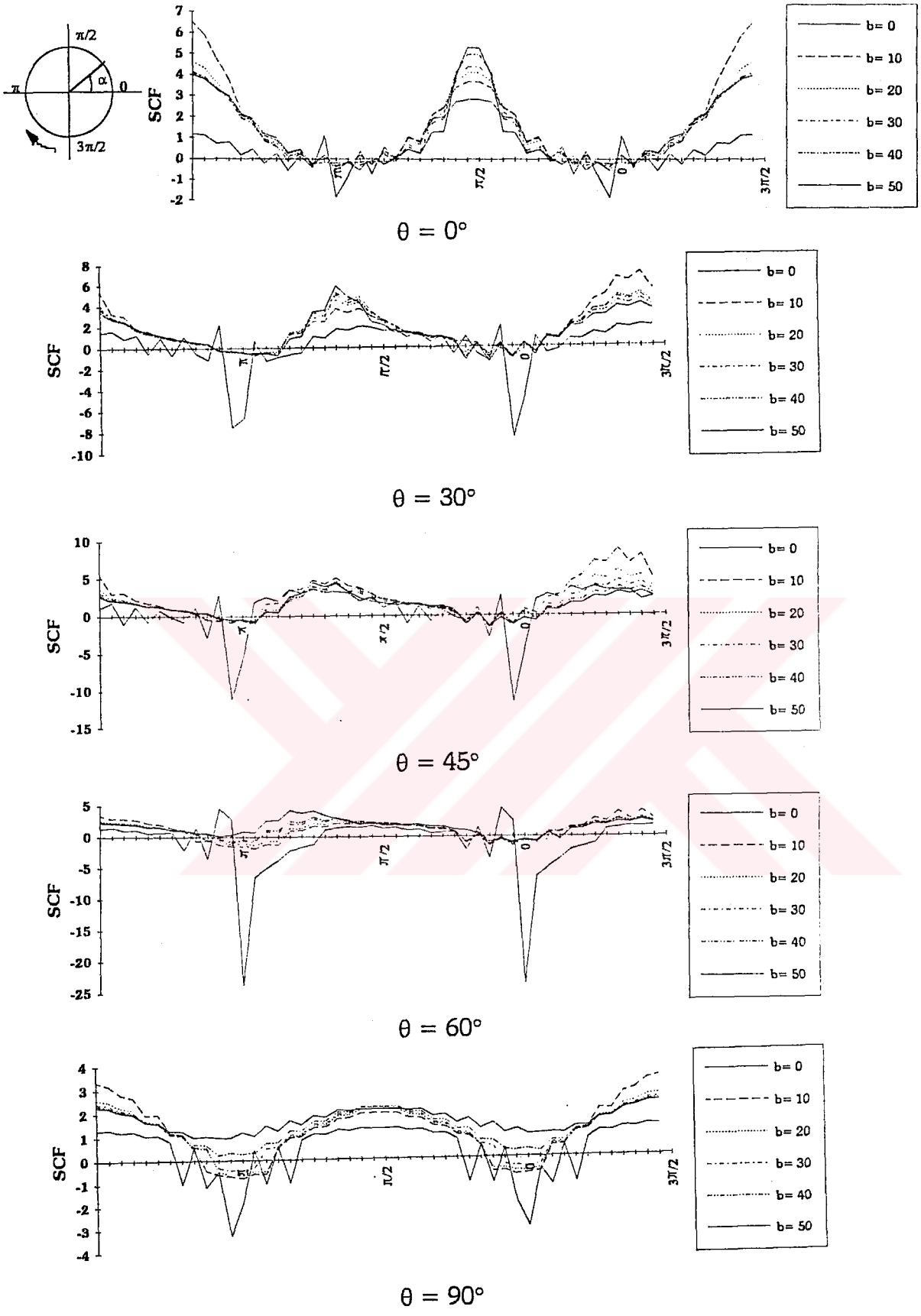

Figure 3.12 Variation of the SCF around the hole for Kevlar

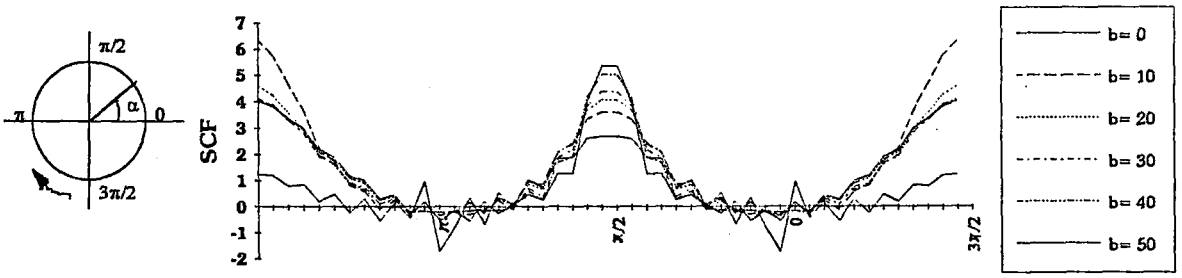

θ = 0°

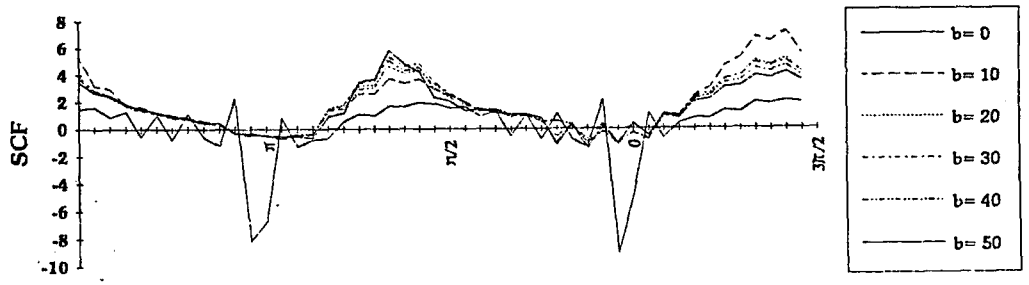

θ = 30°

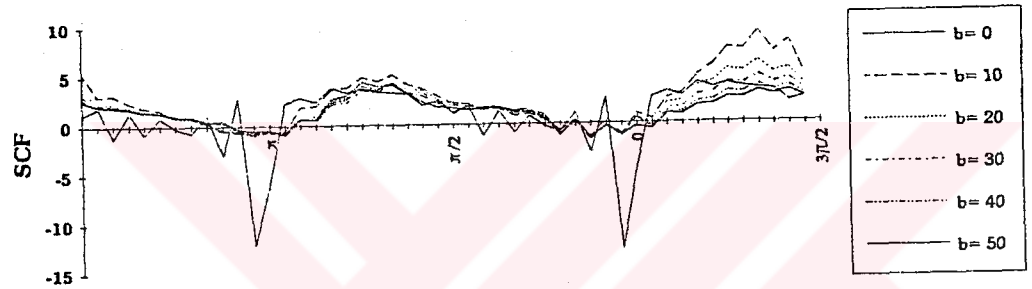

θ = 45°

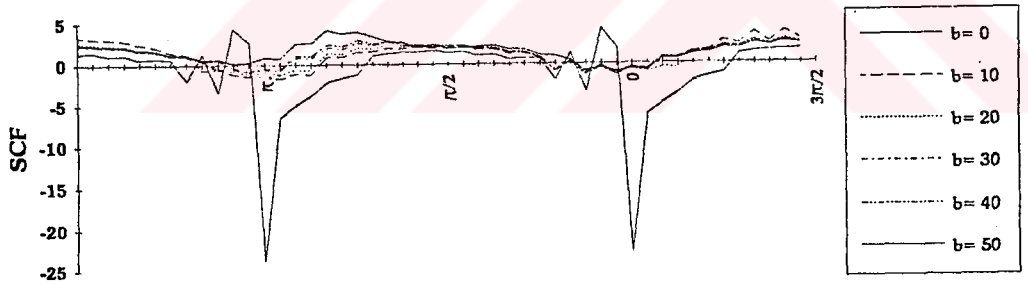

θ = 60°

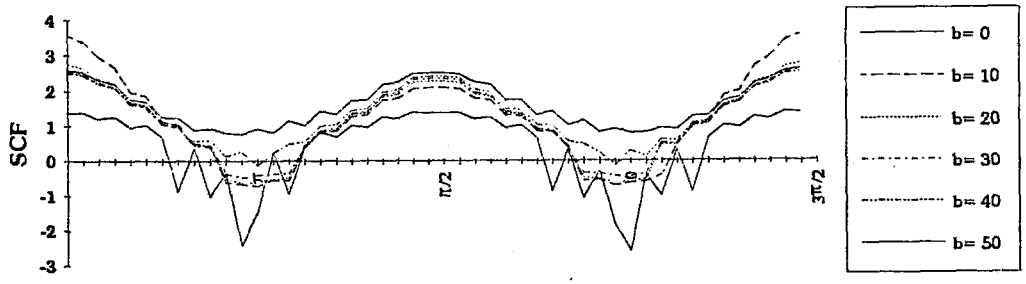

θ = 90°

Figure 3.13 Variation of the SCF around the hole for Boron

3.3. CRITICAL DATA

In our study, the following critical values are determined as follows:

- The critical **b** distances for each beam with 10 mm hole,
- The critical hole diameter $\mathbf{D_{cr}}$ for each **b** distance in the steel beam.

The critic **b** distance for the steel beam with 10 mm hole is 18 mm. The critical **b** distances for composite beams are presented in Fig. 3.14

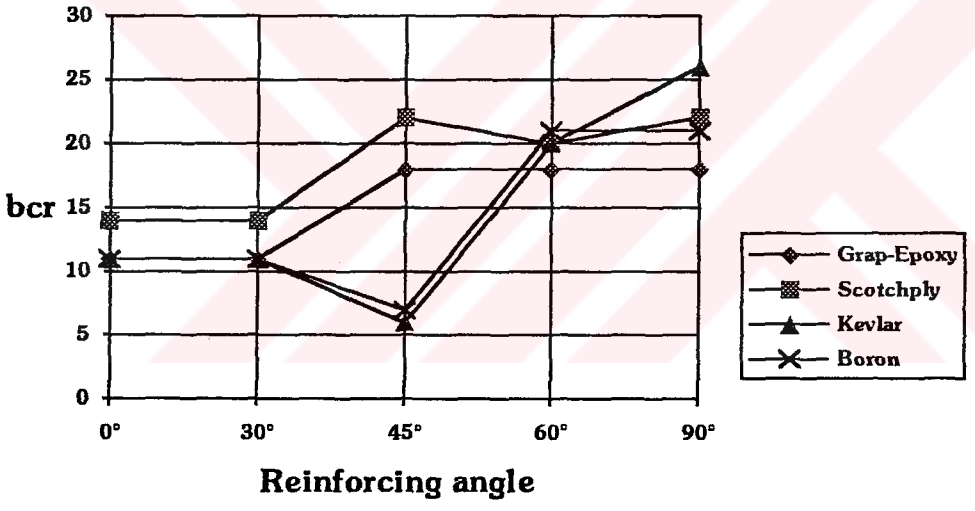

Figure 3.14 The critical **b** distances for each composite beam with 10 mm hole

The stresses are calculated for each **b** distance in a beam with a smaller hole diameter than $\mathbf{D_{cr}}$ do not exceed $(\sigma_{xth})_{max}$. Thus these stresses are not important in practice. In the case the beam has a greater hole diameter than $\mathbf{D_{cr}}$, the stress concentration factor SCF has to be considered. The values of $\mathbf{D_{cr}}$ leading to $(\sigma_{xth})_{max}$ are given in Fig. 3.15

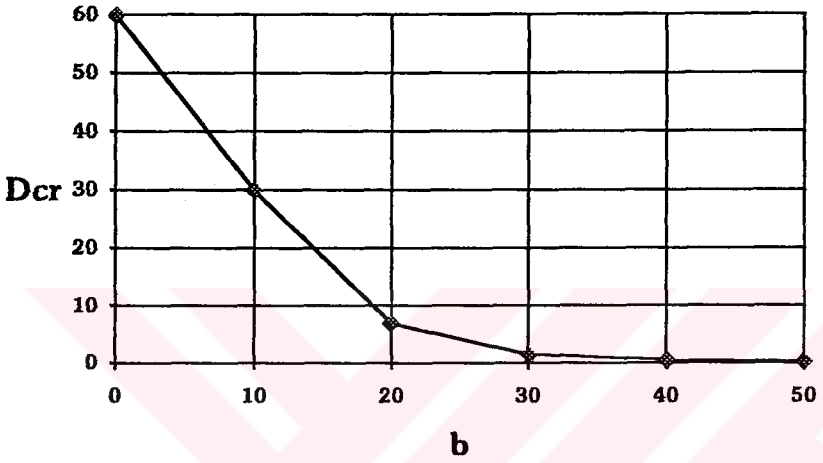

Figure 3.15 $\mathbf{D_{cr}}$ versus **b** graph of the steel beam

CHAPTER 4

CONCLUSIONS

In this study a beam with a circular hole on the transverse axis is investigated under the effect of pure bending. Stress distribution and stress concentration factor around the hole are determined for each position of the hole for steel and composite beams. Besides the critical position of the 10 mm hole with respect to the longitudinal axis is computed for each material. In addition, the value of the critical diameter of the hole leading to the maximum theoretical bending stress is determined for each b distance considered by the FEM. All the numerical values obtained are presented as tables and graphs. We expect that the results of this study will be useful in practice.

REFERENCES

FUNG, Y. C., Foundation of Solid Mechanics. Prentice-Hall of India Private Ltd. New Delhi, 1968

TSAI, S. W., and HAHN, H. T., Introduction To Composite Materials. V. I: Deformation Of Unidirectional And Laminated Composites. OHIO: Air Force Materials Laboratories (AFSC): Wright-Patterson AFB, 1979

CAHN, R. W., DAVIS, E. A., and WORD, I. M., An Introduction to Composite Materials. Cambridge University Press, Cambridge, New York, 1981

VINSON, J. R., and CHOU, T. W., Composite Materials and Their Use In Structures. Applied Science Publishers LTD, London, 1975

SAYMAN, O., and AKSOY, S., Kompozit Malzemeler. Ýzmir, Bornova: D.E.Ü. Mühendislik Fak., 1987

BATHE, K. J., Finite Element Procedures in Engineering Analysis. Prentice-Hall INC. , Englewood Cliffs, New Jersey, 1982

HUEBNER, K. H., and THORNTON, E. A., The Finite Element Method For Engineers. John WILEY & SONS, New York, 1982

ZIENKIEWICZ, O. C., The Finite Element Method. Mc Graw-Hill Co. UK, London, 1979

ZIENKIEWICZ, O. C., and PHILIPS, D. V.,An Automatic Mesh Generation Scheme for Plane and Curved Surfaces by "isoparametric" coordinates. International Journal for Numerical Methods In Engineering 3:519-528(1971)

CHANDRUPATLA, T. R., and BELEGUNDU, A. D., Introduction to Finite Elements in Engineering. Englewood Cliffs, NJ: Prentice-Hall, 1991

CAMPBELL, W. G., and BALLOU, S. V., Form and Style. Dallas, Geneva: Houghton Mifflin Company, 1978

APPENDIX A

SAMPLE DATA FILE, STEEL60.DAT

```
284 240 3 2 1 2 4
400 0 400 11 400 22 400 33 400 44 400 55 383.3333 0 386.4052
11.0352 389.477 22.0704 392.5488 33.1056 395.6206 44.1408 398.6925
55.176 401.3076 55.176 404.3794 44.1408 407.4512 33.1056 410.523
22.0704 413.5948 11.0352 416.6667 0 366.6667 0 372.8361 11.1328
379.0055 22.2656
385.1749 33.3984 391.3444 44.5312 397.5138 55.664 402.4862 55.664
408.6557 44.5312 414.825 33.3984 420.9945 22.2656 427.1639 11.1328
433.3333 0 0 0
35 0 70 0 105 0 140 0 175 0 210 0 245 0 280 0 315 0 350 0
359.2928 11.2928 368.5856 22.5856 377.8784 33.8784 387.1712 45.1712
396.464 56.464 403.536 56.464 412.8288 45.1712 422.1216 33.8784
431.4144 22.5856 440.7072 11.2928 450 0 485 0 520 0 555 0 590 0
625 0 660 0 695 0 730 0 765 0
800 0 0 20 34.16666 20 68.33333 20 102.5 20 136.6667 20 170.8333
20 205 20 239.1667 20
273.3333 20 307.5 20 341.6667 20 352.4662 27.50276
363.2656 35.00551 374.0651 42.50827 384.8645 50.01102
395.664 57.51378 404.336 57.51378 415.1355 50.01102
425.9349 42.50827 436.7344 35.00551 447.5339 27.50276
458.3333 20 492.5 20 526.6667 20 560.8334 20
595 20 629.1667 20 663.3333 20 697.5 20
731.6667 20 765.8333 20 800 20 0 40 33.33333 40
66.66666 40 100 40 133.3333 40 166.6667 40 200 40
233.3333 40 266.6667 40 300 40 333.3333 40
345.7019 43.73849 358.0704 47.47698 370.4389 51.21547
382.8075 54.95396 395.176 58.69244 404.824 58.69245
417.1925 54.95396 429.561 51.21546 441.9296 47.47698
454.2981 43.73849 466.6667 40 500 40 533.3333 40
566.6667 40 600 40 633.3334 40 666.6667 40 700 40
733.3334 40 766.6666 40 800 40 0 60 32.5 60
65 60 97.5 60 130 60 162.5 60 195 60 227.5 60
260 60 292.5 60 325 60 339 60 353 60 367 60
381 60 395 60 405 60 419 60 433 60 447 60
461 60 475 60 507.5 60 540 60 572.5 60 605 60
637.5 60 670 60 702.5 60 735 60 767.5 60
800 60 0 80 33.33333 80 66.66666 80 100 80
```

133.3333 80 166.6667 80 200 80 233.3334 80
266.6667 80 300 80 333.3333 80 345.7019 76.26151
358.0704 72.52302 370.4389 68.78453 382.8075 65.04604
395.176 61.30756 404.824 61.30755 417.1925 65.04604
429.561 68.78453 441.9296 72.52301 454.2981 76.26151
466.6667 80 500 80 533.3334 80 566.6667 80 600 80
633.3333 80 666.6667 80 700 80 733.3333 80
766.6667 80 800 80 0 100 34.16666 100 68.33333 100
102.5 100 136.6667 100 170.8333 100 205 100
239.1667 100 273.3333 100 307.5 100 341.6667 100
352.4662 92.49725 363.2656 84.99448 374.0651 77.49173
384.8645 69.98898 395.664 62.48622 404.336 62.48622
415.1355 69.98898 425.9349 77.49173 436.7344 84.99448
447.5339 92.49725 458.3333 100 492.5 100
526.6667 100 560.8333 100 595 100 629.1666 100
663.3333 100 697.5 100 731.6667 100 765.8333 100
800 100 0 120 35 120 70 120 105 120 140 120
175 120 210 120 245 120 280 120 315 120 350 120
359.2928 108.7072 368.5856 97.4144 377.8784 86.1216
387.1712 74.8288 396.464 63.536 403.536 63.536
412.8288 74.8288 422.1216 86.1216 431.4144 97.4144
440.7072 108.7072 450 120 485 120 520 120 555 120
590 120 625 120 660 120 695 120 730 120 765 120
800 120 366.6667 120 372.8361 108.8672
379.0055 97.73439 385.175 86.60159 391.3444 75.4688
397.5138 64.33601 402.4862 64.33601 408.6557 75.4688
414.825 86.6016 420.9945 97.7344 427.1639 108.8672
433.3333 120 383.3333 120 386.4052 108.9648
389.477 97.9296 392.5488 86.8944 395.6206 75.8592
398.6924 64.82401 401.3076 64.82401 404.3794 75.85921
407.4512 86.89439 410.523 97.9296 413.5949 108.9648
416.6667 120 400 120 400 109 400 98 400 87
400 76 400 65
1 2 8 7 2 3 9 8 3 4 10 9 4 5 11 10
5 6 12 11 7 8 20 19 8 9 21 20 9 10 22 21
10 11 23 22 11 12 24 23 19 20 42 41
20 21 43 42 21 22 44 43 22 23 45 44
23 24 46 45 6 5 14 13 5 4 15 14 4 3 16 15
3 2 17 16 2 1 18 17 13 14 26 25 14 15 27 26
15 16 28 27 16 17 29 28 17 18 30 29
25 26 48 47 26 27 49 48 27 28 50 49
28 29 51 50 29 30 52 51 31 32 64 63
32 33 65 64 33 34 66 65 34 35 67 66
35 36 68 67 36 37 69 68 37 38 70 69
38 39 71 70 39 40 72 71 40 41 73 72
63 64 96 95 64 65 97 96 65 66 98 97
66 67 99 98 67 68 100 99 68 69 101 100
69 70 102 101 70 71 103 102 71 72 104 103

72 73 105 104 95 96 128 127 96 97 129 128
97 98 130 129 98 99 131 130 99 100 132 131
100 101 133 132 101 102 134 133 102 103 135 134
103 104 136 135 104 105 137 136 41 42 74 73
42 43 75 74 43 44 76 75 44 45 77 76
45 46 78 77 73 74 106 105 74 75 107 106
75 76 108 107 76 77 109 108 77 78 110 109
105 106 138 137 106 107 139 138 107 108 140 139
108 109 141 140 109 110 142 141 47 48 80 79
48 49 81 80 49 50 82 81 50 51 83 82
51 52 84 83 79 80 112 111 80 81 113 112
81 82 114 113 82 83 115 114 83 84 116 115
111 112 144 143 112 113 145 144 113 114 146 145
114 115 147 146 115 116 148 147 52 53 85 84
53 54 86 85 54 55 87 86 55 56 88 87
56 57 89 88 57 58 90 89 58 59 91 90
59 60 92 91 60 61 93 92 61 62 94 93
84 85 117 116 85 86 118 117 86 87 119 118
87 88 120 119 88 89 121 120 89 90 122 121
90 91 123 122 91 92 124 123 92 93 125 124
93 94 126 125 116 117 149 148 117 118 150 149
118 119 151 150 119 120 152 151 120 121 153 152
121 122 154 153 122 123 155 154 123 124 156 155
124 125 157 156 125 126 158 157 127 128 160 159
128 129 161 160 129 130 162 161 130 131 163 162
131 132 164 163 132 133 165 164 133 134 166 165
134 135 167 166 135 136 168 167 136 137 169 168
159 160 192 191 160 161 193 192 161 162 194 193
162 163 195 194 163 164 196 195 164 165 197 196
165 166 198 197 166 167 199 198 167 168 200 199
168 169 201 200 191 192 224 223 192 193 225 224
193 194 226 225 194 195 227 226 195 196 228 227
196 197 229 228 197 198 230 229 198 199 231 230
199 200 232 231 200 201 233 232 137 138 170 169
138 139 171 170 139 140 172 171 140 141 173 172
141 142 174 173 169 170 202 201 170 171 203 202
171 172 204 203 172 173 205 204 173 174 206 205
201 202 234 233 202 203 235 234 203 204 236 235
204 205 237 236 205 206 238 237 143 144 176 175
144 145 177 176 145 146 178 177 146 147 179 178
147 148 180 179 175 176 208 207 176 177 209 208
177 178 210 209 178 179 211 210 179 180 212 211
207 208 240 239 208 209 241 240 209 210 242 241
210 211 243 242 211 212 244 243 148 149 181 180
149 150 182 181 150 151 183 182 151 152 184 183
152 153 185 184 153 154 186 185 154 155 187 186
155 156 188 187 156 157 189 188 157 158 190 189
180 181 213 212 181 182 214 213 182 183 215 214

183 184 216 215 184 185 217 216 185 186 218 217
186 187 219 218 187 188 220 219 188 189 221 220
189 190 222 221 212 213 245 244 213 214 246 245
214 215 247 246 215 216 248 247 216 217 249 248
217 218 250 249 218 219 251 250 219 220 252 251
220 221 253 252 221 222 254 253 233 234 256 255
234 235 257 256 235 236 258 257 236 237 259 258
237 238 260 259 255 256 268 267 256 257 269 268
257 258 270 269 258 259 271 270 259 260 272 271
267 268 280 279 268 269 281 280 269 270 282 281
270 271 283 282 271 272 284 283 239 240 262 261
240 241 263 262 241 242 264 263 242 243 265 264
243 244 266 265 261 262 274 273 262 263 275 274
263 264 276 275 264 265 277 276 265 266 278 277
273 274 283 284 274 275 282 283 275 276 281 282
276 277 280 281 277 278 279 280
1 1 1 1 1 1 1 1 1 1 1 1 1 1 1 1 1 1 1 1 1 1 1 1 1 1 1 1 1 1 1
1 1 1 1 1 1 1 1 1 1 1 1 1 1 1 1 1 1 1 1 1 1 1 1 1 1 1 1 1 1 1
1 1 1 1 1 1 1 1 1 1 1 1 1 1 1 1 1 1 1 1 1 1 1 1 1 1 1 1 1 1 1
1 1 1 1 1 1 1 1 1 1 1 1 1 1 1 1 1 1 1 1 1 1 1 1 1 1 1 1 1 1 1
1 1 1 1 1 1 1 1 1 1 1 1 1 1 1 1 1 1 1 1 1 1 1 1 1 1 1 1 1 1 1
1 1 1 1 1 1 1 1 1 1 1 1 1 1 1 1 1 1 1 1 1 1 1 1 1 1 1 1 1 1 1
1 1 1 1 1 1 1 1 1 1 1 1 1 1 1 1 1 1 1 1 1 1 1 1 1 1 1 1 1 1 1
1 1 1 1 1 1 1 1 1 1 1 1 1 1 1 1 1 1 1 1 1 1
61 0 62 0 124 0 458 -1000 496 -1000 200000 .3 0 0

APPENDIX B

SAMPLE PROGRAM OUTPUT, STEELb0.OUT

This output is evaluated by using data file STEELb0.DAT

A:\OUT\ST0°b0.OUT

EL#	Y_c	σ_x	σ_{xt}	S_1	S_2	S_{max}/σ_{xt}
1	-57.674	16.915	16.822	16.934	0.318	1.007
1	-51.319	14.860	14.968	14.872	-0.307	0.994
2	-46.666	13.690	13.611	13.707	0.330	1.007
2	-40.311	11.652	11.757	11.661	-0.289	0.992
3	-35.659	10.478	10.401	10.492	0.329	1.009
3	-29.304	8.425	8.547	8.431	-0.294	0.986
4	-24.652	7.238	7.190	7.250	0.299	1.008
4	-18.296	5.206	5.336	5.210	-0.318	0.976
5	-13.644	4.015	3.980	4.025	0.075	1.011
5	-7.289	2.338	2.126	2.341	-0.432	1.101
225	7.289	-2.337	-2.126	0.442	-2.339	1.100
225	13.644	-4.012	-3.980	-0.065	-4.022	1.011
224	18.296	-5.203	-5.336	0.325	-5.207	0.976
224	24.652	-7.235	-7.190	-0.291	-7.246	1.008
223	29.304	-8.423	-8.547	0.299	-8.429	0.986
223	35.659-	10.477	-10.401	-0.325	-10.491	1.009
222	40.311	-11.653	-11.757	0.292	-11.662	0.992
222	46.666	-13.694	-13.611	-0.328	-13.711	1.007
221	51.319	-14.867	-14.968	0.308	-14.879	0.994
221	57.674	-16.929	-16.822	-0.318	-16.948	1.008
20	-57.674	16.915	16.822	16.935	0.318	1.007
20	-51.319	14.860	14.968	14.872	-0.307	0.994
19	-46.666	13.690	13.611	13.707	0.330	1.007
19	-40.311	11.652	11.757	11.662	-0.290	0.992
18	-35.659	10.479	10.401	10.492	0.329	1.009
18	-29.304	8.425	8.547	8.431	-0.294	0.986
17	-24.652	7.238	7.190	7.250	0.299	1.008
17	-18.296	5.206	5.336	5.210	-0.318	0.976
16	-13.644	4.015	3.980	4.025	0.075	1.011
16	-7.289	2.338	2.126	2.341	-0.433	1.101
236	7.289	-2.337	-2.126	0.442	-2.339	1.100
236	13.644	-4.012	-3.980	-0.065	-4.021	1.011
237	18.296	-5.203	-5.336	0.326	-5.207	0.976

237	24.652	-7.235	-7.190	-0.291	-7.247	1.008
238	29.304	-8.423	-8.547	0.298	-8.429	0.986
238	35.659	-10.477	-10.401	-0.325	-10.491	1.009
239	40.311	-11.653	-11.757	0.292	-11.662	0.992
239	46.666	-13.694	-13.611	-0.328	-13.711	1.007
240	51.319	-14.867	-14.968	0.308	-14.880	0.994
240	57.674	-16.929	-16.822	-0.318	-16.949	1.008
5	-7.289	2.338	2.126	2.341	-0.432	1.101
5	-7.192	2.365	2.098	2.368	-0.492	1.129
10	-7.057	2.207	2.058	2.209	-0.389	1.073
10	-6.787	2.277	1.980	2.280	-0.524	1.152
15	-6.527	1.987	1.904	1.987	-0.290	1.044
15	-6.084	2.100	1.775	2.102	-0.428	1.184
65	-5.531	2.153	1.613	2.155	-0.086	1.336
65	-4.463	2.045	1.302	2.051	-0.167	1.576
70	-3.655	1.813	1.066	1.835	-0.094	1.721
70	-2.515	1.301	0.733	1.371	-0.369	1.869
75	-1.654	0.901	0.483	1.054	-0.154	2.185
75	-0.443	0.153	0.129	0.513	-0.626	-4.842
155	0.443	-0.150	-0.129	0.645	-0.503	-4.985
155	1.654	-0.898	-0.483	0.176	-1.048	2.173
160	2.515	-1.299	-0.733	0.396	-1.368	1.865
160	3.655	-1.811	-1.066	0.120	-1.832	1.719
165	4.463	-2.043	-1.302	0.193	-2.048	1.574
165	5.531	-2.151	-1.613	0.112	-2.153	1.335
215	6.084	-2.096	-1.775	0.449	-2.098	1.182
215	6.527	-1.984	-1.904	0.308	-1.984	1.042
220	6.787	-2.274	-1.980	0.541	-2.277	1.150
220	7.057	-2.206	-2.058	0.402	-2.207	1.072
225	7.192	-2.363	-2.098	0.502	-2.366	1.128
225	7.289	-2.337	-2.126	0.442	-2.339	1.100
236	7.289	-2.337	-2.126	0.442	-2.339	1.100
236	7.192	-2.362	-2.098	0.504	-2.366	1.128
231	7.057	-2.208	-2.058	0.404	-2.209	1.073
231	6.787	-2.276	-1.980	0.544	-2.279	1.151
226	6.527	-1.987	-1.904	0.311	-1.987	1.044
226	6.084	-2.097	-1.775	0.453	-2.100	1.183
176	5.531	-2.151	-1.613	0.113	-2.153	1.334
176	4.463	-2.042	-1.302	0.192	-2.048	1.573
171	3.655	-1.811	-1.066	0.120	-1.832	1.719
171	2.515	-1.299	-0.733	0.396	-1.367	1.864
166	1.654	-0.899	-0.483	0.177	-1.049	2.174
166	0.443	-0.149	-0.129	0.646	-0.503	-4.994
86	-0.443	0.154	0.129	0.515	-0.623	-4.820
86	-1.654	0.903	0.483	1.057	-0.151	2.190
81	-2.515	1.301	0.733	1.371	-0.369	1.869
81	-3.655	1.812	1.066	1.834	-0.094	1.721
76	-4.463	2.043	1.302	2.049	-0.170	1.574

76	-5.531	2.151	1.613	2.153	-0.090	1.335
26	-6.084	2.100	1.775	2.102	-0.432	1.184
26	-6.527	1.987	1.904	1.988	-0.292	1.044
21	-6.787	2.277	1.980	2.280	-0.528	1.152
21	-7.057	2.208	2.058	2.209	-0.391	1.073
16	-7.192	2.364	2.098	2.368	-0.494	1.129
16	-7.289	2.338	2.126	2.341	-0.433	1.101